a0005

6.63 Phototransduction in Microvillar Photoreceptors of *Drosophila* and Other Invertebrates

Roger C Hardie and Marten Postma, Department of Physiology Development and Neuroscience, University of Cambridge, Cambridge, UK

Glossary

g0005 ***ankyrin repeats*** Protein-binding motifs.

g0010 ***Arr1*** Arrestin 1.

g0015 ***Arr2*** Arrestin 2.

g0020 ***ATP*** Adenosine 5′-triphosphate.

g0025 ***BAPTA*** 1,2-bis(*o*-aminophenoxy)ethane-*N*,*N*,*N*′,*N*′-tetraacetic acid, fast Ca^{2+}-specific chelator.

g0030 ***Ca orange*** Calcium indicator.

g0035 ***Ca ATPase*** ATP-dependent Ca^{2+} pump.

g0040 ***CaCaM*** Ca^{2+} calmodulin.

g0045 ***caged Ca^{2+}*** Photolabile compound with tightly bound Ca^{2+} which can be released by photolysis.

g0050 ***Calliphora*** Blowfly.

g0055 ***calnexin*** Gene encoding a Ca^{2+}-binding, chaperone protein.

g0060 ***calphotin*** Gene encoding a Ca^{2+}-binding protein.

g0065 ***CalX*** *Drosophila* sodium/calcium exchanger, belonging to NCX family.

g0070 ***CaM*** Calmodulin.

g0075 ***CaMKII*** Calmodulin kinase II.

g0080 ***CBS*** Calmodulin-binding site.

g0085 ***CC*** Coiled-coil region.

g0090 ***CDP–DAG*** Cytidine 5′-diphosphate–diacylglycerol.

g0095 ***CDP–DAG synthase*** Enzyme that converts PA into CDP–DAG.

g0100 ***cds*** Gene encoding CDP–DAG synthase.

g0105 ***cGMP*** Cyclic guanosine 3,5-monophosphate.

g0110 ***clathrin*** A major constituent of the protein coat of vesicles formed during endocytosis.

g0115 ***CMP*** Cytidine 5′-monophosphate.

CNG Cyclic nucleotide gated. g0120

CTP Cytidine 5′-triphosphate. g0125

DA Dark adapted. g0130

DAG Diacylglycerol. g0135

DAG lipase Enzyme that converts DAG into PUFAs. g0140

DGK Diacylglycerol kinase. g0145

diptera Flies which only have a single pair of wings on the mesothorax. g0150

Drosophila Fruitfly. g0155

EC_{50} The half-maximal concentration for excitation. g0160

eGFP Enhanced green fluorescent protein. g0165

EGTA Ethylene glycol tetraacetic acid, a slow Ca^{2+} chelator. g0170

ER Endoplasmatic reticulum. g0175

ERG Electroretinogram. g0180

Fluo-3 Calcium indicator. g0185

FRET Fluorescence resonance energy transfer. g0190

G Heterotrimeric G protein. g0195

GAP GTPase-activating protein. g0200

GDP Guanosine 5′-diphosphate. g0205

GPRK1 G protein-coupled receptor kinase. g0210

G_q PLC-activating G protein. g0215 AU11

GTP Guanosine 5′-triphosphate. g0220

GTPase GTP-hydrolyzing protein. g0225

Gα Heterotrimeric G protein alpha subunit. g0230

Gβ Heterotrimeric G protein beta subunit. g0235

Gγ Heterotrimeric G protein gamma subunit. g0240

IC_{50} The half-maximal concentration for inhibition. g0245

g0250 ***immunogold labeling*** Antibody labeling using colloidal gold, visible in electron microscope.
g0255 ***ina*** *i*nactivation *n*o *a*fterpotential gene.
g0260 ***INAC*** Eye-specific PKC encoded by *inaC* gene.
g0265 ***INAD*** Scaffolding protein encoded by *inaD* gene.
g0270 ***INDO-1*** Calcium indicator.
g0275 ***$InsP_3$*** Inositol 1,4,5 trisphosphate.
g0280 ***$InsP_3R$*** $InsP_3$ receptor.
g0285 ***ipRGC*** Intrinsically photosensitive retinal ganglion cells.
g0290 ***Kir2.1*** PIP_2-sensitive inward rectifier ion channel.
g0295 ***LA*** Light adapted.
g0300 ***laza*** Lazaro, gene encoding LPP.
g0305 ***LIC*** Light-induced current.
g0310 ***Limulus*** Horseshoe crab.
g0315 ***LMC*** Large monopolar cells (first-order visual interneurons).
g0320 ***LPP*** Lipid phosphate phosphohydrolase.
g0325 ***M*** Metarhodopsin.
g0330 ***Na/K ATPase*** Sodium–potassium pump.
g0335 ***NCKX*** Potassium-dependent sodium/calcium exchange.
g0340 ***NCX*** Na/Ca exchanger with 3Na:1Ca stoichiometry.
g0345 ***nina*** *n*o *i*nactivation *n*o *a*fterpotential gene.
g0350 ***NINAC*** Class III myosin.
g0355 ***norp*** *n*o *r*eceptor *p*otential gene.
g0360 ***NORPA*** Eye-specific PLC encoded by *norpA* gene.
g0365 ***ocelli*** Small, dorsally located simple eyes.
g0370 ***ommatidium*** Cluster of photoreceptor cells and accessory cells underlying each facet lens of the compound eye.
g0375 ***opsin*** Light-sensitive transmembrane G protein-coupled receptor.
g0380 ***P*** Ionic permeability.
g0385 ***PA*** Phospatidic acid.
g0390 ***PC*** Phosphatidylcholine.
g0395 ***PDA*** Prolonged depolarizing afterpotential.
g0400 ***PDZ domain*** (*P*SD95, *d*iscs large, *z*onula adherens) protein binding domain, five of which are found in the scaffolding protein INAD.
g0405 ***phosrestin*** Alternative name for arrestin.
g0410 ***PI*** Phosphatidylinositol.
g0415 ***Pi*** Phosphate.
g0420 ***PI kinase*** Enzyme that phosphorylates PI-producing PIP.
g0425 ***PI synthase*** Enzyme that converts CDP–DAG into PI.
g0430 ***PIP*** Phosphatidylinositol 4-phosphate.
g0435 ***PIP kinase*** Enzyme that phosphorylates PIP-producing PIP_2.
g0440 ***PIP_2*** Phosphatidylinositol 4,5-bisphosphate.
g0445 ***PITP*** PI transfer protein.
g0450 ***PKA*** Protein kinase A.
g0455 ***PKC*** Protein kinase C.
g0460 ***PLC*** Phospholipase C.
g0465 ***PLCβ*** Phospholipase Cβ.
g0470 ***PLD*** Phospholipase D.
g0475 ***PUFA*** Polyunsaturated fatty acid.
g0480 ***quantum bump*** Single-photon response.
g0485 ***R*** Rhodopsin.
g0490 ***R1–6*** Major class of fly photoreceptor cells.
g0495 ***R7 and 8*** Minor classes of fly photoreceptor cells.
g0500 ***rdg*** *r*etinal *d*egeneration *g*ene.
g0505 ***3-hydroxy retinal*** Chromophore of dipteran opsins.
g0510 ***3-hydroxy retinol*** Sensitizing pigment.
g0515 ***RGS*** Regulator of G protein signaling.
g0520 ***rhabdomere*** Light-absorbing structure of the photoreceptor cell.
g0525 ***RK*** Rhodopsin kinase.
g0530 ***RyR*** Ryanodine receptor.
g0535 ***scaffolding protein*** A protein that binds multiple other proteins of different types.
g0540 ***serotonin*** A monoamine neurotransmitter.
g0545 ***Shab*** Potassium channel gene.
g0550 ***Shaker*** Potassium channel gene.
g0555 ***Shal*** Potassium channel gene.
g0560 ***signalplex*** The INAD complex (also referred to as transducisome).
g0565 ***SMC*** Submicrovillar cisternae.
g0570 ***thapsigargin*** Endoplasmic reticulum Ca^{2+}-ATPase inhibitor.
g0575 ***TRP*** Light-activated nonspecific cation channel encoded by *trp* gene.
g0580 ***trp*** *t*ransient *r*eceptor *p*otential gene.
g0585 ***TRPL*** Light-activated nonspecific cation channel encoded by *trpl* gene.
g0590 ***trpl*** *t*ransient *r*eceptor *p*otential-*l*ike gene.
g0595 ***TRPγ*** TRP homologue.
g0600 ***UV*** Ultraviolet light.
g0605 ***WT*** Wild type.

Abbreviation

Arr1	arrestin 1
Arr2	arrestin 2
ATP	adenosine 5′-triphosphate
CBS	calmodulin-binding site
CBS	CaM-binding sites
CC	coiled-coil region
CDP–DAG	cytidine-5′-diphosphate–diacylglycerol
CNG	cyclic nucleotide gated
CTP	cytidine-5′-triphosphate
DA	dark adapted
EGFP	enhanced green fluorescent protein
ER	endoplasmatic reticulum
ERG	electroretinogram
FRET	fluorescence resonance energy transfer
GAP	GTPase-activating protein
GPRK1	G-protein-coupled receptor kinase
ipRGCs	intrinsically photosensitive retinal ganglion cells
LA	light adapted
LIC	light-induced current
LPP	lipid phosphate phosphohydrolase
NinaE	no inactivation no afterpotential e
norpA	no receptor potential a
PAP	phosphatidic acid phosphatase
PDA	prolonged depolarizing afterpotential
RK	rhodopsin kinase
ROS	rod outer segments
TM	transmembrane

s0005

6.63.1 Introduction

p0005 The task of encoding visual information poses photoreceptors with a number of formidable and often conflicting challenges. They must maximize their sensitivity, by being able to absorb a high fraction of the incident light; at the same time they may need to optimize visual acuity, by keeping the cross-sectional area of the light-capturing organelle close to the wavelength of light. Maximum sensitivity also requires the ability to detect single photons, reliably and as rapidly as possible. In addition, they must be able to light adapt in order to operate over the vast environmental range of intensities, which span more than 10 orders of magnitude from starlight to direct sunlight. In the course of evolution, two major classes of ocular photoreceptors have become specialized to perform these functions: ciliary photoreceptors, typified by vertebrate rods and cones (see Yau, K-W., this volume), and the microvillar, or rhabdomeric photoreceptors of many invertebrate groups, including arthropods and most mollusks.

p0010 Ciliary and microvillar photoreceptors diverged very early in metazoan evolution (Arendt, D., 2003), and their separate evolutionary histories have resulted in rather different biological solutions to the challenges photoreceptors face. Although all known ocular photoreceptors use rhodopsin to absorb the incident light energy, and a G protein-coupled signaling cascade to transduce this into changes in conductances in the plasma membrane, the detailed biochemical pathways are quite distinct. Where studied, the transduction cascade of ciliary photoreceptors leads to metabolism of cyclic GMP (cGMP) and modulation of cyclic nucleotide-gated ion channels (CNG channels), whilst microvillar photoreceptors use the more widespread phosphoinositide cascade, characterized by the effector enzyme phospholipase C (PLC) and activation of nonselective cation channels, probably often belonging to the transient receptor potential (TRP) superfamily. Perhaps not surprisingly, the two classes of photoreceptors have in many respects functionally converged; however, there are several intriguing differences in performance. Most notably perhaps, vertebrate eyes usually solve the problems of absolute sensitivity, speed of response and dynamic range by using two classes of photoreceptors: rods, which can detect single photons with limited temporal resolution, but which saturate at moderate photon fluxes; and cones, which cannot detect single photons, but which respond rapidly and can light adapt to signal under the brightest daylight intensities (see Yau, K-W., this volume). By contrast, many invertebrate photoreceptors not only detect single photons, they often do so more rapidly than rods and yet can still light adapt to signal in full sunlight, when photon fluxes per photoreceptor can exceed 10^6 effectively absorbed photons per second. This chapter attempts to describe the cellular and molecular mechanisms that underlie this performance, concentrating on the photoreceptors of the fruit fly *Drosophila,* which has become the preferred model of invertebrate phototransduction, primarily because of its enormous potential for genetic manipulation and

analysis (reviewed in Montell, C., 1999; Minke, B. and Hardie, R. C., 2000; Hardie, R. C. and Raghu, P., 2001; Pak, W. L. and Leung, H. T., 2003). After introducing the structural and electrophysiological framework in sections Photoreceptor and Retinal Morphology and Electrophysiology, sections Molecular Components of the Phototransduction Cascade, Messengers of Excitation, Ca^{2+}-Dependent Feedback and Mechanisms of Adaptation, and Phosphoinositide Metabolismconsider the various molecular components of the cascade and how they are regulated. In section Molecular Strategies of Quantum Bump Generation and Adaptation, we attempt to summarize our current understanding of the molecular strategies underlying the physiological performance, and finally in section Phototransduction Mechanisms in Other Invertebrates we provide a brief overview of phototransduction mechanisms in some other invertebrate preparations.

s0010

6.63.2 Photoreceptor and Retinal Morphology

p0015 Rhodopsin is a transmembrane protein, and in order to maximize absorption of incident light most photoreceptors have evolved structures to increase the surface area of light-absorbing membrane. In vertebrate rods, these are the rod outer segments (ROS) consisting of stacks of internalized membranous discs. Many invertebrates, including arthropods and mollusks, utilize rhabdomeres, which consist of tightly packed arrays of microvilli. Rhabdomeres in *Drosophila* consist of ~30–50 000 microvilli, each 1–2 μM long and 60 nm in diameter (Figure 1). They develop from the apical surface of the cell to which they are attached by a narrow neck. Each microvillus contains ~1000 rhodopsin molecules closely packed in the microvillar membrane at a density of ~4000 μM^{-2}. Together, the microvilli form the rhabdomere, a 80- to100-μm-long and 1- to 2-μm-diameter tapering rod-like structure, which functions as a waveguide, trapping some 50% of the incident axial light at the wavelength of peak absorption (reviewed in Hardie, R. C., 1985).

p0020 Eight such photoreceptors are assembled in a so-called ommatidium behind each of the ~750 facets of the *Drosophila* compound eye. In cross section, the rhabdomeres form a precise hexagonal array with six peripheral rhabdomeres (R1–6) all containing the same visual pigment (Rh1 with $\lambda_{max} = 480$ nm), and a central tiered rhabdomere (R7 in the distal two

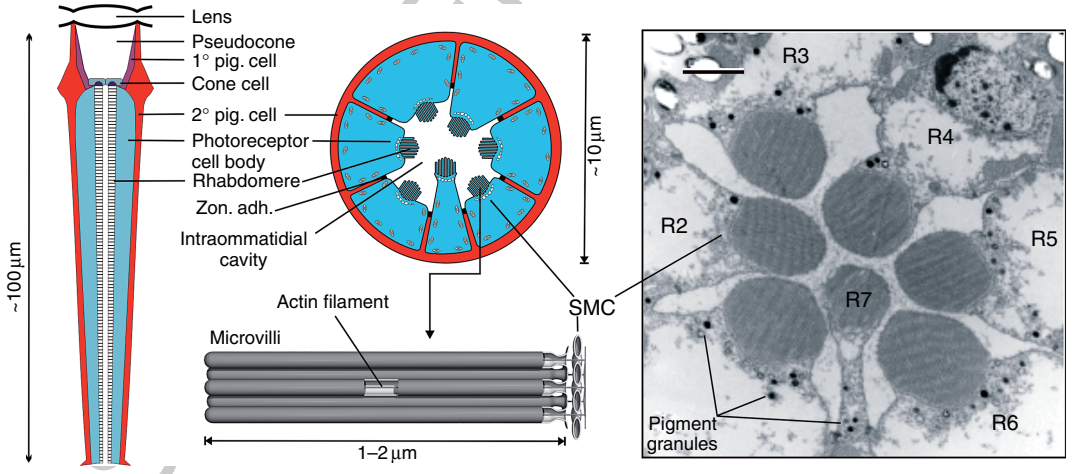

f0005 **Figure 1** Photoreceptor and retinal morphology in *Drosophila*. *Left*: Schematic of ommatidium showing the photoreceptors with the microvillar rhabdomeres, surrounded by secondary pigment cells. Light is focussed on the rhabdomere tips by the overlying lens through the pseudocone. The pseudocone is filled with fluid secreted by the underlying cone cells (Semper cells), and surrounded by primary pigment cells. The schematic cross section shows the hexagonal array of rhabdomeres, projecting into the intraommatidial cavity. The central photoreceptor is R7 (an ultraviolet (UV) receptor), the rest are R1–6 cells. The eighth photoreceptor R8, whose rhabdomere is contiguous with that of R7, lies proximally in the ommatidium. The photoreceptors are connected by specialized junctions, called zonula adherens, or desmosomes, which separate the apical (medial) membrane of the cell from the basolateral membrane. The detailed schematic (below) shows how the rhabdomere is formed from tightly packed microvilli, with a system of submicrovillar cisternae (SMC) lining their base. *Right*: The electron micrograph shows the six R1–6 cells with large rhabdomeres and the central R7 cell; pigment granules can be seen close to the base of the rhabdomeres (scale bar 1 μm).

thirds of the ommatidium, R8 in the proximal third). R7 and R8 cells have a variety of visual pigments (λ_{max} ~340, 370, 440, and 510 nm), which subserve the fly's color vision. As far as is known, the basic mechanism of phototransduction is the same in the different classes of photoreceptors, and apart from the rhodopsins, there appear to be no cell-specific isoforms of the various component of the transduction cascade as is the case in vertebrate rods and cones (see Yau, K-W., this volume). However, the majority of studies have been performed on the major class of photoreceptors, R1–6.

p0025 The rhabdomeres project toward the center of the ommatidium into a large extracellular space (the intraommatidial cavity), delimited by specialized junctions (desmosomes, or zonula adherens) between neighboring photoreceptors. Photoreceptors are derived from epithelial cells, and these junctions separate the apical (rhabdomere and stalks) membrane from the basolateral membrane, which forms the outer surface of the photoreceptor cluster (Figure 1). Unlike tight junctions, desmosomes do not represent a diffusion barrier between the intraommatidial cavity and the rest of the extracellular space (Chi, C. and Carlson, S. D., 1981). Completing the ommatidium are a number of accessory cells: four distal cone, or Semper cells, that form the floor of the fluid-filled transparent pseudocone, which forms the optical path between the rhabdomere tips and the facet lens; two primary pigment cells, which surround the distal ends of the photoreceptors and form the walls of the pseudocone, and 12 secondary and tertiary pigment cells, shared between ommatidia (Ready, D. F., 1989). Also referred to as pigmented glia, the pigment cells surround the photoreceptors, optically isolating the ommatidia over the depth of the retina. At the base of the retina, the R1–6 photoreceptors project short axons to the first neuropile (lamina), where they form histaminergic synapses with second-order cells, the large monopolar cells (Hardie, R. C., 1989; Sarthy, P.V., 1991). The microvilli contain no internal membranous structures; however, each contains a single central F-actin filament. With appropriate fixation, the actin filament can be seen to be connected to the microvillar membrane via sidearms (see Figure 6), which may be formed by the class III unconventional myosin NINAC (Kumar, J. P. and Ready, D. F., 1995; Hicks, J. L. *et al.*, 1996). Closely apposed (10 nm) to the base of the microvilli, is an array of submicrovillar cisternae (SMC), which are derived from smooth endoplasmic reticulum (ER). These have been considered to represent internal Ca^{2+} stores, and similar, more extensively developed structures in many arthropods (including bee and *Limulus*) mediate light-induced Ca^{2+} release (see Phototransduction Mechanisms in Other Invertebrates, reviewed in Nasi, E. *et al.*, 2000). However, in *Drosophila* and many other Diptera, the SMC are much reduced in size with a very narrow lumen and it is questionable whether they perform any significant role in the release of Ca^{2+} (Ca^{2+} Signals). They effectively form a fenestrated double-layered membranous curtain lining the bases of the microvilli and they may be more important as a site for PI recycling (Phosphoinositide Metabolism), and also perhaps as a diffusion barrier or baffle between the rhabdomere and the rest of the cell.

p0030 The cell body contains numerous ~0.1 μm pigment granules, which migrate toward the rhabdomere in response to light, functioning as a cell autonomous pupil. Since the rhabdomere acts as a waveguide, a significant fraction of the light actually travels outside its perimeter (evanescent wave). The pupil pigment granules can therefore effectively bleed light from the rhabdomere, thereby attenuating up to 90–99% (Roebroek, J. G. H. and Stavenga, D. G., 1990) of the incident light. The pupil also significantly improves spatial resolution by narrowing the acceptance angle, whilst causing a blue shift in the spectral sensitivity (Hardie, R. C., 1979; Stavenga, D. G., 2004). Pupil pigment migration, which is intensity dependent, occurs over a time course of ~5 s following onset of illumination. The exact mechanism remains obscure, but it is Ca^{2+} dependent (Kirschfeld, K. and Vogt, K., 1980), and since it can be readily monitored with optical techniques in the intact animal, it can be used as an *in vivo* measure of photoreceptor performance and Ca^{2+} signaling (e.g., Hofstee, C. A. and Stavenga, D. G., 1996).

p0035 The immediately obvious function of the rhabdomeric structure is to provide the light capturing waveguide required for maximizing absorption whilst preserving spatial sensitivity. The parallel arrays of microvilli also provide the rhabdomere with an intrinsic dichroism, which forms the basis for the ability of arthropods and mollusks to detect and discriminate polarized light (Wehner, R., 1989). In addition, the microvillar structure is also the key to understanding many aspects of the photoreceptors' performance (see Molecular Strategies of Quantum Bump Generation and Adaptation). All the major

components of the transduction cascade, from rhodopsin to the light-sensitive channels are localized in the microvillus, and it seems likely that the immediate effect of single-photon absorption is more or less limited to activation of enzymes and channels in the microvillus where it was absorbed. This extreme compartmentalization is crucial for the rapid kinetics of the response to light, as it minimizes diffusional delays, and also greatly increases the effective concentration of molecular components and metabolic intermediates in the transduction cascade (see Molecular Strategies of Quantum Bump Generation and Adaptation). For example, within the volume of one microvillus, just a single molecule represents a concentration of ~1 μM; whilst the average resting concentration of free Ca^{2+} (100–200 nM) would represent just one-quarter of a Ca^{2+} ion in solution at any one instant!

6.63.3 Electrophysiology

6.63.3.1 Invertebrate Photoreceptors Depolarize

p0040 Ever since the first photoreceptor intracellular recordings in the 1960s, it has been known that vertebrate photoreceptors hyperpolarize in response to light due to closing of cation channels, whilst invertebrates depolarize. Under many conditions, this difference may be of minor functional significance, since both types of photoreceptors signal via graded potentials and under most situations are responding to fluctuations of intensity (contrast) around a mean background. However, there are important implications under certain conditions, such as the ability to detect single photons. In rods, there are $\sim 10^4$ channels open in the dark, and a large number need to be closed to make significant difference. Thus, a typical quantum bump in a vertebrate rod represents the closing of ~200 channels, generating a response of ~1 pA (see Yau, K-W., this volume). By contrast, in microvillar photoreceptors the channels are closed in the dark, membrane resistance is at its highest, and only a few channels may need to be opened to generate a significant depolarization. Indeed, in *Drosophila* only ~15 channels are activated during a quantum bump (Henderson, S. R. *et al.*, 2000), generating a 10-pA current and a voltage response of ~1–2 mV in the intact eye (Wu, C. F. and Pak, W. L., 1978; Johnson, E. C. and Pak, W. L., 1986).

6.63.3.2 Voltage-Clamped Light-Induced Current

Because of their small size, intracellular recordings p0045
from *Drosophila* photoreceptors are technically challenging (see Other Channels and Transporters); however, it has also proved possible to record from single photoreceptors using whole-cell patch clamp techniques from dissociated ommatidia of both pupae and young adults. This preparation, developed independently in two laboratories (Hardie, R. C., 1991a; 1991b; Ranganathan, R. *et al.*, 1991), allows isolation of the light-induced current (LIC) with excellent recording quality, whereby responses to single photons, single G proteins, and even single channels can be clearly resolved. This preparation, in combination with the molecular genetic potential of *Drosophila*, has been particularly important for recent advances in our mechanistic and quantitative understanding of phototransduction.

In the dark, photoreceptors have a resting potential of ~−70 to −80 mV, which is close to the potassium equilibrium potential (−85 mV) under standard recording conditions. The cells have a high input resistance (~2 GΩ) and a large capacitance (~60 pF), the majority (>80%) of which can be attributed to the surface area of the microvillar membrane. This results in a slow membrane time constant (12 ms for the dark-adapted (DA) values above), but intracellular recordings in the intact animal suggest that the membrane properties do not compromise the temporal resolution of even DA responses in the voltage domain, and may even be advantageous in filtering out high-frequency noise (Juusola, M. and Hardie, R. C., 2001). p0050

An ongoing barrage of ~2-pA events at rates of 1–4 s^{-1} can be resolved in complete darkness (Figure 2), which is eliminated in mutants of the G protein α subunit and therefore probably represents activation of the cascade by spontaneous activation of single G proteins (Hardie, R. C. *et al.*, 2002). Recent evidence indicates that the rate is only kept this low by the presence of approximately twofold excess of G protein β subunits, and, the spontaneous dark noise is greatly increased in heterozygote mutations of Gβ when there are approximately equal numbers of β and α subunits (Elia, N. *et al.*, 2005). Much more rarely, random thermal rhodopsin isomerizations generate spontaneous quantum bumps at rates of less than 1 min^{-1} (Henderson, S. R. *et al.*, 2000). p0055

With dim illumination individual quantum bumps p0060
can be clearly resolved (Figure 2). Strict adherence to

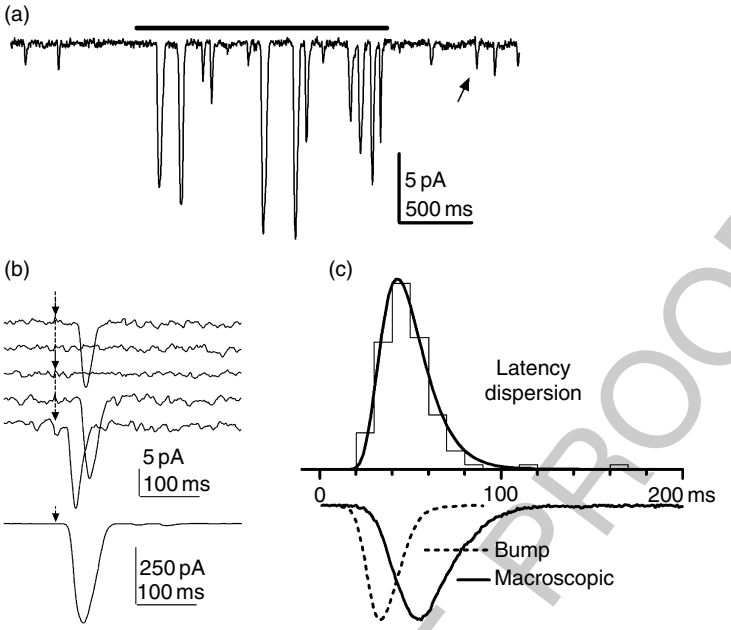

f0010 **Figure 2** Quantum bumps. (a) Response of a whole-cell voltage-clamped photoreceptor to 2 s of dim illumination (~2 effectively absorbed photons per second, bar). In the dark, small ~2-pA events (e.g., arrow) are likely to represent spontaneous activation of single G proteins. Light induces a train of ~10-pA quantum bumps. (b) Responses to brief (1 ms) flashes (arrows), containing on average 0.5 effective photons. Some flashes induce no response (failures), others induce single quantum bumps with a variable latency; below, the macroscopic response of the same cell to a flash containing ~100 photons is broader than the individual quantum bumps. (c) *Top*: latency distribution (histogram) of quantum bumps elicited by brief flashes (as in (b)); below, normalized waveforms of quantum bump and macroscopic response. The smooth curve in the top trace, obtained by mathematically deconvolving the two waveforms, is an excellent fit to the latency distribution, confirming that the waveform of the macroscopic response represents the convolution of the bump latency distribution and AU2 bump waveform. (Hardie unpublished data; for further details, see Henderson, S. R. *et al.*, 2000).

Poisson statistics, as well as frequency of seeing curves, indicate that these represent responses to single-photon absorptions (Wu, C. F. and Pak, W. L., 1975; Henderson, S. R. *et al.*, 2000). The quantum bumps have a mean amplitude of ~10 pA (range ~2–20 pA) representing the simultaneous opening of ~15 channels. This is consistent with the opening of channels in a single microvillus, which, according to quantitative biochemical estimates in the larger fly *Calliphora*, should contain about 25 channels (Huber, A. *et al.*, 1996a). Quantum bumps have a duration (halfwidth) of ~20 ms and are generated with a characteristically variable latency of between ~20 and 100 ms (mean ~40–50 ms). Consequently, the waveform of the macroscopic response to brief flashes represents the convolution of the bump waveform and its latency dispersion. Unlike the situation in rods, voltage-clamped quantum bumps sum linearly over a large range, and the macroscopic response to brief flashes containing up to at least several hundred photons can be accurately reconstructed from the linear superposition of the underlying bumps (Henderson, S. R. *et al.*, 2000). The essential kinetic description of the DA flash response is thus embodied in the bump waveform and its latency distribution (Figure 2).

With longer steps of light, the bumps fuse to form p0065 a noisy maintained inward current, and as the intensity increases there is an increasingly rapid transition from peak to plateau representing the onset of light adaptation. At higher intensities this overshoots giving rise to what is effectively a damped oscillation (Figure 3(d)). Peak responses can greatly exceed 20 nA, but are not accurately voltage-clamped, whilst the steady-state plateau saturates at ~500 pA. Increments of intensity superimposed upon maintained backgrounds elicit responses with the classic features of light adaptation (Figure 4): gain is decreased as a function of background intensity, whilst the kinetics are significantly accelerated. In the current (voltage-clamped) domain, the shift of the response along the intensity (I) axis with light adaptation can simply be described as multiplicative reduction in gain (Gu, Y. *et al.*, 2005); in the voltage

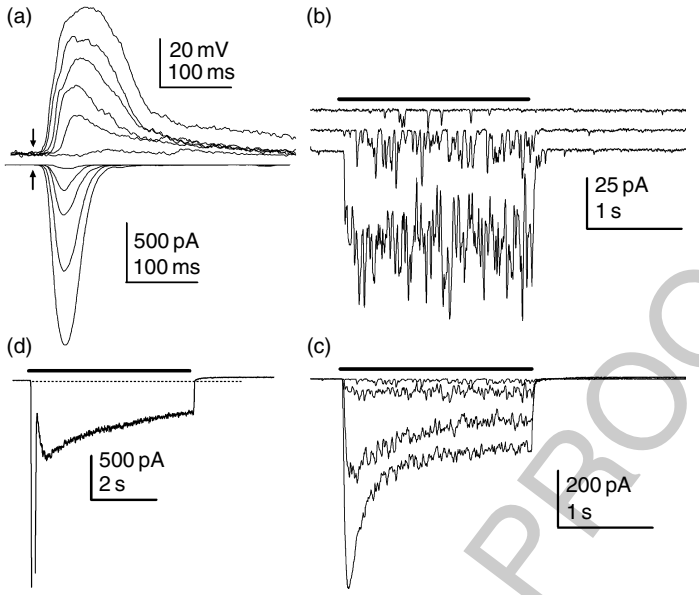

f0015 **Figure 3** Whole-cell recordings of light responses in *Drosophila* photoreceptors. (a) Lower traces: Voltage-clamped responses recorded by whole-cell patch clamp from a dissociated ommatidium to brief (1 ms) flashes of increasing intensity (~5 to ~500 effective photons): responses in this range scale linearly with intensity. Upper family of traces: voltage recordings in current clamp mode from the same cell. (b)–(c) Responses to 2-s steps of light of increasing intensity (note different scales in (b) and (c)): bumps fuse to form noisy inward currents, which then show an increasingly rapid peak–plateau transition as intensity increases ((b): 3, 30, and 300 photons per second; (c) 30, 300, 3000, and 18 000 photons per second). This transition is a direct manifestation of light adaptation. (d) Response to a bright stimulus (3×10^5 photons per second), approximating daylight intensities: the peak response (>10 nA and off-scale) rapidly adapts, generating a notch before reaching a plateau that then slowly relaxes to the final steady-state level. After light off, there is a small outward current due to the electrogenic Na^+/K^+ ATPase. (Hardie, R. C., unpublished data.)

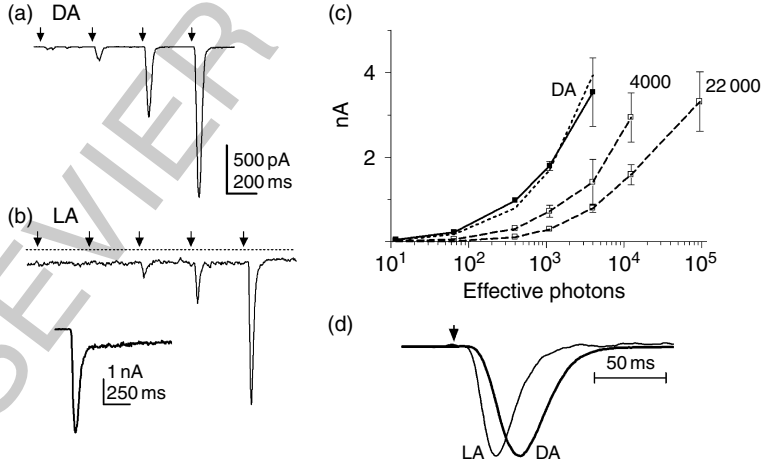

f0020 **Figure 4** Light adaptation. (a) and (b) Voltage-clamped responses to brief (1 ms) flashes of increasing intensity in the dark, and the same flashes superimposed on a maintained background of ~22 000 effectively absorbed photons per second, generating a plateau response of ~150 pA (dotted line shows zero current). Inset shows the onset of the adapting light. (c) Response intensity functions from recordings, similar to those shown in (a) and (b), in dark-adapted (DA) and light-adapted (LA) states (intensity in effective photons per second). The DA response intensity function is accurately reproduced by simple linear scaling of a LA response intensity function (dotted line), indicating that light adaptation at this level can be simply described by a multiplicative reduction in gain. (d) Normalized flash responses of DA and LA responses show the acceleration in kinetics typical of light adaptation. (Adapted from Gu, Y. *et al.*, 2005 with permission.)

domain, this translates into a more complex behavior (shifted $V/\log I$ functions, slope increasing with intensity) due to the passive and voltage-dependent properties of the membrane.

s0030 **6.63.3.3 Potassium Channels**

p0070 In the voltage domain, the overall response is further shaped by passive membrane properties, as well as a variety of voltage-sensitive conductances and electrogenic transporters. Dominant amongst these are at least four classes of potassium channels, which play important, though often subtle roles in shaping the voltage response.

(1) A very rapidly activating and inactivating A current, I_A, encoded by the prototypical voltage-gated K^+ channel gene, *Shaker* (Hardie, R. C., 1991a; Hardie, R. C. *et al.*, 1991). The voltage operating range of this current is more negative (V_{50}act $= -24$ mV) than for other reported *Shaker* currents, though it can be shifted to a more positive range by serotonin (Hevers, W. and Hardie, R. C., 1995). Modeling and intracellular recordings from photoreceptors in the intact animal suggest that the voltage dependence of the so-called window current, representing the overlap of the steady-state activation and removal from inactivation voltage dependences, can effectively amplify voltage signals and thus results in a significant improvement in the information capacity (Niven, J. E. *et al.*, 2003). The *Shaker* channels are densely expressed on the outer (basolateral) membrane of the photoreceptors and are almost always encountered at high density in cell-attached patch recordings (Hardie, R. C., 1991a).

AU3 (2) A slowly activating delayed rectifier, I_{Ks} (Hardie, R. C., 1991a), which is encoded by the *Shab* gene (Vahasoyrinki, M. *et al.*, 2006). Although generating similar sized currents to I_A, I_{Ks} channels are only very rarely encountered in cell-attached patch recordings, suggesting they have a different localization, possibly on the apical membrane. I_{Ks} has a more positive voltage operating range than I_A (V_{50} act $= \sim 0$ mV) and inactivates much more slowly with a time constant of ~ 1 s. This is the dominant maintained outward current at depolarized potentials, which would be predicted to counteract the depolarization and help prevent saturation. Interestingly, the *Shab* conductance is only expressed in R1–6, but not in R7 and R8 cells (Anderson, J. and Hardie, R. C., 1996).

(3) A fast delayed rectifier, I_{Kf} with intermediate kinetics (inactivation $\tau \sim 50$ ms) and a slightly more negative operating range than I_A. From its properties, I_{Kf} is most likely encoded by *Shal*. This conductance is found in R1–6, R7, and R8, but is not uniformly expressed, and is entirely lacking in some cells (Hardie, R. C., 1991a; Vahasoyrinki, M. *et al.*, 2006). One may speculate that it fine tunes the kinetics of the voltage output and may be expressed preferentially in certain eye regions with specific demands on temporal resolution.

(4) A very slowly activating and noninactivating K current which has been revealed in *Sh*;*Shab* double mutants (Vahasoyrinki, M. *et al.*, 2006).

p0075 In addition, the photoreceptors may express two classes of Ca^{2+}-activated K channels (*Slo* and *Sk*), and preliminary data using intracellular voltage recording in the intact animal suggest that mutants lacking these channels have subtle defects in their peak-to-plateau transition (Wolfram, V., 2004).

6.63.3.4 Other Channels and Transporters s0035

p0080 As well as K^+ channels, the photoreceptors also express a noninactivating voltage-gated Ca^{2+} conductance, which can be recorded in the cell body, but is presumably more important in synaptic release at the photoreceptor axon terminal (Hardie, R. C. and Mojet, M. H., 1995; Anderson, J. and Hardie, R. C., 1996). In addition, the photoreceptors exhibit inward rectification due to a hyperpolarization-activated chloride current (Hardie, R. C. and Minke, B., 1994b), recently characterized in detail by Ugarte G. *et al.* (2005), who suggest it is encoded by *clc-2*.

p0085 Finally, the photoreceptors express at least two electrogenic transporters:

(1) A Na^+/K^+ ATPase, which is expressed predominantly on the basolateral surface of the cell away from the rhabdomere (Yasuhara, J. C. *et al.*, 2000). It generates an outward current (or afterhyperpolarization in the voltage domain) following bright stimulation (e.g., Figure 3) and can make a significant contribution to the depolarized plateau potential level (Jansonius, N. M., 1990).

(2) An electrogenic Na^+/Ca^{2+} exchanger (*calx* gene), which is predominantly expressed in the microvillar membrane, and which can generate

currents of up to ~100 pA (Hardie, R. C., 1995; Wang, T. *et al.*, 2005b). Belonging to the NCX family (Schwarz, E. M. and Benzer, S., 1997), it represents the dominant mechanism of Ca^{2+} extrusion, and plays an essential role in clearing the Ca^{2+} influx associated with the light-sensitive current (Wang, T. *et al.*, 2005b) (see also Ca^{2+} Transients in the Rhabdomeres). A second, K^+-dependent Na^+/Ca^{2+} exchanger gene (NCKX) has also been reported to be expressed in the photoreceptors (Haug-Collet, K. *et al.*, 1999), but has not been detected electrophysiologically (Wang, T. *et al.*, 2005b).

s0040 ### 6.63.3.5 Intracellular Recordings of Voltage Responses

p0090 Intracellular recordings of photoreceptors in the intact animal are demanding, and values for resting potential, and input resistance may often be underestimated due to the shunt resistance introduced by electrode penetration. The best recordings report resistances of up to ~200–500 MΩ, and resting potentials of ~−70 mV (Juusola, M. and Hardie, R. C., 2001). Apart from the shunt resistance, the difference between these values and values recorded in dissociated cells may also reflect the contribution from the axon terminal, which is severed during the dissociation. Thus, recent evidence suggests there is a significant depolarizing synaptic feedback at the receptor terminal, and when synaptic transmission was blocked by warming the temperature-sensitive *shibire* mutation, the photoreceptors hyperpolarized by a further 10–15 mV (Zheng, L. *et al.*, 2006). Responses to brief flashes show broadly similar kinetics to the LIC, but are slightly faster in rise time with a more skewed waveform; quantum bumps of ~1–2 mV can be resolved with dim illumination (Wu, C. F. and Pak, W. L., 1975; 1978). As in most arthropod photoreceptors, saturating responses reach ~70 mV, close to the reversal potential of the light-sensitive channels, with a maintained plateau of ~30 mV above resting potential. $V/\log I$ curves are sigmoidal, covering 4–5 log units of intensity with a log-linear region of ~2 log units.

p0095 Photoreceptors in wild type (WT) flies light adapt and continue responding to contrast fluctuations up until at least 10^6 effectively absorbed photons per second, equivalent to vision under the brightest daylight conditions. Contrast sensitivity and temporal resolution improve with light adaptation, allowing transmission of signals up to ~100 Hz (3 dB cutoff at 25 Hz) with an information capacity of ~200 bits per second at 25 °C (Juusola, M. and Hardie, R. C., 2001).

s0045 ### 6.63.3.6 Electroretinogram

p0100 Extracellular electroretinogram (ERG) recordings can be made straightforwardly with an electrode placed on the surface of the cornea (Figure 5). The ERG represents the summed activity of all the photoreceptors, and also higher-order neurons and glial cells. The sustained corneal negative component

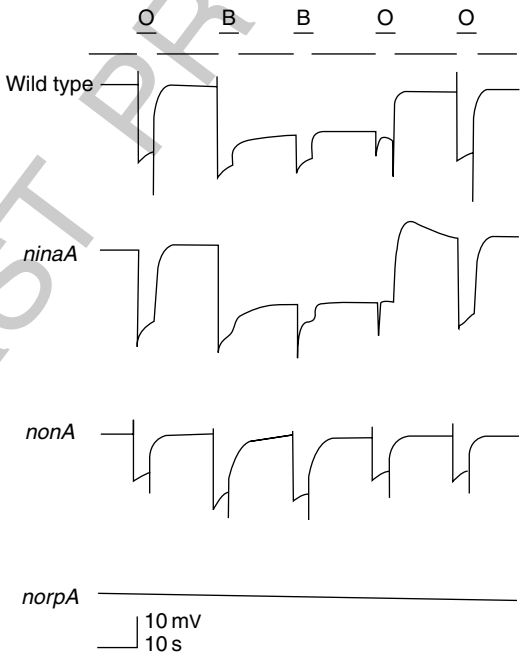

f0025 **Figure 5** Electroretinogram (ERG) recordings. In a wild-type (WT) fly a 5-s pulse of orange light elicits a typical ERG with on and off transients and a maintained corneal negative component. At light off, the potential returns rapidly to baseline; however, a blue stimulus which converts >50% of R to M, creates a prolonged depolarizing afterpotential (PDA), whilst a second blue test flash elicits a much reduced (inactivated) response lacking the transients, and which is primarily mediated by the R7 cells. A subsequent orange stimulus, which reconverts M to R, terminates the PDA and restores sensitivity. In the *no i*nactivation *no a*fterpotential mutant, *ninaA*, there is no PDA and no loss of sensitivity (inactivation) to the second blue test flash. This is the classical *nina* phenotype found in a variety of mutants that have low levels of rhodopsin (*ninaA* encodes a chaperone required for rhodopsin folding and targeting). The *nonA* mutant lacks the on and off transients, but is otherwise normal, suggesting a defect in synaptic transmission. The *norpA* mutant (encoding PLC) has no detectable response. (Reproduced with permission from Pak, W. L., 1995.)

of the response is maximally ~20–30 mV. It is normally attributed to the photoreceptors, although experiments using a perfused preparation suggest caution in interpretation, since with bright light, slow components in particular may become dominated by depolarization of the pigmented glia (secondary pigment cells) by the build up of extracellular K^+ (Minke, B., 1982; Minke, B. and Selinger, Z., 1992). Nevertheless, it reflects indirectly at least the photoreceptor response and has been widely used as an easily recorded measure of photoreceptor output. The ERG also has rapid on (positive) and off (negative) transients, which reflect the activity of the second-order interneurons (large monopolar cells or LMCs) which have an amplified and transient response of inverted polarity due to sign-inverting synapses using the photoreceptor neurotransmitter, histamine, which activates histamine-gated chloride channels on the LMCs (Hardie, R. C., 1989).

6.63.4 Molecular Components of the Phototransduction Cascade

6.63.4.1 Strategies for Gene Discovery

The discovery and characterization of the molecular components of the transduction cascades in vertebrates and invertebrates (Figures 6 and 7) exploited two very different approaches. In vertebrates the ability to isolate ROS *en masse*, particularly from bovine retina, greatly facilitated the purification, and subsequent molecular identification of the elements of the cascade (see Yau, K-W., this volume). In invertebrates, discovery relied in the first instance on classical forward genetic approaches in *Drosophila* to identify and positionally clones genes involved in phototransduction. The pioneers in this enterprise, starting in the late 1960s were Seymour Benzer (Hotta, Y. and Benzer, S., 1970) and Bill Pak (Pak, W. L. *et al.*, 1970). Benzer had a wider agenda, wanting to identify genes involved in vision generally, and thus isolated behavioral mutants defective in phototaxis. Pak was more focussed on the early events in vision and embarked upon a labor intensive, but ultimately rewarding electrophysiological screen to detect subtle defects using the readily recorded ERG.

At least 50 different complementation groups representing distinct genes were isolated. Some 30 of these had defects in the ERG transients and represent genes involved in synaptic transmission or responses of second-order neurons. Most of the remainder has turned out to be photoreceptor genes, many of which are directly involved in the transduction cascade (Table 1, reviewed in: Pak, W. L., 1995; Pak, W. L. and Leung, H. T., 2003). A number of important genes were not discovered in these early screens, but were identified by molecular approaches, such as subtractive hybridization and/or homology to vertebrate genes. Mutants of several these, including arrestin (Dolph, P. J. *et al.*, 1993), G protein (Scott, K. *et al.*, 1995), and the TRPL light-sensitive channels (Niemeyer, B. A. *et al.*, 1996), were generated in a second wave of mutagenesis based on antigenicity, i.e., using antibodies to screen for mutants generated by random chemical mutagenesis lacking the proteins in question (see also Koundakjian, E. J. *et al.*, 2004).

6.63.4.2 Rhodopsin

The *no inactivation no afterpotential* E (*ninaE*) mutant was isolated by Pak and coworkers using the ERG screen (Figure 5). Even before it was cloned, it was implicated as the gene encoding rhodopsin in R1–6 (Rh1) since it affected the visual pigment concentration in a gene dosage-dependent manner (Scavarda, N. J. *et al.*, 1983). It was cloned and sequenced a couple of years after vertebrate rhodopsin (O'Tousa, J. E. *et al.*, 1985), itself the first member of the G protein-coupled receptor (GPCR) family, with the now classical seven transmembrane helix structure (Figure 7). Rh1 (*ninaE*) shares ~36% identity with bovine rhodopsin, including the lysine in the seventh transmembrane helix, which forms the covalent Schiff base linkage with the chromophore, and potential phosphorylation sites near the C-terminal. Six further genes with a similar *nina* mutant ERG phenotype are involved either in rhodopsin trafficking (*ninaA, calnexin* (Baker, E. K. *et al.*, 1994; Rosenbaum, E. E. *et al.*, 2006), or chromophore production (*ninaB*, *ninaD*, *ninaG*, and *pinta*, see below). An additional five *Drosophila* opsin genes, identified by homology to Rh1, account for the visual pigments of the ocelli (Rh2) and the various spectral classes of R7 (Rh3 and Rh4), and R8 (Rh5 and Rh6) (Feiler, R. *et al.*, 1992; Salcedo, E. *et al.*, 1999).

More than 60 invertebrate opsin genes have been cloned in the meantime (reviewed in Gärtner, W., 2000), and although recognizable as such they form a distinct subfamily from the majority of vertebrate opsins. An intriguing exception is melanopsin (Provencio, I. *et al.*, 1998), which appears to belong within the invertebrate opsin family, but is a vertebrate opsin found in a recently discovered novel class

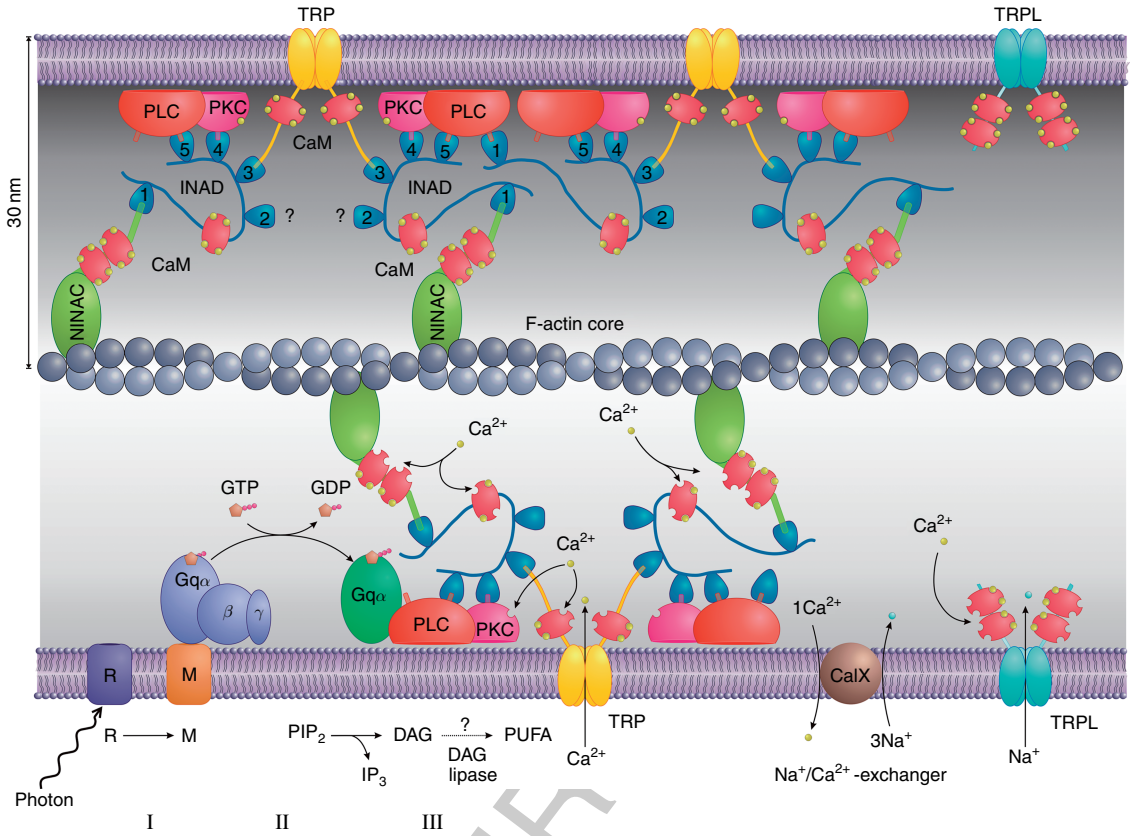

f0030 **Figure 6** Overview of the phototransduction cascade in *Drosophila*. *Lower half*: (I) Photoisomerization of rhodopsin (R, encoded by *ninaE* gene) to metarhodopsin (M) activates G_q via GTP–GDP exchange, releasing the $G_q\alpha$ subunit (*Gαq* gene); (II) $G_q\alpha$ activates phospholipase C (PLC, *norpA* gene), generating $InsP_3$ and DAG from PIP_2. DAG is also a potential precursor for polyunsaturated fatty acids (PUFAs) via DAG lipase; although PUFAs can activate the channels, there is no direct evidence for this enzyme in the cascade. (III) Two classes of light-sensitive channels (*trp* and *trpl* genes) are activated by an unknown mechanism. TRP is primarily Ca^{2+} permeable; Ca^{2+} influx feeds back at multiple sites, including calmodulin (CaM), which itself has multiple targets, and PKC (see Ca^{2+}-Dependent Feedback and Mechanisms of Adaptation, Table 3). Ca^{2+} is extruded by the CalX Na^+/Ca^{2+} exchanger. All components drawn approximately to scale within a schematic microvillus. *Upper half*: Several components of the cascade, including TRP, protein kinase C (PKC, *inaC* gene), and PLC are assembled into a signaling complex by the scaffolding protein, INAD, which may be linked to the F-actin core via the NINAC class II myosin. The INAD protein contains five PDZ domains (1–5) joined by short linker regions. Each PDZ domain associates preferentially with different targets (Huber, A. *et al.*, 1996a; Shieh, B. H. and Zhu, M. Y., 1996; Chevesich, J. *et al.*, 1997; Tsunoda, S. *et al.*, 1997; Xu, X. Z. S. *et al.*, 1998). The precise composition of the native complex is uncertain as some PDZ domains are reported to bind at least two different targets, and there are several possibilities for multimerization: by homophilic interactions between INAD (PDZ domains 3 and 4) (Xu, X. Z. S. *et al.*, 1998); involvement of up to four TRP subunits and linkage of two INAD molecules via PLCβ which is reported to bind both PDZ1 and PDZ5 (van Huizen, R. *et al.*, 1998). Several of these scenarios are depicted in the figure. CaM binds to the linker region between PDZ1 and PDZ2 (Xu, X. Z. S. *et al.*, 1998) and also to NINAC, TRP, and TRPL.

of intrinsically photosensitive retinal ganglion cells (ipRGCs). Melanopsin mediates a range of nonvisual responses such as circadian entrainment and the pupillary response (reviewed in Fu, Y. *et al.*, 2005) (see Yau, K-W., this volume). The ipRGCs also respond to light by depolarization, and at least in heterologous expression systems, melanopsin has been found to activate a G_q/PLC/TRP cascade as in invertebrates (Melyan, Z. *et al.*, 2005; Panda, S. *et al.*, 2005; Qiu, X. *et al.*, 2005).

6.63.4.2.1 Chromophore

s0065

Unusually, the chromophore of *Drosophila* opsin, as in most Diptera and a few other insect orders, is not retinal but a hydroxylated derivative, 11-*cis* 3-hydroxy retinal (Figure 8 (Vogt, K. and Kirschfeld,

p0125

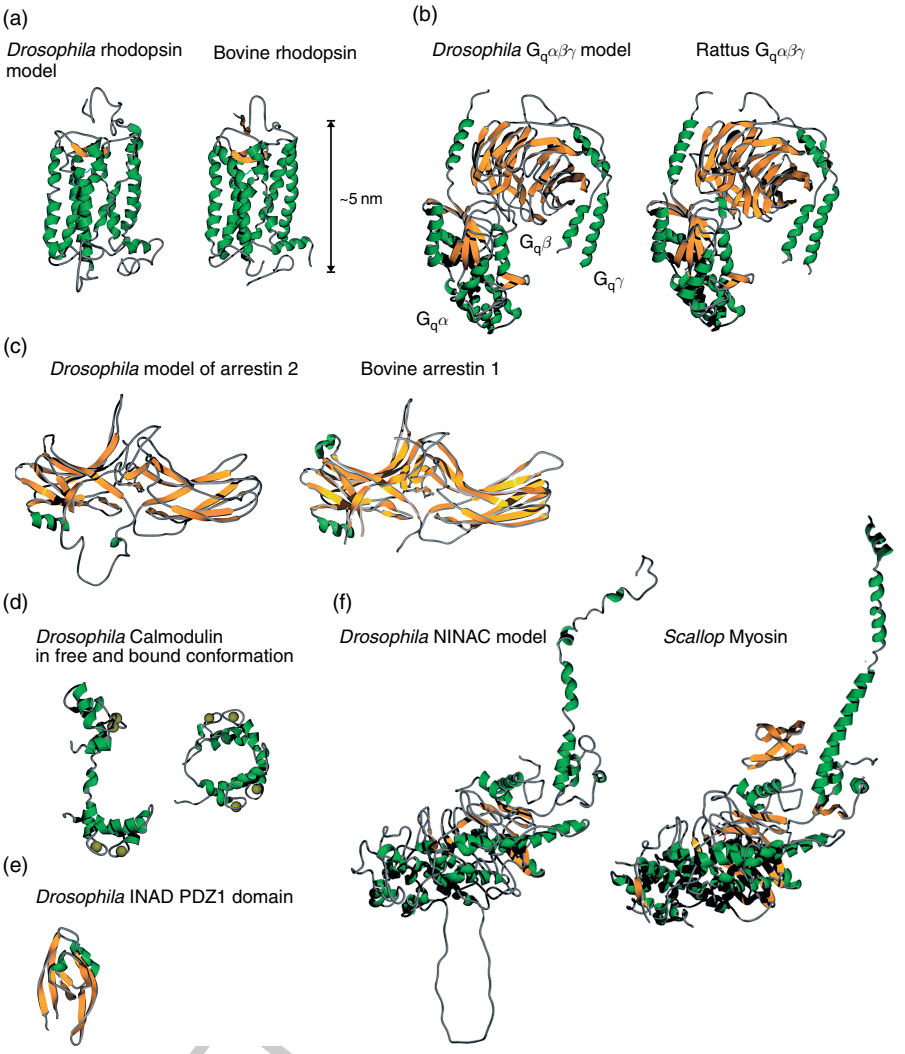

f0035 **Figure 7** Molecular models of some key transduction proteins. Modeled protein structures of several proteins involved in fly phototransduction based on solved crystal structures of homologous proteins. (a) The solved structure of bovine rhodopsin (left structure, 1F88) was used to model *Drosophila* Rhodopsin (*ninaE*). (b) Vertebrate (*Rattus*, 1GP2) G_q was used to model the structure of *Drosophila* G_q. (c) Bovine arrestin 1 (1G4R) was used to model the structure of *Drosophila* arrestin 2. (d) Structure of free and α-helix-bound *Drosophila* CaM (4CLN, 2BBN). (e) Structure of the first PDZ domain (PDZ1, 1IHJ) of *Drosophila* INAD, the other four PDZ domains have similar sizes (1IHJ) (f) Structure of single-headed scallop myosin (1B7T) used to model *Drosophila* NINAC. The models were generated using Geno3D: http://geno3d-pbil.ibcp.fr/ (Geourjon, C. *et al.*, 2001; Combet, C. *et al.*, 2002). References: 1F88 (Palczewski, K. *et al.*, 2000); 1GP2 (Wall, M. A. *et al.*, 1995); 1G4R (Han, M. *et al.*, 2001); 1B7T (Houdusse, A. *et al.*, 1999); 4CLN (Taylor, D. A. *et al.*, 1991); 2BBN (Ikura, M. *et al.*, 1992); 1IHJ (Kimple, M. E. *et al.*, 2001).

K., 1984)). Whilst this appears to function in an essentially identical manner to the more conventional 11-*cis* retinal, Diptera are remarkable in also using a second chromophore, 3-hydroxy retinol, that functions as a sensitizing or antenna pigment (Kirschfeld, K. and Franceschini, N., 1977). The sensitizing pigment has a characteristic three-fingered absorption peak in the ultraviolet (peaks at ~330, 350, and 370 nm). It transfers the energy of an absorbed photon by fluorescence resonance energy transfer (FRET) to the chromophore proper, which then photoisomerizes exactly as if it had absorbed the photon directly (Kirschfeld, K. *et al.*, 1983). This rare biological example of FRET enhances quantum catch by extending the spectral sensitivity of the photoreceptors into the ultraviolet (Figure 8).

t0005 **Table 1** List of mutants of genes involved in *Drosophila* phototransduction, all of which have been cloned and sequenced

Mutant	*Protein*	*Function*
Excitation		
Gαq	G_q α subunit	Heterotrimeric G protein
Gβe	G_q β subunit	Heterotrimeric G protein
InaD	PDZ domain scaffolding protein	Signalplex scaffold
inaF	Novel	Required for TRP function
ninaE	Rhodopsin (Rh1)	Visual pigment
norpA	Phospholipase Cβ	Key effector enzyme
trp	TRP channel	Light-sensitive channel
trpl	TRPL channel	Light-sensitive channel
Deactivation and adaptation		
arr1	39-kDa arrestin1	Rhodopsin endocytosis
arr2	49-kDa arrestin 2	Rhodopsin deactivation
Cam	Calmodulin	Ca^{2+}-dependent inactivation and Ca^{2+} buffer
inaC	Protein kinase C	Ca^{2+}-dependent inactivation
ninaC	Class III myosin kinase	CaM binding, response inactivation
rdgA	DAG kinase	Response termination, PIP_2 recycling
Phosphoinositide turnover		
cds	CDP–DAG synthase	PIP_2 recycling
laza	Lipid phosphate phosphohydrolase	DAG production from PA
rdgB	PITP	PIP_2 recycling
Calcium homeostasis		
calnexin	Calnexin	Rh1 chaperone and Ca^{2+} buffer
calphotin	Ca^{2+}-binding protein	Ca^{2+} buffer
calx	Na^+/Ca^{2+} exchanger	Ca^{2+} extrusion
Rhodopsin and chromophore biogenesis and pigment cycle		
ninaA	Peptidyl-prolyl *cis–trans* isomerase (cyclophilin)	Rh1 chaperone
ninaB	Dioxygenase	Chromophore synthesis
ninaD	Class B scavenger receptor	Chromophore synthesis (carotenoid uptake)
ninaG	Oxidoreductase	Chromophore synthesis
pintA	Retinoid-binding protein	Vitamin A uptake into pigment cells
rdgC	Rhodopsin phosphatase	Rhodopsin dephosphorylation
GPRK1	Rhodopsin kinase	Rhodopsin phosphorylation

Mutant genes have been classified according to their major function – excitation, deactivation, PI turnover, Ca^{2+} homeostasis, and visual pigment cycle and biogenesis (not mutually exclusive, though each gene listed only once). References in text.

p0130 Recent biochemical and mutant analysis has identified several key genes required for chromophore production, including a class B scavenger receptor (*ninaD*), required for cellular uptake of dietary carotenoids (Kiefer, C. *et al.*, 2002), and a dioxygenase (*ninaB*), which cleaves the 40C carotenoids into the 20C chromophore precursor, vitamin A (all-*trans* retinol) (von Lintig, J. and Vogt, K., 2000; von Lintig, J. *et al.*, 2001). Whilst these stages take place outside the retina (Gu, G. *et al.*, 2004), uptake of vitamin A into the retina probably occurs first in the pigment cells, with the essential involvement of a recently identified retinal-binding protein, PINTA (Wang, T. and Montell, C., 2005). Finally, oxidization of the retinal ring to generate the hydroxylated 3-hydroxy retinal appears to take place in the photoreceptors via an oxidoreductase encoded by the recently discovered *ninaG* gene (Sarfare, S. *et al.*, 2005).

6.63.4.2.2 Invertebrate rhodopsins are bistable

s0070

p0135 Although *de novo* biosynthesis of chromophore from carotenoids is relatively complex, chromophore recycling following photoisomerization is much simpler than in vertebrates. Most invertebrate rhodopsins represent bistable, photointerconvertible pigment systems, whereby all-*trans* retinal can be directly reconverted to 11-*cis* by absorption of a second photon whilst still attached to the opsin. *Drosophila* Rh1, which has been extensively studied, absorbs maximally in the blue–green (480 nm), and

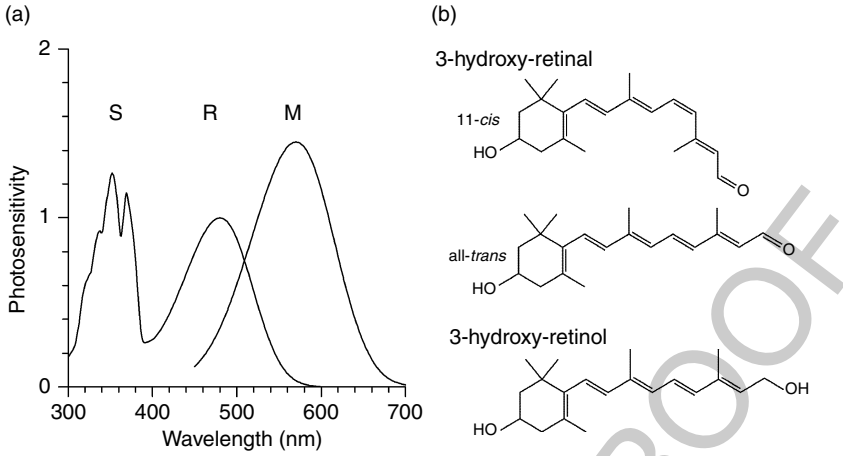

f0040 **Figure 8** Chromophores and absorption spectra. *Left*: Idealized photosensitivity spectra of the Rh1 pigment system in *Drosophila* R1–6 cells, normalized to the rhodopsin (R) peak. Responses in the UV (300–400 nm) are primarily mediated by absorption of the sensitizing pigment (S: 3-hydroxy retinol), which transfers the energy of absorption to the chromophore proper (11-*cis* 3-hydryoxy retinal), which absorbs maximally at 480 nm in Rh1. Photoisomerization to all-*trans* 3-hydroxy retinal converts R to metarhodopsin (M), which absorbs maximally at 570 nm. The sensitizing pigment can also transfer energy to M, which is thus also effectively photoisomerized by UV light (not shown). Spectra based on rhodopsin nomograms (Govardovskii, V. I. *et al.*, 2000), combined with estimates of the sensitizing pigment spectrum. Right: Chemical structures of the chromophores of R and M (11-*cis* and all-*trans* 3-hydroxy retinal) and the sensitizing pigment (3-hydroxy retinol).

on absorption of a photon, the 11-*cis* to all-*trans* isomerization leads to generation of a metarhodopsin (M) absorbing maximally at 570 nm (Figure 8). Metarhodopsin is thermostable, but can be photoisomerized back to the rhodopsin state (R) by absorption of further photon. Such a bistable pigment system reaches a photoequilibrium determined by the spectral content of the illuminating light and the absorption spectra of the R and M states (reviewed in Hillman, P. *et al.*, 1983; Hardie, R. C., 1985; Stavenga, D. G., 1996). It is no coincidence that the screening pigments in the eye are transparent to long-wavelength (red) light – hence the red eye color of most flies – and the red light diffusing through the eye reconverts M, ensuring that there is always a high fraction of R (reviewed in Hardie, R. C., 1986). Compared to the complex chromophore recycling of the vertebrate retina, this would appear to represent a much more efficient, rapid, and economical mechanism for pigment regeneration.

p0140 Under experimental conditions, however, particularly with white-eyed mutants lacking the screening pigments, or in biochemical preparations of purified photoreceptor membranes, it is possible to generate essentially any photoequilibrium simply by adjusting the wavelength of illumination. With blue light, which favors R → M conversion, up to ~80% of the pigment can be converted to the M form (it is not possible to create more than this as both R and M have second, overlapping photosensitivity peaks at short wavelengths due to β absorption peaks and sensitizing pigment). When flashes are delivered that result in more than ~20% of the pigment being converted to M, the photoreceptors develop a prolonged depolarizing afterpotential (PDA), that can last for several hours (Figure 5). This is because thermostable M remains active and capable of exciting the phototransduction cascade until it is inactivated by binding to arrestin (see Arrestins Terminate Active Metarhodopsin below). The photoreceptors contain only one arrestin molecule for every five rhodopsins, and thus, once more than 20% of the pigment exists in the M state, all arrestin is bound to M, and any further M molecules generated can no longer be inactivated. Although the PDA may last for several hours in *Drosophila*, it can be terminated at any time simply by delivering a bright long-wavelength (e.g., orange/red) flash, which inactivates M by reconverting it to R (Figures 5 and 9).

6.63.4.3 Visual Pigment Cycle s0075

6.63.4.3.1 Arrestins terminate active metarhodopsin s0080

p0145 Arrestins are small soluble cytosolic proteins implicated in response termination and trafficking of most

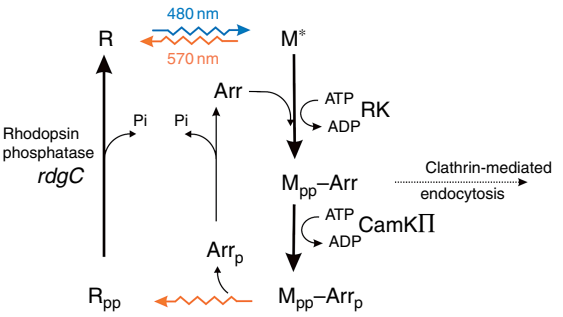

f0045 **Figure 9** Visual pigment cycle in *Drosophila*. Photoisomerization of rhodopsin (R) by blue light (480 nm) generates active metarhodopsin (M^*). M^* is thermostable and continues to activate G_q until it binds arrestin (Arr). Arr2 is the dominant arrestin, but Arr1 can perform this function more slowly in its absence. M is also multiplely phosphorylated by rhodopsin kinase (RK), but this is not required for Arr2 binding and may even occur after Arr2 binding (Plangger, A. *et al.*, 1994). The M_{pp}–Arr state is a target for clathrin-mediated endocytosis, but this is inhibited by the CaMKII-dependent phosphorylation of Arr2 (Alloway, P. G. *et al.*, 2000; Kiselev, A. *et al.*, 2000b). Reconversion of M_{pp} to R_{pp} leads to the release of Arr_p. Finally, R_{pp} is dephosphorylated by the CaCaM-dependent rhodopsin phosphatase (encoded by *rdgC*) to recreate the ground state, R (Byk, T. *et al.*, 1993; Lee, S. J. and Montell, C., 2001).

G protein-coupled receptors. *Drosophila* photoreceptors express two arrestin isoforms: a 39 kDa protein (Arr1, originally called phosrestin 2) and 49 kDa Arr2 (or phosrestin 1). Arr2 is approximately fivefold more abundantly expressed than Arr1, and apart from Rh1 is the most abundant protein in the retina. As such, it was the only element of the cascade to be sequenced by protein purification and microsequencing (Yamada, T. *et al.*, 1990), whilst Arr1 was cloned by a subtractive hybridization strategy (Hyde, D. R. *et al.*, 1990). Both share ~40% identity with human arrestin, showing closer similarity to β-arrestins than the vertebrate visual arrestins (Figure 7). Mutants of both *arr1* and *arr2* genes were isolated by screening for loss of protein in Western blots (Dolph, P. J. *et al.*, 1993). As expected from its abundance, Arr2 is dominant with respect to inactivation of M. Thus *arr1* mutants have no overt physiological phenotype, though they undergo light-independent degeneration (Satoh, A. K. and Ready, D. F., 2005). By contrast, *arr2* mutants have a pronounced deactivation defect, with responses to brief flashes decaying slowly over 1–2 s (Figure 10). *arr2* mutants also enter a PDA state with much lower levels of illumination

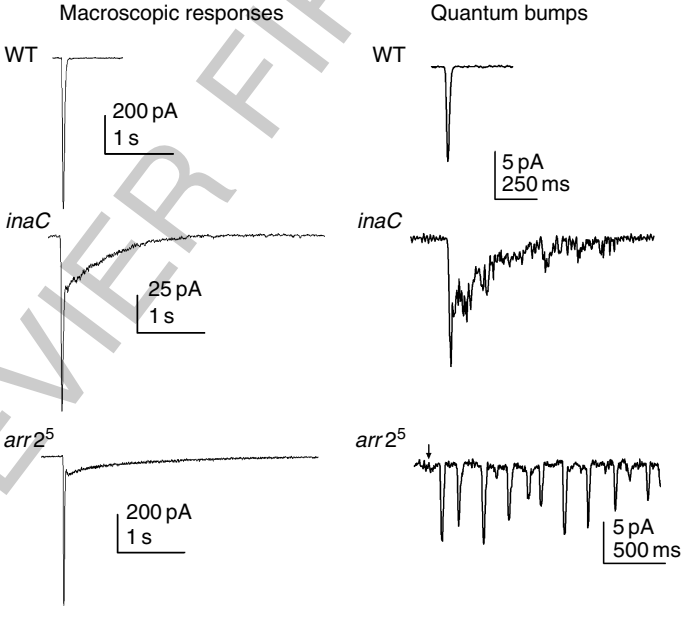

f0050 **Figure 10** Responses in inactivation mutants. *Left*: Whole-cell voltage-clamped responses to brief (1 ms) flashes of light in wild type (WT) and two mutants (*inaC* and $arr2^5$) with defects in inactivation. *Right*: quantum bumps elicited by single-photon absorptions in the same mutants. Macroscopically, both *inaC* and *arr2* mutants show a similar inactivation defect, with responses decaying over a period of 1–2 s. In the PKC mutant *inaC*, this defect is recapitulated in the bump waveform, and is due to a defect late in the transduction cascade (failure to inactivate PLC and the channels); however, in the arrestin 2 mutant ($arr2^5$) the defect manifests itself as a train of multiple bumps in response to a single absorbed photon, and represents a failure to terminate the activity of active metarhodopsin. (Hardie, R. C., unpublished data; see also Hardie, R. C. *et al.*, 1993; Scott, K. *et al.*, 1997; Gu, Y. *et al.*, 2005.)

(Dolph, P. J. *et al.*, 1993). Although these phenotypes indicate that Arr2 binding to M is the dominant mechanism of M inactivation, Arr1 is also capable of binding to and inactivating M, since response deactivation in *arr1*;*arr2* double mutants lacking both arrestin isoforms is at least 10× slower than in *arr2* alone (Dolph, P. J. *et al.*, 1993). A recent study indicates that Arr1 also has a dedicated role in light-induced Rh1 endocytosis, a generic mechanism of receptor turnover found in most G protein-coupled signaling cascades required for receptor turnover and cell maintenance (Satoh, A. K. and Ready, D. F., 2005).

s0085 #### 6.63.4.3.2 Arrestin translocation

p0150 Light-induced translocation of components of the transduction cascade in both vertebrates and invertebrates has recently been appreciated as an important and widespread phenomenon, likely to be involved in long-term light and dark adaptation (reviewed in: Arshavsky, V. Y., 2003; Frechter, S. and Minke, B., 2006). In *Drosophila*, both arrestins, along with the G protein and the TRPL channel, have been reported to translocate in response to illumination. In DA cells most Arr2 is distributed throughout the cytosol, with only ~30% immunolocalized in the rhabdomeres, whilst Arr1 is only detectable in the cytosol; however, within 5 min of illumination by white or blue light, both Arr2 and Arr1 are predominantly localized in the rhabdomere (Lee, S. J. *et al.*, 2003; Satoh, A. K. and Ready, D. F., 2005). Arr2 remains in the rhabdomere during illumination, returning slowly (within 3 h) to the cytosol in the dark (Figure 11). The translocation of Arr2 into the rhabdomeres appears to have physiological consequences, as the ERG response to bright stimuli terminated more quickly in flies that had been preexposed to light to stimulate translocation (Lee, S. J. *et al.*, 2003). Arr1 translocation is more dynamic and transient, and even in continuous illumination Arr1 retreats from the rhabdomere within 30 min and is then found internalized in vesicles in association with Rh1 (Figure 11), indicative of a role in physiological Rh1 endocytosis (Satoh, A. K. and Ready, D. F., 2005).

p0155 Lee S. J. *et al.* (2003) found that Arr2 binds to PIP_3 *in vitro* (and less avidly to PIP_2), and that translocation was disrupted by neutralization of three basic residues in Arr2 required for this interaction (lysines 228, 231, and 257), or by genetic manipulation of PIP_3 metabolism. Lee S. J. and Montell C. (2004) also reported that translocation was disrupted in *ninaC* mutants (see Myosin Kinase NINAC) and proposed a model whereby Arr2 is transported by a NINAC myosin motor in PIP_3-enriched vesicles. However, a more recent study found that translocation of both Arr1 and Arr2 was unaffected by the *ninaC* mutation calling aspects of this model into question (Satoh, A. K. and Ready, D. F., 2005).

6.63.4.3.3 Rhodopsin kinase and phosphatase

s0090

p0160 In vertebrate rods, metarhodopsin inactivation is a two-stage process, whereby M must first be phosphorylated by a rhodopsin kinase (RK) before

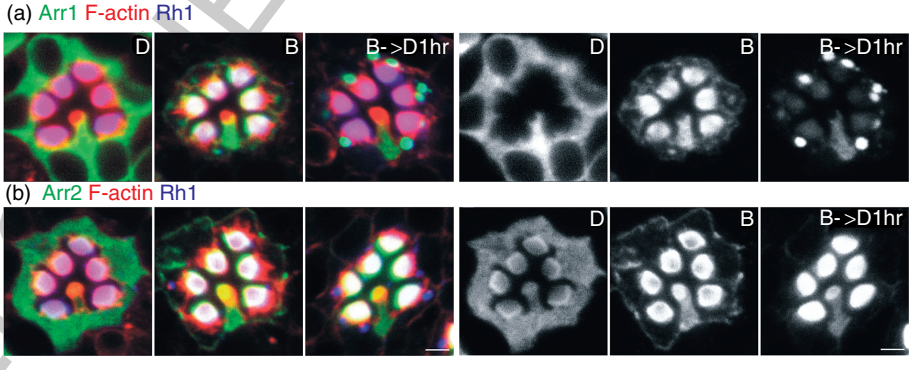

f0055 **Figure 11** Translocation of arrestin. Immunostaining of Arr1 and Arr2 (green) in dark-adapted (D) retina, 5 min after illumination for 2 min by bright blue light (B), and 1 h after the same blue illumination (B > D 1 h). Sections are also stained for Rh1 (blue) and actin (red). The black and white image shows just the arrestin antibody staining. In the dark, all Arr1 is localized in the cytosol, whilst Arr2 is found in both cytosol and rhabdomere. Five minutes after illumination, both arrestins are found almost exclusively in the rhabdomeres. One hour later in the dark, Arr2 remains bound in the rhabdomeres, but Arr1 is now found predominantly in vesicles in the cell body, which also stain positive for Rh1. (Images courtesy of Akiko Satoh and Don Ready, unpublished; see also Satoh, A. K. and Ready, D. F., 2005 for further details.)

arrestin can bind and complete the inactivation (see Yau, K-W., this volume). Unexpectedly, although fly rhodopsin is also multiplely phosphorylated at several serine residues in the C-terminal (Bentrop, J. and Paulsen, R., 1986; Byk, T. *et al.*, 1993), this appears not to be required for arrestin binding (Figure 9). Thus, transgenic flies in which the rhodopsin is replaced by a truncated version lacking the serine residues ($ninaE^{\Delta 356}$), or by a construct in which the serines have been individually mutated to alanine, show responses apparently normal in every respect including bump amplitude and waveform (Hardie, R. C., unpublished) and response inactivation (Vinos, J. *et al.*, 1997). The mutant Rh1 constructs also still bind Arr2 in biochemical assays (Kiselev, A. *et al.*, 2000a). Recently, Satoh A. K. and Ready. D. F. (2005) reported that translocation of Arr1 and subsequent endocytosis of Arr1–Rh1 complexes was suppressed in these Rh1 phosphorylation mutants, suggesting that Rh1 phosphorylation may be specifically important for Rh1 binding to Arr1 (and/or its subsequent endocytosis) rather than Arr2.

p0165 A *Drosophila* G protein-coupled receptor kinase (GPRK1) with homology to β-adrenergic receptor kinases has recently emerged as a strong candidate for RK. It is highly expressed in the photoreceptors where it associates with and phosphorylates rhodopsin (Lee, S. J. *et al.*, 2004). Interestingly, mutant flies expressing lower levels of GPRK1 had a significantly larger ERG responses, but without obvious response termination defects. Although responses were not measured at the single-cell level, at first sight this seems inconsistent with the lack of effect of the Rh1 phosphorylation site mutants on the response, which indicates that GPRK1 may also have a protein kinase-independent function.

p0170 After photoreisomerization from M to R, Arr2 is released from R, which must then be dephosphorylated before it can be used again (Figure 9). Dephosphorylation, which only takes place after Arr2 has been released, is mediated by a Ca^{2+} calmodulin (CaCaM)-dependent rhodopsin phosphatase encoded by the retinal degeneration C (*rdgC*) gene (Steele, F. R. *et al.*, 1992; Byk, T. *et al.*, 1993; Vinos, J. *et al.*, 1997; Lee, S. J. and Montell, C., 2001). *rdgC* mutants have a slow deactivation phenotype, but this may reflect a secondary defect, e.g., in Arr2 function, and is unlikely to be an immediate and direct consequence of the failure to dephosphorylate R, since by this stage in the rhodopsin cycle, the active M form should already have been inactivated by arrestin binding (Vinos, J. *et al.*, 1997). The original and most obvious phenotype of *rdgC* mutants, namely the severe light-dependent retinal degeneration, is suppressed by the truncated Rh1 phosphorylation site mutant $ninaE^{\Delta 356}$, and also by *arr2* mutations, suggesting that the accumulation of hyperphosphorylated M–Arr2 complexes may act as a trigger for apoptosis (Vinos, J. *et al.*, 1997; Kiselev, A. *et al.*, 2000a).

6.63.4.3.4 Arrestin phosphorylation

s0095

p0175 Both arrestin isoforms are themselves also phosphorylated in a light-dependent manner, and in fact Arr2 is the major phosphoprotein revealed in proteomic analysis (Matsumoto, H. and Pak, W. L., 1984). It is also the most rapidly detectable phosphorylated protein in the eye, being phosphorylated by calmodulin-dependent kinase II (CaMKII) at a single serine residue (Ser^{366}) on a subsecond timescale following illumination (Matsumoto, H. and Pak, W. L., 1984; Matsumoto, H. *et al.*, 1994). Although it was originally speculated that CaMKII-dependent phosphorylation of Arr2 may be a necessary first step in the binding of arrestin to M, this seems not to be the case. Arr2 phosphorylation is prevented by mutating Ser^{366} to alanine ($Arr2^{S366A}$) or in the $arr2^{1}$ allele, in which the protein is truncated prior to this site (Alloway, P. G. and Dolph, P. J., 1999). However, Arr2 still binds normally to M in either of these mutants. The defect appears rather to be in the subsequent dissociation of Arr2 from rhodopsin after reconversion to R (Figure 9). Thus normally, Arr2 dissociates rapidly from M after it has been reconverted to R by long-wavelength light, but remains bound in $Arr2^{S366A}$ or $arr2^{1}$ (Alloway, P. G. and Dolph, P. J., 1999). Related to this, the phosphorylation also controls the subsequent trafficking of M–Arr2 complex, which become internalized by clathrin-mediated endocytosis if Arr2 fails to be phosphorylated (Kiselev, A. *et al.*, 2000a). This has the consequence that following light exposure, the nonphosphorylated mutant Arr2 becomes sequestered in stable complexes with phosphorylated rhodopsin, again triggering apoptosis and retinal degeneration. Before the onset of degeneration, it also results in a deactivation phenotype similar to an *arr2* hypomorph, presumably because there is no longer sufficient free Arr2 to inactivate M (Alloway, P. G. and Dolph, P. J., 1999; Alloway, P. G. *et al.*, 2000; Kiselev, A. *et al.*, 2000a).

p0180 In summary, it appears that, whilst having no direct role in the electrophysiological response, the rhodopsin and arrestin phosphorylation and

dephosphorylation cycles (Figure 9) play vital, though still incompletely understood roles in rhodopsin turnover and photoreceptor maintenance and survival. Thus, as described above, *rdgC* mutants undergo light-dependent degeneration because of the accumulation of hyperphosphorylated metarhodopsin bound to arrestin. Since the *rdgC* rhodopsin phosphatase is dependent on the Ca^{2+} influx associated with the light response, hyperphosphorylated rhodopsin also accumulates in any mutants of the transduction cascade that block transduction, such as *norpA* (see below), and these mutants probably degenerate by a similar mechanism (Byk, T. *et al.*, 1993; Alloway, P. G. *et al.*, 2000; Kiselev, A. *et al.*, 2000a). Alloway P. G. *et al.* (2000) speculate that the clathrin-mediated endocytosis of M–Arr2 complexes may be a mechanism for removal of defective rhodopsin molecules, whilst Satoh A. K. and Ready D. F. (2005) suggest that Arr1 may play a scavenging role, binding phosphorylated M before it can accumulate in the lethal Arr2–M-p complexes. In support of this, they found that the light-independent degeneration in *arr1* mutants is actually rescued in the *arr1*;*arr2* double mutant.

s0100 **6.63.4.4 Heterotrimeric G Protein**

p0185 Heterotrimeric G proteins are holoenzymes composed of α, β, and γ subunits, with the α subunit bound to GDP in the (heterotrimeric) resting state (Figure 7). In common with all such G proteins, the G protein in the *Drosophila* photransduction cascade is activated by interaction with the active receptor (M), which catalyzes the exchange of GDP for GTP on the α subunit, resulting in release of the active GTP-bound α subunit (Figure 6). The α subunit binds and activates its effector enzyme (in this case PLC), which then remains active until the GTP is hydrolyzed to GDP promoting dissociation of $G_q\alpha$ from PLC and its reassociation with $G\beta\gamma$.

p0190 Curiously, no mutants of any of the three G protein subunits were isolated in the early mutagenesis screens, but a strong candidate gene for the α subunit was identified amongst a collection of retinal genes identified by subtractive hybridization (Lee, Y. J. *et al.*, 1990). This G protein showed ~75% identity to mouse $G_q\alpha$, the isoform known to specifically couple to PLC. A role in transduction was indicated by showing it was localized in the rhabdomeres and by overexpressing a constitutively active form in the retina, which resulted in constitutive GTPase activity in the eye and suppression of the light response (Lee, Y. J. *et al.*, 1994). Definitive confirmation came with the characterization of a severe hypomorphic mutant $G\alpha q$, again isolated by screening for antigenicity, in which protein levels were reduced to <1%. Sensitivity to light in these mutants was reduced ~1000-fold (Figure 12), but this could be rescued in a dose-dependent manner by $G_q\alpha$ cDNA expressed under control of a heat-shock promoter (Scott, K. *et al.*, 1995).

The responses of $G\alpha q$ mutants also appear to have p0195
a slow response deactivation (Figure 12); however, analysis of the underlying quantum bumps indicated, that this actually represents generation of bumps with delayed latencies, thereby substantially broadening the latency distribution. This can be readily understood by considering that one of the determinants of latency is the time taken for G protein to encounter the active M by diffusion in the microvillar membrane (see Fast Nonlinear Response Kinetics). Clearly, if the number of G proteins per microvillus is greatly reduced, then it will take longer on average for a G protein to encounter the single activated M in the microvillus (Scott, K. *et al.*, 1995).

Quantum bump amplitudes in $G\alpha q$ (Scott, K. *et al.*, p0200
1995), and also in hypomorphic PLC (*norpA*) mutants (Deland, M. C. and Pak, W. L., 1973; Cook, B. *et al.*, 2000), were originally reported to be the same as in WT, leading to the concept that amplification of the quantum bump was determined entirely downstream of PLC – i.e., PLC activation serves only as a trigger for the quantum bump. However, it was subsequently found that quantum bumps were reduced by approximately fivefold in both these mutant backgrounds, indicating that G_q and PLC also contribute to the amplification process, and that normally activation of several G protein and PLC molecules is required to generate a full size quantum bump (Figures 12 and 13, Hardie, R. C. *et al.*, 2002). The discrepancy was attributed to the omission of ATP from the patch electrodes solution in earlier studies, resulting in artefactual amplification of the small bumps, probably as a consequence of reduced DAG kinase activity (Hardie, R. C. *et al.*, 2002) (see also Figure 16 and Evidence for Activation by Lipid Messengers).

6.63.4.4.1 G protein β and γ subunits s0105

A G protein β subunit that is expressed predomi- p0205
nantly in the rhabdomeres has also been identified (Yarfitz, S. *et al.*, 1991; Yarfitz, S. L. *et al.*, 1994). Mutants ($G\beta e$), subsequently isolated by screening for antigenicity, also show a greatly (~100-fold)

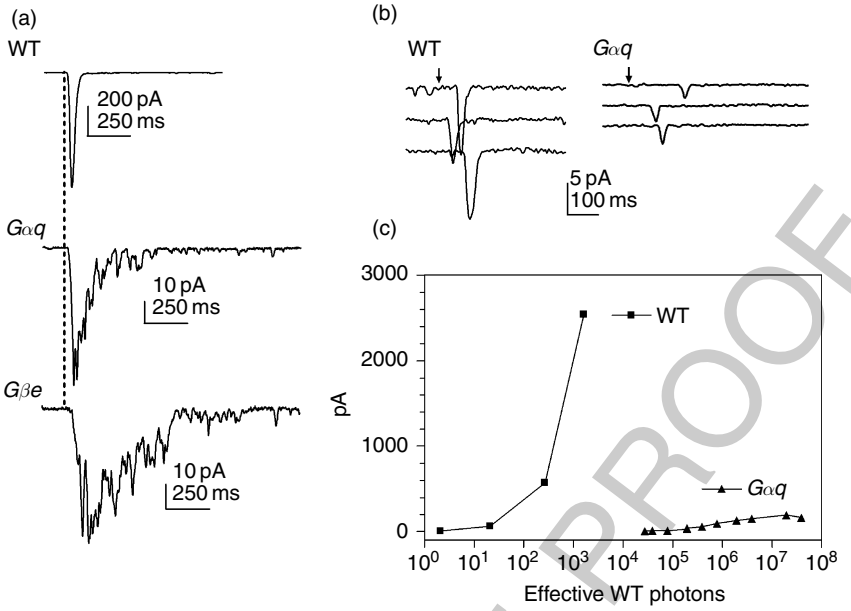

f0060 **Figure 12** Responses in mutants of G_q. (a) Whole-cell voltage-clamped responses to brief (1 ms) flashes of light in wild type (WT), and in *Gαq* and *Gβe* mutants: (intensity for *Gαq* ~1000 times, and for Gβe ~100 times greater than for WT). Apart from the greatly reduced sensitivity, responses in both *Gαq* and *Gβe* show slow kinetics. For *Gαq* this is explained by delayed activation leading to longer bump latency (Scott, K. *et al.*, 1995), but in *Gβe* an additional defect in deactivation has been proposed (Dolph, P. J. *et al.*, 1994). (b) Individual quantum bumps elicited by dim flashes in *Gαq* are ~5× smaller than in WT. (c) Response intensity functions for WT and *Gαq* mutants: intensity expressed in effectively absorbed photons in WT photoreceptors. (Adapted with permission from Hardie, R. C. *et al.*, 2002; see also Dolph, P. J. *et al.*, 1994; Scott, K. *et al.*, 1995; Hardie, R. C. *et al.*, 2002.)

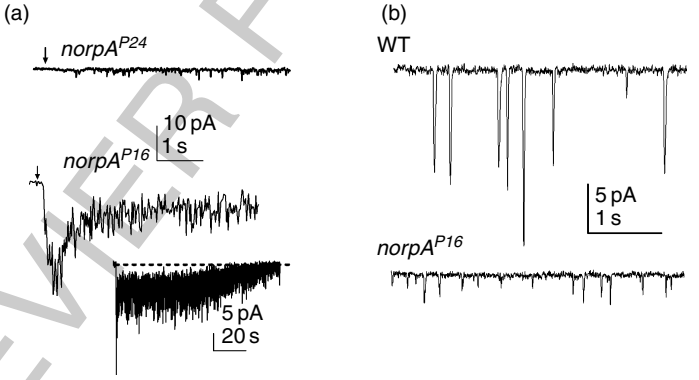

f0065 **Figure 13** *norpA* mutant responses. (a) Whole-cell voltage-clamped responses to brief flashes of light (containing ~10^5 effectively absorbed photons) in the null PLC mutant *norpA*^{P24} and the severe hypomorph *norpA*^{P16}. Even in the supposedly null *norpA*^{P24}, a few ~1-pA bumps are elicited in response to bright illumination, whilst the same intensity elicits a small response in *norpA*^{P16} (these intensities would generate saturating responses in wild-type (WT) flies). Inset, on a slower timescale shows that the response in *norpA*^{P16} lasts for several minutes. (b) Quantum bumps in *norpA*^{P16} (recorded in the tail of a response to a weaker flash), are greatly reduced compared to WT (above). (Adapted with permission from (Hardie, R. C. *et al.*, 2002.)

decreased sensitivity to light (Dolph, P. J. *et al.*, 1994) as well as reduced light-induced GTPγS binding to retinae of cryosectioned heads (Yarfitz, S. L. *et al.*, 1994). Although this may indicate that Gβ is essential for effective coupling of $G_q\alpha$ with M, a recent study found that the majority of $G_q\alpha$ was mislocalized to the cytosol in *Gβe* mutants, i.e., the reduced sensitivity could in principle also be explained as

consequence of G protein and rhodopsin being in separate cellular compartments (Elia, N. *et al.*, 2005). Interestingly, *Gβe* mutants also show a distinct deactivation defect, which is more severe than in *Gαq* mutants (Figure 12), suggesting a distinct role for Gβ in response termination (Dolph, P. J. *et al.*, 1994). There are no null or hypomorphic mutants of the G protein γ subunit; however, a dominant negative construct lacking the farnesylation site require for membrane anchoring also reduces light sensitivity as measured by ERG, presumably by sequestering Gβ subunits away from the membrane (Schillo, S. *et al.*, 2004).

s0110 #### 6.63.4.4.2 G_q translocation

p0210 Along with the arrestins (Arrestin Translocation) and the TRPL channels (Transient Receptor Potential-Like Translocation), G_q is one of three components of the *Drosophila* cascade that has been shown to translocate in response to illumination. In the dark, the majority of the G protein is found concentrated in the microvilli. However, following saturating illumination with blue light, ~50% of the $G_q\alpha$ is released from the membrane and moves out into the cell body over a time course of 50 min, returning to the rhabdomere slightly more slowly in the dark (Kosloff, M. *et al.*, 2003). Translocation was little affected by mutations in PLC, though curiously was largely blocked in mutants of the TRP channel. Like other G proteins, G_q is not a transmembrane protein, but can be anchored to the membrane by reversible palmitoylation of the α subunit, suggesting that depalmitoylation may be required to initiate the translocation (Kosloff, M. *et al.*, 2003). The return of $G_q\alpha$ in the dark was blocked in *Gβe* mutants, indicating that targeting to the microvillar membrane also requires Gβ or, more likely, Gβγ with involvement of the farnesylation of the γ subunit in membrane anchoring.

s0115 ### 6.63.4.5 Phospholipase C (NORPA)

p0215 Severe mutants of the *n*o *r*eceptor *p*otential *A* (*norpA*) gene have effectively no response to light, and were isolated independently by both the Pak and the Benzer groups (Hotta, Y. and Benzer, S., 1970; Pak, W. L. *et al.*, 1970). Although evidence had already implicated the PI cascade in invertebrate phototransduction (Brown, J. *et al.*, 1984; Fein, A. *et al.*, 1984; Inoue, H. *et al.*, 1985; Devary, O. *et al.*, 1987), the finding that *norpA* encoded a PI-specific PLC (Bloomquist, B. T. *et al.*, 1988) provided clear genetic evidence that PLC was the effector enzyme of the phototransduction cascade in *Drosophila* and represented a key milestone in the analysis of invertebrate phototransduction. Appropriate for its role, the NORPA protein was found to be highly enriched in the eyes and immunogold labeling showed it to be specifically localized to the rhabdomeres (Schneuwly, S. *et al.*, 1991). Although the obligatory control demonstrating that *norpA* cDNA could genetically rescue the mutant phenotype was not performed until much later (McKay, R. R. *et al.*, 1995); importantly, possible pleiotropic developmental effects of this mutation had already been effectively excluded by the availability of temperature-sensitive alleles of *norpA* in which the light response was rapidly and reversibly abolished by warming to 35 °C (Deland, M. C. and Pak, W. L., 1973).

p0220 NORPA, one of the first PI-specific PLCs to be cloned, is clearly recognizable as a PLCβ isoform, which unlike PLCγ and PLCδ, are activated by interaction with heterotrimeric G proteins. Thus, NORPA has up to 60% identity with mammalian PLCβs in the conserved X and Y domains, which form the catalytic core of the enzyme and contains a C2 domain that may be involved in Ca^{2+}-dependent targeting to the membrane (reviewed in Pak, W. L., 1995). Interestingly, one of the vertebrate PLCβ isoforms (PLCβ4) is more closely related to NORPA than any other vertebrate PLC isoform and is predominantly expressed in the vertebrate cones (Ferreira, P. A. and Pak, W. L., 1994). Its role in vertebrate photoreceptors is not known, but may hint at some distant evolutionary common ancestral photoreceptor.

s0120 #### 6.63.4.5.1 Phospholipase C is also a GAP

p0225 Numerous mutant alleles of the *norpA* gene have been isolated, which vary widely in their severity (Pearn, M. T. *et al.*, 1996). The most severe, such as $norpA^{P24}$, which has a 28-bp deletion resulting in a frameshift and a premature stop codon, have essentially no response to even saturating flashes (but see Figure 13 and Hardie, R. C. *et al.*, 2003) and no detectable protein. However, others such as $norpA^{P57}$ and $norpA^{P16}$ have residual protein and substantial responses to bright illumination. As well as a marked reduction in sensitivity, such hypomorphic alleles also have dramatically prolonged responses to light that can persist for many minutes, the time course increasing with the severity of the mutation (Figure 13, Scott, K. and Zuker, C. S., 1998; Cook,

B. *et al.*, 2000). A combined electrophysiological and biochemical study indicated that this reflects the requirement for PLC to act as a GTPase-activating protein (GAP), essential to terminate the activity of $G_q\alpha$ subunit (Cook, B. *et al.*, 2000). With severely reduced PLC levels, it appears that $G_q\alpha$ subunits remain active indefinitely (for many minutes), before finally encountering and binding to a PLC molecule, only then initiating a cycle of bump generation, PLC inactivation, and response termination. GAP activity of the effector enzyme is a common feature in G protein signaling and as in vertebrate rods, such a mechanism is important in ensuring the fidelity of the response to light. Thus, firstly the G protein stays active until it has had the chance to activate its target (PLC), but then it is rapidly inactivated ensuring that only one bump is generated. Whether or not RGS proteins are also involved as GAP proteins, as in vertebrate photoreceptors, is not known.

s0125 #### 6.63.4.5.2 Measuring Phospholipase C activity

p0230 Light- and *norpA*-dependent PLC activity, generating DAG and $InsP_3$ from PIP_2 has directly been demonstrated in biochemical assays, using radiolabeled inositol or PIP_2 (Inoue, H. *et al.*, 1985; Devary, O. *et al.*, 1987; Toyoshima, S. *et al.*, 1990; Running Deer, J. L. *et al.*, 1995). Like other PLCs, *Drosophila* NORPA shows *in vitro* dependence on Ca^{2+}, both basal and light-activated PLC activity being increased in the range from 10 nm to 1 μM, and inhibited in the high micromolar range (Toyoshima, S. *et al.*, 1990; Running Deer, J. L. *et al.*, 1995).

p0235 The only available quantitative biochemical measurements come from squid, indicating that ~500 PIP_2 molecules can be hydrolyzed per absorbed photon (Szuts, E. Z., 1993). However, semiquantitative *in vivo* estimates of PIP_2 hydrolysis rates in *Drosophila* have recently been made using biosensors in the guise of PIP_2-sensitive inward rectifier ion channels (Kir2.1), genetically targeted to the rhabdomeres (Hardie, R. C. *et al.*, 2001; 2004). These channels are activated by PIP_2, and their open probability is simply related to PIP_2 concentration. When they replace the light-sensitive channels, they generate a constitutively active inward current maintained by the endogenous resting PIP_2 levels. This current is suppressed in an intensity-dependent manner by illumination, providing a rather direct *in vivo* measure of PIP_2 hydrolysis. The suppression of the Kir2.1 current by light indicated that PLC activity corresponded to rates of ~150% of the PIP_2 in the microvillus per second per effectively absorbed photon (Figure 14, Hardie, R. C. *et al.*, 2004). Interestingly, in complete darkness, a remarkably high basal PLC activity could also be readily resolved after blocking PIP_2 synthesis by ATP deprivation. Although ~1000× less than maximum light-induced rates, this was still sufficient to effectively deplete the rhabdomere of PIP_2 within 5–10 min (Figure 14).

p0240 Kir2.1 biosensors, in combination with manipulation of cytosolic Ca^{2+}, also allowed *in vivo* measurements of the Ca^{2+} dependence of basal and light-induced PLC activity. Broadly, these confirmed *in vitro* measurements; however, facilitation by Ca^{2+} was only noted in the range ~10–100 nM, and maximal activity appeared already to be reached at physiological resting levels of Ca^{2+} (Hardie, R. C., 2005). As discussed later (Ca^{2+} Signals Are Dominated by Ca^{2+} Influx), much higher concentrations (>50 μM) strongly inhibited PLC activity *in vivo*.

s0130 ### 6.63.4.6 Light-Sensitive Channels TRP and TRPL

p0245 The *Drosophila* transient receptor potential mutant, *trp*, was first isolated as a spontaneously occurring mutation, in which the photoreceptor's response to light decayed to baseline during prolonged illumination (Cosens, D. J. and Manning, A., 1969; Minke, B. *et al.*, 1975). After the gene was positionally cloned (Montell, C. and Rubin, G. M., 1989), it was found to encode a novel transmembrane protein. Since mutants still had a light response, it was originally considered unlikely that TRP represented the light-sensitive channel. However, Hardie R. C. and Minke B. (1992) demonstrated that the Ca^{2+} selectivity of the light-sensitive current was reduced 10-fold in *trp* mutants, leading to the proposal that it represented the major, Ca^{2+} selective component of the light-sensitive current, and that a second, less Ca^{2+} permeable channel was responsible for the residual response in the *trp* mutant. At the same time, Phillips A. M. *et al.* (1992) reported the sequence of a second channel-like gene (TRP-like, or TRPL), now known to be responsible for this residual response (Niemeyer, B. A. *et al.*, 1996; Reuss, H. *et al.*, 1997). Both TRP and TRPL have been shown to be predominantly localized in the microvilli by immunogold labeling (Niemeyer, B. A. *et al.*, 1996), although as detailed below (TRPL Translocation), TRPL may also be found in the cell body following translocation.

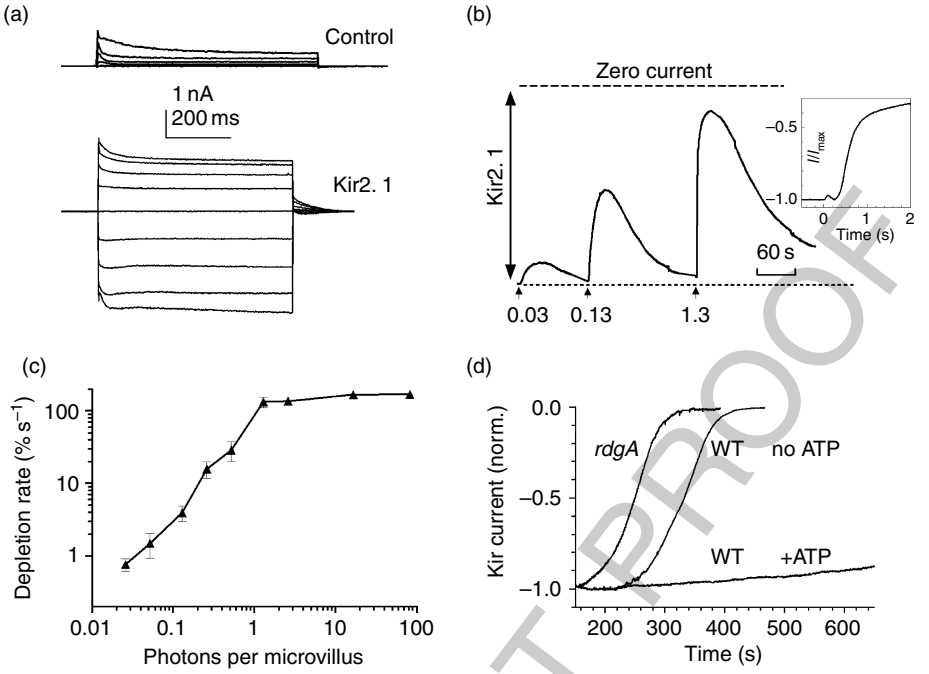

f0070 **Figure 14** PIP_2 hydrolysis monitored with PIP_2 biosensor channels Kir2.1. Whole-cell recordings of inward K^+ currents in photoreceptors expressing the PIP_2-sensitive inwardly rectifying Kir2.1 channel. (a) Voltage steps (from −100 to −20 mV in 10 mV steps). In control cells, only outward K currents (mainly *Shaker* and *Shab*) are activated, but in cells expressing Kir2.1 large inwardly rectifying currents are seen at negative potentials. (b) When expressed in photoreceptors of *trpl*;*trp* double mutants, Kir2.1 is the only light-sensitive conductance in the cell. In the dark a large, ~1-nA constitutive current is activated by the prevailing PIP_2 levels (extent indicated by double arrow). Calibrated stimuli (0.03 etc., expressed in effectively absorbed photons per microvillus) suppress the current due to hydrolysis of PIP_2 by PLC: flashes containing one photon per microvillus deplete the entire rhabdomere of the majority of detectable PIP_2 within ~1 s (inset shows a response on a faster timescale). The Kir2.1 current is reactivated with a half time of ~60 s in the dark, representing the resynthesis of PIP_2. (c) Intensity response function of PLC activity – measured from the maximum slope of individual flash responses as in (b). Note that there is no Ca^{2+} influx associated with the light response in these experiments: under normal conditions, Ca^{2+} influx via TRP channels rapidly inhibits PLC activity, so that these rates of PLC activity will only be reached and briefly sustained during the latent period of the quantum bump (see Ca^{2+}-Dependent Negative Feedback). (d) Basal PLC activity monitored *in vivo* as a function of time after establishing the whole-cell configuration: a control (wild type (WT)) cell held in the dark with ATP in the patch pipette shows only very gradual rundown of the Kir2.1 current over 10 min. Without ATP however, the current decays to near zero within ~6 min. A similar behavior is seen in the *rdgA* mutant demonstrating ongoing basal PLC activity in this mutant as well. (Adapted from Hardie, R. C. *et al.*, 2004.)

s0135 ### 6.63.4.6.1 Structure of TRP and TRPL

p0250 The TRPL protein shares 40% identity to TRP and both sequences show structural similarity with the voltage-gated Ca^{2+} channel family with six transmembrane (TM) helices and a pore loop (Phillips, A. M. *et al.*, 1992). Unlike Ca^{2+} channel genes, which encode four such 6TM domains in a single peptide, the *trp* and *trpl* genes encode only one such domain, and consequently, like voltage-gated K channels or CNG channels, TRP channels are believed to be composed of homo- or heterotetramers. The identification of TRP as a PLC-regulated cation channel heralded the discovery of some 30 vertebrate isoforms, divided into seven subfamilies (TRPC, TRPV, TRPM, TRPML, TRPP, TRPA, and TRPN). They have remarkably diverse functions throughout the body, most notably, but by no means exclusively, in sensory transduction (reviewed in: Clapham, D. E., 2003; Montell, C., 2005; Ramsey, I. S. *et al.*, 2006).

p0255 *Drosophila* TRP and TRPL share closest homology with the vertebrate TRPC (*c*anonical TRP) subfamily, with similar overall topology, including four N-terminal ankyrin repeats (protein binding motifs) and a coiled-coil (CC) region in the N-terminal, and six transmembrane segments with a pore loop between S5 and S6 (Figure 15). The most highly conserved region is the so-called TRP domain, which is

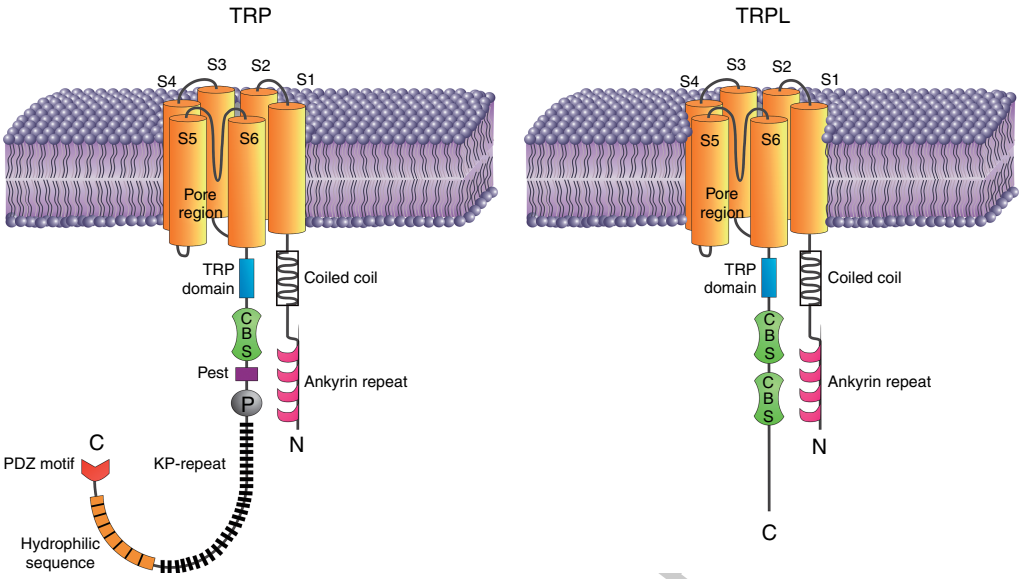

f0075 **Figure 15** Structural features of the TRP and TRPL channel subunits. TRP and TRPL both belong to the overall superfamily of voltage-gated Ca^{2+}/Na^{+} and K^{+} channels and CNG channels; and represent subunits of tetrameric channels. Each subunit has six transmembrane helices (S1–S6), with a pore helix and pore loop between S5 and S6. The S4 helix lacks the positively charged residues characteristic of the voltage-gated members of the family. Their N-termini contain a coiled-coil region (CC) and four ankyrin repeats, which are potential protein–protein interaction domains. The most highly conserved region is the TRP domain adjacent to S6, with the motif EWKFAR found in all TRPC channels, and which is still recognizable in other TRP subfamilies. TRP has one, and TRPL, two CaM-binding sites (CBS) in the C-termini. TRP has an extended C-terminus with a PEST sequence, a proline-rich region with 29 KP repeats, multiple repeats of a hydrophilic eight to nine peptide sequence DKDKKP(A/G)D, and a PDZ domain binding motif in the last three amino acids required for binding to the INAD protein. Ser^{982} has been implicated as an *in vivo* PKC phosphorylation site (P) required for effective response termination (Popescu, D. C. *et al.*, 2006).

immediately adjacent to S6. In vertebrate TRPC1, part of this domain can serve as a binding site for a scaffolding protein, Homer, which is proposed to mediate interaction with $InsP_3$ receptor ($InsP_3R$) (Yuan, J. P. *et al.*, 2003). However, given that TRP channels are activated normally in the $InsP_3R$ null mutants in the photoreceptors (Evidence for Activation by Lipid Messengers), the significance of this region in the *Drosophila* TRPs is not known. The rest of the C-terminal is rather divergent – both between TRP and TRPL and the vertebrate TRPCs – though all include one or more consensus CaM-binding domains (see Calmodulin). TRP has a conspicuously long C-terminal domain containing a proline-rich region, eight to nine peptide repeats of unknown function and a consensus PDZ-binding motif that binds to the scaffolding protein INAD (Scaffolding Protein INAD).

s0140 ***6.63.4.6.2 Channel properties***

p0260 The properties of the native TRP- and TRPL-dependent currents *in vivo* have been characterized by exploiting null mutants of both genes to isolate the respective currents, providing characteristic biophysical fingerprints (Table 2, Reuss, H. *et al.*, 1997). TRP channels (isolated in *trpl* mutants) are highly selective for Ca^{2+} (P_{Ca}:P_{Na} ~100:1) and have a rather small single-channel conductance (~8 pS) with rapid kinetics (mean open time ~0.5 ms). TRP (but not TRPL) channels are completely blocked by micromolar levels of La^{3+}. TRPL channels, isolated in *trp* mutants are relatively nonselective (P_{Ca}:P_{Na}~4:1) with a conductance of 35 pS and slightly slower channel open times (1–2 ms). The only reported specific blocker is cinnamyl-dihidroxy-cyanocinnamate, with an IC_{50} of 1 μM (Chyb, S. *et al.*, 1999b). An interesting feature of the TRP channel is a pronounced voltage-dependent open channel block by physiological concentrations of Mg^{2+} (IC_{50} ~1 mM). The block is relatively weak around resting potential (−70 mV), but intensifies as the cell depolarizes. This means that the effective single-channel conductance should decrease as the cell depolarizes in response to light, and potentially would seem to be an elegant

t0010 **Table 2** Biophysical properties of TRP and TRPL channels

Permeability ratios	***TRP (in trpl)***	***TRPL (in trp)***	***WT***			
A						
P_{Ca}:P_{Cs}	110	4.3	45.1			
P_{Mg}:P_{Cs}	13.0	1.4	5.7			
P_{Na}:P_{Cs}	1.27	0.84	1.16			
P_{Li}:P_{Cs}	0.89	0.80	0.89			
	γ (pS) (divalent free)	***γ (pS)***	***τ (ms)***	***IC_{50} Mg^{2+} (mM), 0 Ca^{2+}***	***IC_{50} Mg^{2+} (mM), 1.5 Ca^{2+}***	***La^{3+} block (10 μM)***
B						
TRP (in *trpl*)	35	8	2, 0.2	0.28	1.3	Total
TRPL (in *trp*)	70	35	0.4	4	4	None

A: Permeability ratios (P_x:P_{Cs}) derived from bi-ionic reversal potential data. Values expressed with respect to internal Cs^+ (130 mM) and determined in respective mutants, i.e., TRPL channels measured in the *trp* mutant, TRP-dependent channels in *trpl*. (Data from Reuss, H. *et al.*, 1997.)

B: Estimates of single-channel characteristics and ion block. Single-channel conductances (γ, pS) derived from noise analysis in both divalent free and physiological Ringer's. Time constant (τ) refer to Lorentzian fits to power spectra. Mg^{2+} block has been determined only in WT (dominated by TRP channels) and *trp* mutant. (Data from Hardie, R. C. and Minke, B., 1994b; Hardie, R. C. and Mojet, M. H., 1995; Hardie, R. C. *et al.*, 1997; Reuss, H. *et al.*, 1997; Raghu, P. *et al.*, 2000b and Hardie, R. C., unpublished.)

and economical mechanism for light adaptation (Hardie, R. C. and Mojet, M. H., 1995).

p0265 Both TRP and TRPL have also been expressed in heterologous expression systems, indicating that they encode bona fide channels (Vaca, L. *et al.*, 1994; Gillo, B. *et al.*, 1996; Hardie, R. C. *et al.*, 1997; Xu, X. Z. S. *et al.*, 1997). TRPL has been successfully expressed by many groups (Hu, Y. *et al.*, 1994; Harteneck, C. *et al.*, 1995; Gillo, B. *et al.*, 1996; Lan, L. *et al.*, 1996; Hardie, R. C. *et al.*, 1997), and its biophysical properties found to be indistinguishable from those of the native TRPL-dependent current isolated in *trp* mutants (Hardie, R. C. *et al.*, 1997; Chyb, S. *et al.*, 1999b). Together with the complete elimination of the native current by the *trpl* mutation (Niemeyer, B. A. *et al.*, 1996; Reuss, H. *et al.*, 1997) , the close functional equivalence of native and heterologously expressed TRPL channels leaves little doubt as to their identification (Hardie, R. C. *et al.*, 1997). Although there is good evidence that TRPL can associate as a heteromultimer with TRP (Xu, X. Z. S. *et al.*, 1997), it seems questionable whether the *in vivo* light-sensitive TRPL-dependent conductance includes TRP subunits as well. Thus the WT light-sensitive conductance can readily be accounted for by the independent sum of TRP and TRPL, whilst blocking TRP channels with La^{3+} quantitatively mimics the effect of the *trp* mutation leaving TRPL channels indistinguishable from those found in *trp* mutants (Reuss, H. *et al.*, 1997). A third TRP homologue, TRPγ, has also been identified and found to be expressed in the photoreceptors (Xu, X. Z. S. *et al.*, 2000). TRPγ was also reported to form heteromultimers with TRPL (but not TRP) in expression systems and a dominant negative construct suppressed the TRPL-dependent light response *in vivo* suggesting that the native channels might also represent TRPL–TRPγ heteromultimers. However, unlike TRP and TRPL, recent evidence suggests that TRPγ is not particularly eye-enriched (Jors, S. *et al.*, 2006) and until a mutant is generated, its role remains uncertain.

p0270 By contrast, it has generally proved very difficult to express TRP, and the few published reports of its biophysical properties in expression studies (Vaca, L. *et al.*, 1994; Gillo, B. *et al.*, 1996; Xu, X. Z. S. *et al.*, 1997) do not closely match the properties of the *in vivo* TRP-dependent current (isolated in *trpl* mutants). This therefore raises the question of whether TRP actually represents a pore-forming channel subunit *in vivo*. This concern has recently been addressed by the identification of a unique aspartate residue (Asp^{621}) within the TRP pore region as the major determinant of Ca^{2+} permeation, most likely forming a ring of four such acidic residues in a tetramer, as in other Ca^{2+}-selective channels. Neutralizing Asp^{621} (to glycine) almost completely eliminated Ca^{2+} permeation *in vivo*, whilst more conservative substitutions resulted in intermediate ionic selectivities (Hardie, R. C. *et al.*, in preparation-b). Systematic alteration of

pore properties by site-directed mutagenesis of the pore represents the most rigorous demonstration of channel identity, and thus these results conclusively demonstrate that TRP does indeed form a pore-forming subunit of the *Drosophila* light-sensitive channel *in vivo*.

s0145 ### 6.63.4.6.3 *trp* and *trpl* phenotypes

p0275 Apart from the changes in permeation properties and pharmacology of block, both *trp* and *trpl* mutants have a number of intriguing secondary phenotypes. The original *trp* phenotype is the decay of the response to baseline during maintained illumination, associated with a complete loss of sensitivity that slowly recovers in the dark. After some debate, this now appears to be attributable to the complete loss of PIP_2 due to the failure of Ca^{2+}-dependent inhibition of PLC (see Figure 20 and Ca^{2+}-Dependent Negative Feedback). With weaker illumination, or brief flashes, responses in *trp* mutants are superficially similar to WT; however, they have a ~10-fold reduced sensitivity, their kinetics are slightly slower and fail to accelerate during light adaptation. Indeed, virtually all aspects of light adaptation are lacking, and the loss of response during light adaptation regimes is better described as exhaustion of the excitatory process (Minke, B., 1982). Whilst intracellular recordings originally suggested that quantum bumps were similar in WT and *trp*, the improved resolution of whole-cell recordings clearly showed a reduction in bump amplitude to ~3–4 pA (Niemeyer, B. A. *et al.*, 1996; Henderson, S. R. *et al.*, 2000). Given that the TRPL single-channel current is ~2 pA, this implies that bumps in *trp* usually consist of only one to two channel openings.

p0280 By contrast, quantum bumps and macroscopic flash responses in *trpl* mutants are almost indistinguishable from WT, and initially the only phenotypes found in whole-cell recordings of the LIC were changes in ionic selectivity and the complete block of the light response by La^{3+} (Niemeyer, B. A. *et al.*, 1996; Reuss, H. *et al.*, 1997). This suggests that the TRP channels make the dominant contribution to the WT light response, and it has been estimated that ~95% of the DA LIC in flash responses is attributable to TRP (Reuss, H. *et al.*, 1997). However, subsequent studies using prolonged illumination performed under more physiological conditions, using either the ERG or intracellular voltage recordings, revealed further distinct phenotypes. These include a reduced plateau potential, oscillations superimposed on the response and an impaired ability to light adapt to very dim background lights (Leung, H. T. *et al.*, 2000). With the possible exception of the reduced ability to light adapt (see TRPL Translocation), it remains unclear however, how these phenotypes relate to the known properties of the two channels. Leung H. T. *et al.* (2000) also reported an intriguing genetic interaction between *trpl*, *trp*, and a mutant of the scaffolding protein INAD (Scaffolding Protein INAD), $InaD^{P215}$, which has a point mutation disrupting its binding to TRP. Specifically, whilst *trpl* and $InaD^{P215}$ mutants have normal or near normal levels of TRP protein, the *trpl*,$InaD^{P215}$ double mutant has greatly reduced (<10%) levels of TRP and an even more profound loss of response, which could not be entirely accounted for by the loss of protein. This suggests that when TRP is not bound to INAD, it requires TRPL in order to maintain TRP protein levels and to generate significant responses (Leung, H. T. *et al.*, 2000).

6.63.4.6.4 TRPL translocation

s0150

p0285 Another feature that distinguishes the TRPL from the TRP channel is that the former, like arrestin and G_q, also undergoes a massive light-induced translocation. Translocation of the TRPL protein out of the rhabdomere in response to illumination, and its return in the dark has been shown both by immunocytochemistry and by tracking an enhanced green fluorescent protein (eGFP)-tagged TRPL protein *in vivo* (Bahner, M. *et al.*, 2002; Meyer, N. E. *et al.*, 2006). In the larger fly *Calliphora*, translocation has also been confirmed by quantitative Western blotting of cytosolic and rhabdomeral fractions (Bahner, M. *et al.*, 2002). In *Drosophila*, at least 80% of eGFP-tagged TRPL leaves the rhabdomere during bright illumination with a halftime of 3.25 h, returning rather more quickly in the dark (halftime 1 h). The translocation mechanism appears to require operation of the full transduction cascade, being blocked in *Gαq*, *norpA*, and *trp* mutants, and also by removal of extracellular Ca^{2+}, whilst it is impaired in the *ninaC* and *arr2* mutants (Meyer, N. E. *et al.*, 2006). Importantly, whole-cell recordings confirmed the removal (and return) of functional TRPL channels from the rhabdomeres, assayed by their reversal potential and insensitivity to La^{3+}. One of the physiological consequences of the translocation of TRPL protein out of the rhabdomere following light exposure, namely an impaired inability to adapt to weak background lights, closely mimics one of the *trpl* mutant phenotypes (*trp* and *trpl* Phenotypes). A possible

explanation for this is that the TRPL channel may be subject to more pronounced Ca^{2+}-dependent inactivation than the TRP channel, and that consequently low levels of Ca^{2+} influx associated with weak background illumination have more effect in inhibiting TRPL channels than TRP channels, and hence this cause less reduction in sensitivity when only TRP is present (Bahner, M. *et al.*, 2002).

s0155 **6.63.4.7 INAF, a Novel Protein Required for TRP Function**

p0290 The *inaF* gene encodes a small, highly eye-enriched protein with no homologies to other proteins in the databases and no predicted transmembrane domains. Null *inaF* mutants have substantially reduced (~10% of WT levels) TRP protein levels and a phenotype that resembles that of a *trp* null mutant, whilst TRPL channel function appears intact (Li, C. J. *et al.*, 1999). Interestingly, the residual TRP protein in *inaF* mutants is still localized to the rhabdomeres, yet the phenotype is as severe as in *trp* mutants in which there is no immunodetectable protein. Therefore, although the reduced levels of TRP protein may contribute to the phenotype, Li C. J. *et al.* (1999) suggest that the INAF protein may also have a direct regulatory role in TRP channel function.

s0160 **6.63.4.8 Scaffolding Protein INAD**

p0295 Along with translocation, one of the most intriguing recent developments in invertebrate photransduction has been the realization that not only are the molecular elements of the cascade highly compartmentalized within microvilli, but that several key proteins are also organized into a multimolecular signaling complex by a scaffolding protein, INAD (Figure 6). The first mutant allele of *InaD* ($InaD^{P215}$) was isolated by Pak and coworkers, and after it was cloned the gene was found to encode a protein with five so-called PDZ domains (Shieh, B. H. and Niemeyer, B., 1995; Shieh, B. H. and Zhu, M. Y., 1996; Chevesich, J. *et al.*, 1997; Tsunoda, S. *et al.*, 1997). PDZ domains are modules, which anchor a variety of protein targets, typically though not always by a short (three amino acids) C-terminal target sequence (see Figures 6 and 7). The final composition of the complex is still debated, but there is general agreement that a core set of three proteins TRP, PLC, and PKC, are bound to INAD in a stoichiometric (1:1:1:1) manner (Huber, A. *et al.*, 1996a; Tsunoda, S. *et al.*, 1997; Li, H. S. and Montell, C., 2000). Other reported targets include rhodopsin, the second ion channel (TRPL), NINAC (Myosin Kinase NINAC), which is a class III myosin that has been proposed to link the complex to the actin cytoskeleton, CaM, and the immunophilin FKBP59 (Montell, C., 1999; Goel, M. *et al.*, 2001; Huber, A., 2001). INAD can also form homophilic interactions with itself; together with the likelihood of linkage via TRP, which forms tetrameric channels, this in principle would provide the potential for extended complexes containing multiple channels and PLC molecules (Figure 6).

p0300 The precise functional role of the INAD complex (sometimes referred to as signalplex or transducisome) remains uncertain. It has been reasonably speculated that tethering PLC and the channels together would minimize diffusional delays, thus contributing to the rapid kinetics. It has also been suggested that the INAD complex represents the molecular framework responsible for the quantum bump (Scott, K. and Zuker, C. S., 1998), but definitive evidence for this is lacking. The null $InaD^{1}$ mutant has greatly reduced sensitivity and quantum bumps are much reduced in size (Scott, K. and Zuker, C. S., 1998); however, this could simply reflect reduced levels of microvillar PLC since INAD is also required for targeting PLC to the microvillar membrane (Tsunoda, S. *et al.*, 2001). It is also possible to genetically disrupt specific INAD interactions; for example, the TRP channel's interaction with INAD can be disrupted by mutations either in the TRP-specific PDZ domain on the INAD protein (as in the original $InaD^{P215}$ mutation), or by mutation in the C-terminal PDZ-binding motif of the TRP protein (Li, H. S. and Montell, C., 2000). In either case, there is little, if any, defect in the kinetics or amplification of excitation, although there is a specific deactivation defect (quantum bumps terminate abnormally slowly) in the $InaD^{P215}$ mutant (Shieh, B. H. and Niemeyer, B., 1995; Henderson, S. R. *et al.*, 2000). Most recently, a similar deactivation defect, albeit measured in the ERG, was reported after engineering a point mutation of a key PKC phosphorylation site in the TRP protein, suggesting that the association of TRP with INAD and PKC (also a member of the signalplex) is critical for TRP phosphorylation (Popescu, D. C. *et al.*, 2006) (see also Protein Kinase C). Whether or not the proximity of PLC and TRP on a molecular scale is also essential for normal excitation, one of the vital roles of INAD is to maintain TRP and PLC and PKC in the microvillus in high concentrations (~100 copies per microvillus) and in stoichiometric relationship. In fact both TRP and

INAD are essential for the long-term maintenance of the complexes in the rhabdomeres. Thus, whilst both TRP and INAD are initially correctly targeted to the rhabdomere in the absence of the other, over a period of days, TRP protein disappears from the rhabdomere in *InaD* mutants, whilst INAD protein is similarly destabilized in *trp* mutants (Tsunoda, S. *et al.*, 1997; Li, H. S. and Montell, C., 2000).

s0165 ### 6.63.4.9 Myosin Kinase NINAC

p0305 The *ninaC* locus encodes two photoreceptor-specific class III myosins characterized by an N-terminus kinase domain followed by a myosin-like domain (Figure 7). A long form (174 kDa) is localized in the rhabdomeres, whilst a short cytosolic variant (132 kDa) is found only in the cell body (Montell, C. and Rubin, G. M., 1988). The rhabdomeric 174-kDa protein may be linked to the F-actin core of the microvillus (Hicks, J. L. *et al.*, 1996). *ninaC* null mutants or mutants lacking the rhabdomeric 174-kDa variant show defects in response termination and light adaptation, including an abnormally large steady-state plateau response (Porter, J. A. *et al.*, 1992; Porter, J. A. and Montell, C., 1993; Hofstee, C. A. *et al.*, 1996; Arnon, A. *et al.*, 1997a), and also undergo light-dependent retinal degeneration (Porter, J. A. *et al.*, 1992). The mechanistic basis for these phenotypes remains uncertain, though the deactivation defect can be attributed, at least in part, to its role as the major CaM-binding protein in the retina (Porter, J. A. AU4 *et al.*, 1993) (see Section 6.3.1). NINAC is also a phosphoprotein and an *in vitro* target for PKC and possibly other kinases. Targeted mutagenesis of two putative phosphorylation sites in NINAC resulted in an unusual ERG phenotype, with slow oscillations in the dark following a bright flash (Li, H. S. *et al.*, 1998). *ninaC* mutants have also been reported to be defective in a putative PKA-mediated modulation of response latency (Chyb, S. *et al.*, 1999a). More recently, *ninaC* mutants have been reported to show defects in the translocation of both arrestin (Lee, S. J. and Montell, C., 2004) (disputed by Satoh, A. K. and Ready, D. F., 2005) and the TRPL channels (Meyer, N. E. *et al.*, 2006), possible indicative of a motor function.

s0170 ## 6.63.5 Messengers of Excitation

p0310 Genetic and other evidence have clearly established that fly phototransduction involves rhodopsin, G_q protein, and PLC, followed by activation of TRP and TRPL channels; however, the final steps of activation downstream of PLC, and in particular, the messenger of excitation are controversial and have still not been unequivocally resolved.

6.63.5.1 Evidence for Activation by Lipid Messengers s0175

p0315 $InsP_3$ is the most familiar product of PIP_2 hydrolysis by PLC, and its major target is the $InsP_3R$ – an intracellular Ca^{2+} release channel found on internal Ca^{2+} stores. Although it was originally widely believed that $InsP_3$-induced Ca^{2+} release from the SMC was an essential step in excitation in *Drosophila*, as appears to be the case, e.g., in *Limulus* (see Phototransduction Mechanisms in Other Invertebrates), most recent evidence suggests it plays no role. Firstly, neither $InsP_3$ nor Ca^{2+} has been found to activate the light-sensitive channels, even when released instantaneously by flash photolysis of caged precursors (Hardie, R. C., 1995; Hardie, R. C. and Raghu, P., 1998). Furthermore, although light induces a massive rise in cytosolic Ca^{2+}, this is almost entirely due to Ca^{2+} influx (see Ca^{2+} Signals are Dominated by Ca^{2+} Influx, Peretz, A. *et al.*, 1994; Ranganathan, R. *et al.*, 1994; Hardie, R. C., 1996b). Most importantly, all aspects of phototransduction appear to be completely normal in mutants of the only known $InsP_3R$ gene in *Drosophila* (Acharya, J. K. *et al.*, 1997; Raghu, P. *et al.*, 2000a). Although some pharmacological evidence has implicated the ryanodine receptor (RyR) in phototransduction in *Drosophila* (Arnon, A. *et al.*, 1997b), null mutants of the RyR again failed to shown any discernible phenotype (Sullivan, K. M. C. *et al.*, 2000).

p0320 By contrast, genetic evidence, particularly involving mutations of the *rdgA* gene encoding diacylglycerol kinase (DGK), strongly implicates DAG in the excitatory pathway (Figure 16). The first indication was the finding that both TRP and TRPL channels were constitutively active in the dark in *rdgA* mutants, consistent with activation by build up of DAG by basal PLC activity (Raghu, P. *et al.*, 2000b). Recently, strong evidence for the requisite basal hydrolysis of PIP_2 by PLC has been obtained *in vivo* using the genetically targeted PIP_2 biosensor (Kir2.1 channel) in both WT and *rdgA* mutants (Figure 14 and Measuring Phospholipase C Activity). A second powerful argument is that DGK mutations massively facilitate the response to light in severe *norpA* or *Gαq* hypomorphs (Figure 16). In such

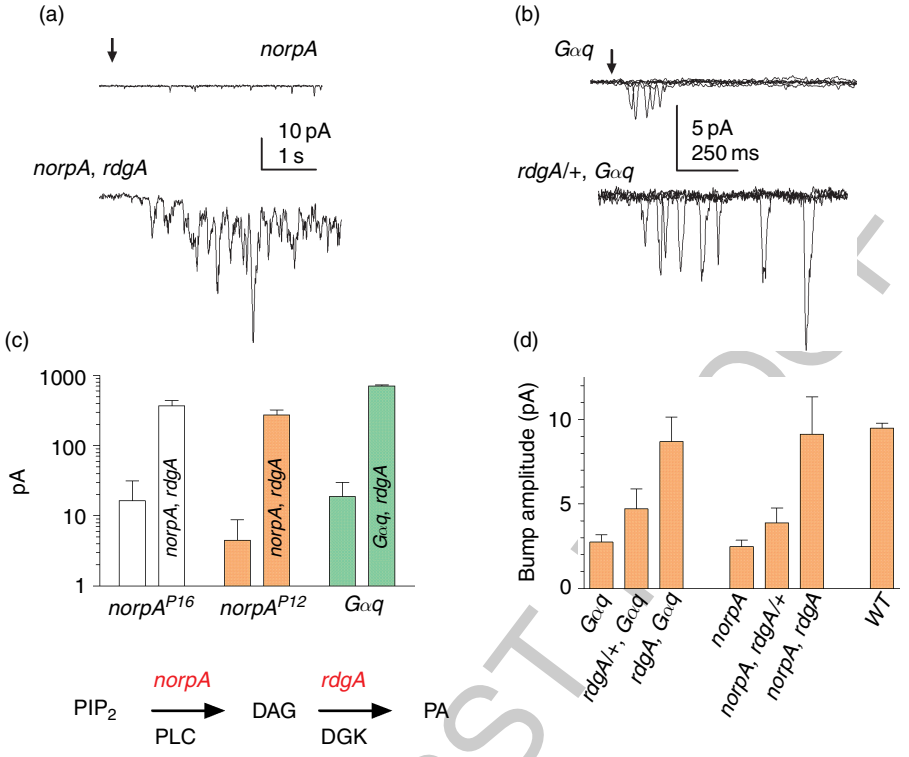

f0080 **Figure 16** Genetic evidence for excitatory role of DAG. Mutations in DAG kinase (DGK, *rdgA* gene) greatly facilitate responses in PLC and *Gαq* hypomorphs. (a) A bright flash in a severe *norpA* hypomorph (*norpA*^{P12}) elicits no more than a few sporadic 1- to 2-pA bumps; in the double mutant *norpA*^{P12},*rdgA*^{1} the response to the same intensity is enhanced ~100-fold. (b) In a *Gαq* mutant, repeated flashes elicit small ~2-pA quantum bumps (traces superimposed); however, the bump amplitude is greatly increased even in a *rdgA*/+ heterozygote where the DGK levels are reduced by only ~50%. (c) Summary of averaged data (mean ± SEM) for macroscopic response amplitude in two *norpA* alleles (P12 and P16) and also the *Gαq* mutant (left bar, single mutant; right bar, in double mutant combination with *rdgA*) – note the logarithmic scale. (d) Summary of data on quantum bump amplitudes in *Gαq* and *norpA*^{P12}, showing dosage-dependent rescue by the *rdgA* mutation. *Below*: reference to the roles of PLC and DGK shows how the data can be readily interpreted if it is assumed that DAG is an excitatory messenger. (Adapted with permission from Hardie, R. C. *et al.*, 2002.)

mutants, bump amplitudes are reduced 5- to 10-fold (Figures 12 and 13) and the macroscopic response to light can be reduced 100- to 1000-fold. However, when combined with the *rdgA* mutation, responses are massively facilitated and quantum bump amplitudes restored to WT levels (Hardie, R. C. *et al.*, 2002). The possibility that pleiotropic effects of the *rdgA* mutation mediate such effects are effectively excluded by finding that even a ~50% knockdown of DGK activity in *rdgA*−/+ heterozygotes (themselves otherwise fully WT in behavior) is sufficient to substantially amplify responses in these PLC and G_q hypomorphic backgrounds (Figure 16, and Hardie, R. C. *et al.*, 2002).

p0325 The *Drosophila* TRP channels can also be activated by metabolic inhibition, and activate spontaneously for example in whole-cell recordings made without ATP in the electrode (Hardie, R. C. and Minke, B., 1994b; Agam, K. *et al.*, 2000). Whilst this has been taken as evidence of protein dephosphorylation – possibly of the channels themselves – contributing to their activation (Agam, K. *et al.*, 2000), a recent study found that activation by metabolic inhibition had an absolute requirement for PLC activity, and proposed that the primary mechanism was failure of DGK activity, combined with basal PLC activity, resulting in buildup of DAG (Hardie, R. C. *et al.*, 2004). An apparent additional requirement of Ca^{2+} inferred from the ability of high concentrations of BAPTA to block the spontaneous activation (Agam, K. *et al.*, 2004) may have been due to the suppression of PLC activity by low Ca^{2+} levels, and a previously unrecognized action of BAPTA as an inhibitor of PLC activity (Hardie, R. C., 2005).

p0330 Whilst DAG has been strongly implicated by these and other studies, and is now also widely accepted as an activator of several vertebrate TRPC

channels (reviewed in: Hardie, R. C., 2003), at least two obstacles remain. Firstly the only data on DGK immunolocalization indicate that it is found predominantly in the SMC and not in the microvilli (Masai, I. *et al.*, 1997). However, the resolution was not sufficient to exclude presence at the base of the microvilli, which would potentially be sufficient to control DAG levels in the microvilli. Secondly, exogenous application of DAG either to photoreceptors or to heterologously expressed TRPL channels has little or no effect (Hardie, R. C. unpublished; Estacion, M. *et al.*, 2001). The only potential agonists yet found to activate the *Drosophila* channels are in fact poly- or monounsaturated fatty acids (PUFAs), such as arachidonic acid or linolenic acid. PUFAs activate TRPL channels in inside-out patches from heterologously expressed channels as well as both TRP and TRPL channels in whole-cell recordings from photoreceptors with an EC_{50} of $\sim$10 μM (Chyb, S. *et al.*, 1999b). More recently, PUFAs, but not DAG have also been shown to activate the only other TRPC family member in *Drosophila*, namely TRPγ (Jors, S. *et al.*, 2006). PUFAs could in principle be released from DAG by DAG lipase or from phospholipids by PLA_2; however, to date there is no evidence for the existence of such enzymes in the transduction cascade in *Drosophila*. Although a mutation in a putative DAG lipase (*r*olling *b*lack *o*ut, *rbo*) recently described by Huang F. D. *et al.* (2004) did in fact result in a severe block in phototransduction, details of its phenotype, were not consistent with such a proposed role. Thus, *rbo* mutants were reported to show reduction in light-induced DAG production, interpreted as an apparent inhibition of PLC activity, whilst the mutant flies only stopped responding to light after continuous bright illumination.

p0335 One possible resolution to this problem is suggested by quantitative estimates of the rate of PIP_2 hydrolysis in the photoreceptors, again using the Kir2.1 channel as a PIP_2 biosensor. These measurements indicate that a single-photon absorption results in PLC activity at rates sufficient to hydrolyze all the PIP_2 (and probably also the PI and PIP reserve) in a single microvillus within less than 1 s (Figure 14, Hardie, R. C. *et al.*, 2001; 2004). Given that a single microvillus contains several thousand PI, PIP, and PIP_2 molecules, a simple calculation based on the surface area and volume of a microvillus suggests that, locally, DAG concentrations within the microvillus can be expected to reach near millimolar levels. DAG is notoriously insoluble and if the TRP channels respond to DAG levels in this concentration range, it may be experimentally impossible to apply exogenous DAG at such concentrations, whilst the more soluble PUFAs may act as surrogate, nonphysiological agonists on the same channels.

6.63.5.2 PIP_2 Depletion

s0180

p0340 In addition to mounting evidence for the role of DAG, recent studies have also raised the possibility that PIP_2 reduction may contribute to excitation. The first indication was the finding that recombinant TRPL channels in inside-out patches, previously activated by application of exogenous PLCβ, could be inhibited by application of PIP_2 (Estacion, M. *et al.*, 2001). However, recordings of light-activated TRPL channel activity, isolated in *trp* mutants, suggest a different picture *in vivo*. In the *trp* mutant prolonged illumination leads to complete loss of PIP_2 in the microvillar membrane, because Ca^{2+} influx via the TRP channels appears to be required for inhibition of PLC activity (see Ca^{2+}-Dependent Negative Feedback), but under these conditions the remaining TRPL channels rapidly close and remain profoundly inactivated until PIP_2 is resynthesized (Hardie, R. C. *et al.*, 2001). This collapse of the response is consistent with a role for DAG in excitation, since the substrate for its generation is exhausted, but clearly contrary to what would be expected if PIP_2 depletion directly activated the channels. Interestingly, however, TRP channels behave rather differently. The Ca^{2+} influx required to prevent excessive PIP_2 hydrolysis by PLC can also be blocked by removing extracellular Ca^{2+}: under these conditions flashes of light which deplete a substantial fraction of PIP_2 usually result in a failure of the TRP channels to close after termination of the light flash. A similar failure in response termination can also be observed in mutants of the *rdgB* gene, which encodes an essential component of the PIP_2 recycling pathway (Vihtelic, T. S. *et al.*, 1993; Milligan, S. C. *et al.*, 1997; Hardie, R. C. *et al.*, 2001) see Phosphoinositide Metabolism and Figure 17). Finally, when TRP channels are activated following ATP deprivation they remain active indefinitely, and long after all detectable PIP_2 has disappeared from the microvilli (Gu, Y. *et al.*, 2005). Since large amounts of DAG are also produced under all these conditions, activation cannot necessarily be attributed to PIP_2 depletion alone; however, a hypothesis worth further investigation is that channels may be activated by simultaneous generation of DAG and depletion of PIP_2. For example, the TRP protein (or associated proteins) might incorporate domains capable of binding PIP_2 and DAG (or PUFA); binding to PIP_2

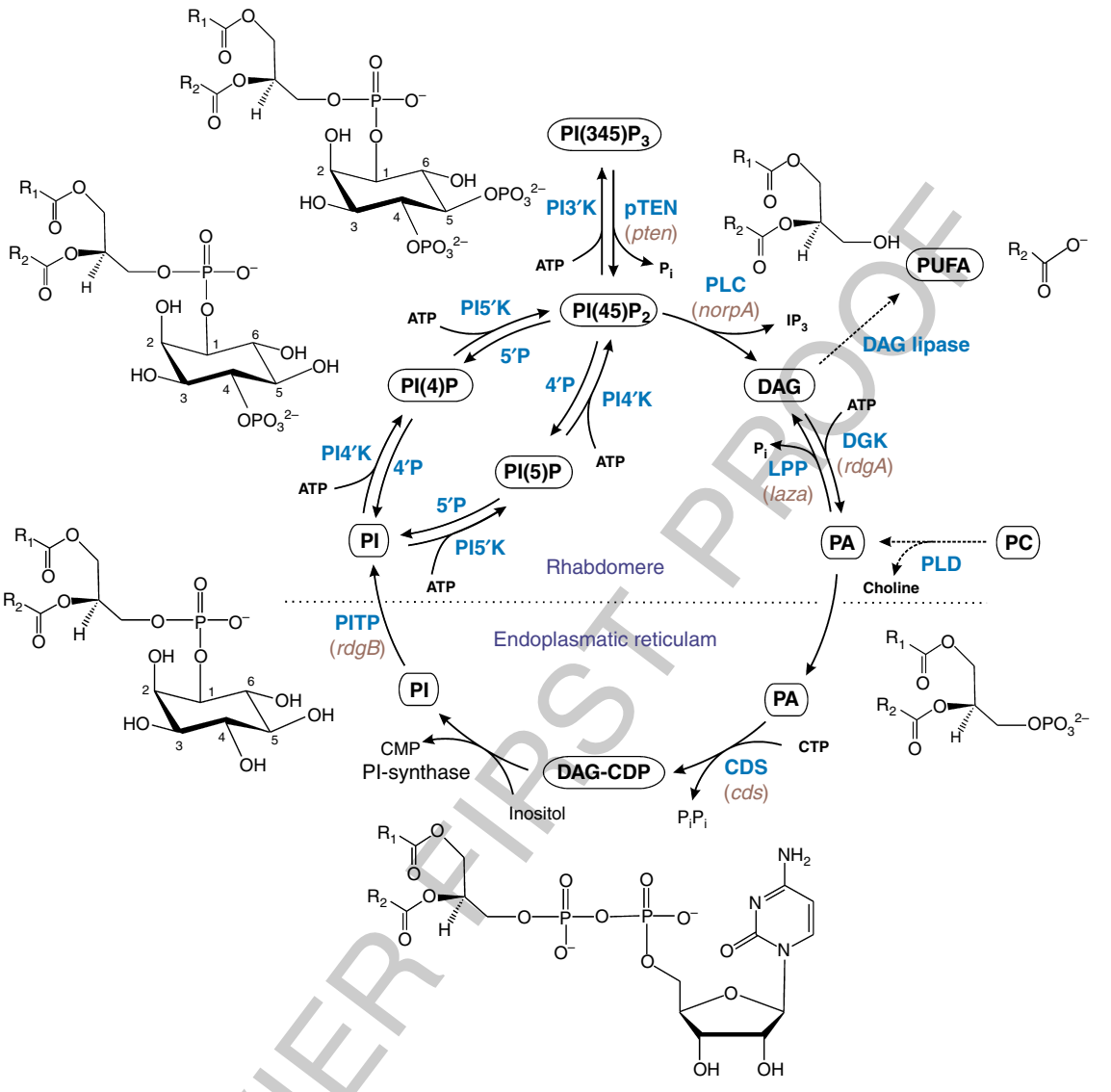

f0085 **Figure 17** Phosphoinositide cycle. PIP_2 is hydrolyzed by PLC (*norpA* gene), generating diacylgylcerol (DAG) and $InsP_3$. DAG is converted to phosphatidic acid (PA) via DAG kinase (*rdgA*), the reverse reaction (PA to DAG) is catalyzed by LPP (*laza*); DAG may also be converted to PUFAs by a DAG lipase. PA can also be synthesized *de novo* by acylation of glycerophosphate and can be released from phosphatidylcholine (PC) by PLD. PA is combined with CTP to form CDP–DAG via CD synthase (*cds*) in the SMC. This in turn undergoes condensation with inositol to form to phosphatidylinositol (PI) via PI synthase. PI is transported back to the microvillar membrane by a PI transfer protein (*rdgB*). PI is converted to PIP_2 via sequential phosphorylation (PI kinase and PIP kinase) in the microvilli to reconstitute PIP_2. PIP_2 may also be further phosphorylated to PIP_3 via PI3′ kinase and reconverted via a PIP_3-specific lipid phosphatase (pTEN).

would stabilize the closed state, whilst DAG/PUFA would stabilize the open state.

p0345 Further support for the roles of DAG and/or PIP_2 in excitation comes from recent studies of mutants (*laza*) of an eye-enriched phosphatidic acid phosphatase (PAP). More correctly referred to as lipid phosphate phosphohydrolase (LPP), this enzyme catalyzes the reverse reaction from DGK, namely PA to DAG (see Figure 17, Garcia-Murillas, I. *et al.*, 2006; Kwon, Y. and Montell, C., 2006). Analysis of *laza* mutants indicates that LPP acts antagonistically with DGK (*rdgA*) to regulate the levels of DAG and PA. Thus the normally slow response termination in the ERG of a hypomorphic *rdgA* mutant ($rdgA^3$) was accelerated in the $rdgA^3$; *laza* double mutant, but further slowed by overexpression of LPP using a

WT *laza* transgene (Garcia-Murillas, I. *et al*., 2006). Similarly, using an independently generated *laza* mutant, (Kwon, Y. and Montell, C., 2006) found that response amplitudes (measured by ERG) were reduced and response decay times accelerated in *laza* mutants. Similar genetic interactions between *laza* and *rdgA* were also seen in their retinal degeneration phenotypes – in that *laza* mutants suppress, and *laza* overexpression enhances degeneration in *rdgA* (Garcia-Murillas, I. *et al*., 2006).

p0350 On the one hand, these results would appear to support a role for DAG in excitation and degeneration, since *laza* mutations would be expected to decrease DAG levels (at the expense of PA), whilst overexpression of LPP would increase DAG. However, Garcia-Murillas I. *et al.* (2006) also found that PI levels are reduced in *rdgA* mutants, particularly in combination with *laza* overexpression, due, not only to the involvement of PA as substrate for PI recycling (Phosphoinositide Metabolism), but also because transcript levels of PI synthase, an essential enzyme for PIP_2 recycling were greatly reduced in these mutant backgrounds. Garcia-Murillas I. *et al.* (2006) also noted that whilst PA levels have been shown to be decreased in *rdgA* mutants (a finding which they confirm), DAG levels have been reported to remain unaltered (Inoue, H. *et al*., 1989), and therefore interpret their results as support for the suggestion that the decrease in PIP_2 may underlie the degeneration, and possibly contribute to the excessive and prolonged activation of TRP channels.

p0355 In summary, there is little evidence to support a role for $InsP_3$ in excitation in *Drosophila*, whilst a number of recent studies have suggested that the alternative, membrane-delimited products of PLC activity (i.e., DAG, PUFAs, and PIP_2) may be the relevant messengers of excitation. However, this area is still controversial and final resolution of the mechanism of excitation is likely to require, *inter alia*, identification and characterization of lipid-binding sites on the channel molecules, further biochemical analysis of light-induced lipid metabolism, and molecular identification and mutant analysis of any further gene products required for activation.

s0185 6.63.6 Ca^{2+}-Dependent Feedback and Mechanisms of Adaptation

p0360 Whilst current evidence argues that the primary agent of excitation is a membrane-delimited lipid messenger, the importance of Ca^{2+} influx via the channels as regulator of phototransduction and mediator of adaptation can hardly be overstated. This was graphically illustrated in some of the first whole-cell recordings from *Drosophila* photoreceptors investigating the effect of removing extracellular Ca^{2+} (Hardie, R. C. 1991b; Ranganathan, R. *et al*., 1991). Both onset and offset kinetics are greatly slowed, quantum bump amplitudes are reduced ~10-fold (Henderson, S. R. *et al*., 2000), and the peak–plateau transition characteristic of light adaptation is largely abolished (Figure 18). The mechanisms underlying this Ca^{2+}-dependent regulation are diverse and still not entirely understood, but they include both positive and negative feedback regulation, the latter in particular probably affecting most steps in the transduction cascade. Although Ca^{2+}-dependent positive feedback is arguably the most distinguishing feature of invertebrate phototransduction (in vertebrates, Ca^{2+}-dependent feedback is always operationally negative, see Yau, K-W., this volume), there is little information on the underlying molecular mechanism(s) in *Drosophila*. Electrophysiologically, positive feedback is manifest as a ~10-fold increase in the amplitude of the quantum bumps and an even larger increase in the absolute slope of the rising phase of the response. The feedback can be mimicked by cytosolic release of caged Ca^{2+}, which accelerates the light response with a submillisecond latency (Hardie, R. C., 1995). This would suggest that it acts at a very late stage in transduction – either on the channels themselves, and/or PLC which is facilitated by Ca^{2+} in the range from 10 nM to 1 μM (Running Deer, J. L. *et al*., 1995) (see Measuring Phospholipase C Activity and Fast Nonlinear Response Kinetics for further discussion).

6.63.6.1 Ca^{2+} Signals s0190

p0365 Crucial to an understanding of Ca^{2+}-dependent feedback is an appreciation of the Ca^{2+} signals actually experienced by the photoreceptors during stimulation.

6.63.6.1.1 Ca^{2+} signals are dominated by Ca^{2+} influx s0195

p0370 Ca^{2+} indicator dyes, including fluo-3, Ca orange, or INDO-1, loaded via the patch pipette reveal a massive and rapid light-induced rise in Ca^{2+} (Peretz, A. *et al*., 1994; Ranganathan, R. *et al*., 1994; Hardie, R. C., 1996b). Absolute estimates in *Drosophila*, made using ratiometric dyes indicate that Ca^{2+} are ~160 nM in

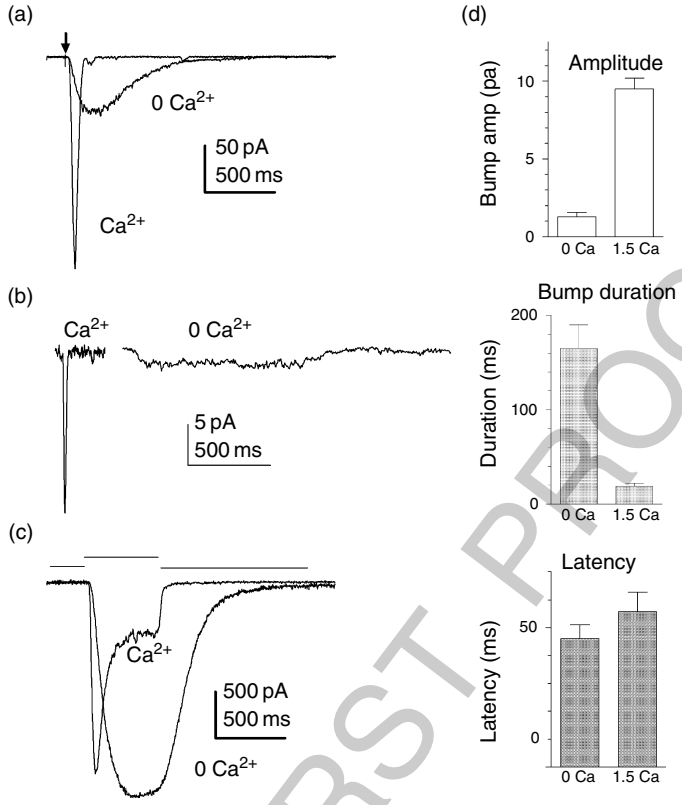

f0090 **Figure 18** Ca^{2+}-dependent feedback. (a) Responses recorded in normal bath (Ca^{2+}) and after perfusing with EGTA-buffered Ca^{2+}-free Ringer (0 Ca^{2+}) reveal the profound influence of Ca^{2+} influx on the light response. Both rising and falling phases are greatly slowed down suggesting that Ca^{2+} influx mediates both positive and negative feedback. (b) This behavior is also seen at the level of the quantum bumps, which are greatly reduced in amplitude and prolonged in the absence of external Ca^{2+}. (c) Ca^{2+} influx is also essential for light adaptation: the peak-to-plateau transition during a 500-ms stimulus is eliminated in the absence of external Ca^{2+}. (d) Quantum bump parameters; amplitude, duration (half-width), and latency, measured in normal (1.5 mM Ca^{2+}) and Ca^{2+}-free bath. Note that the amplitude is reduced and the duration increased, but the latency is unaltered. (For further details, see Henderson, S. R. *et al.*, 2000.)

the dark, and can transiently reach light-induced values of ~50 μM, measured globally throughout the cell (Hardie, R. C., 1996b). The overwhelming majority of this signal derives from Ca^{2+} influx via the light-sensitive channels, since the Ca^{2+} signal is undetectable (Peretz, A. *et al.*, 1994; Ranganathan, R. *et al.*, 1994), or greatly reduced (Hardie, R. C., 1996b) when extracellular Ca^{2+} is removed. However, a small fluorescent signal, in principle representing a rise of ~20 nM free Ca^{2+}, can still be detected with bright illumination under optimal conditions in Ca^{2+}-free solutions (Hardie, R. C., 1996b; Cook, B. and Minke, B., 1999). Whilst this signal is clearly dependent on phototransduction (e.g., it is absent in *norpA* mutants), it was not significantly reduced in $InsP_3R$ mutants (Raghu, P. *et al.*, 2000a), but was eliminated in the absence of external Na^+ (Hardie, R. C., 1996b; Cook, B. and Minke, B., 1999). It therefore can even be questioned whether it represents release from internal stores; alternative possibilities might include release of buffered Ca^{2+} or a dye artefact induced by massive (bio)chemical changes and/or monovalent ion fluxes associated with responses under these conditions.

6.63.6.1.2 Ca^{2+} transients in the rhabdomeres s0200

Notwithstanding the uncertainties concerning the origin and significance of the residual signal detected under Ca^{2+}-free conditions, the Ca^{2+} signal under physiological conditions is clearly predominantly mediated by Ca^{2+} influx via the TRP channels. TRPL channels are also permeable to Ca^{2+} and can sustain a reduced influx signal in *trp* mutants (Peretz, A. *et al.*, 1994; Hardie, R. C. 1996b) until they close following PIP_2 depletion. Both TRP and TRPL p0375

channels are localized along the length of the microvilli (Niemeyer, B. A. *et al.*, 1996), and spatial imaging of the Ca^{2+} influx in *Drosophila* also shows influx to be initially localized to the rhabdomeres (Ranganathan, R. *et al.*, 1994). Rather more accurate and informative Ca^{2+} imaging has been made in the larger fly *Calliphora*, using intracellular indicator dye-injection in the intact animal combined with imaging of the rhabdomeres through the fly's own optics (Oberwinkler, J. and Stavenga, D. G., 1998; 2000). By using a range of indicator dyes with different affinities, Ca^{2+} levels in the rhabdomeres were found transiently to reach values well in excess of 200 μM during bright illumination, before rapidly relaxing (within ~100 ms) to steady-state levels of maximally ~10 μM with the brightest illumination. Under light-adapted (LA) conditions, however, because of the reduction in gain associated with adaptation, incremental flashes generate greatly reduced inward currents and the Ca^{2+} transients in the microvilli now reached only ~50–100 μM (Figure 19). Whilst such measurements were made from the whole rhabdomere in *Calliphora*, theoretical considerations suggest that a similar situation should hold in *Drosophila*, and also that similar values are reached at the level of single microvilli in response to single-photon absorptions (Postma, M. *et al.*, 1999). In fact, the Ca^{2+} levels reached in single microvilli are probably even higher, since measurements will inevitably average the responses of both stimulated and unstimulated microvilli. The time course of the microvillar transients is also likely to be faster, as the measured responses will be smeared by the bump latency dispersion. Finally, the Ca^{2+} levels reached in individual microvilli in between photon absorptions in LA cells are likely to be lower than the measured steady-state level, again because this will represent the average of excited and unstimulated microvilli.

s0205 p0380

6.63.6.1.3 Ca^{2+} buffers and homeostasis

Invertebrate photoreceptors such as *Drosophila* experience more extreme Ca^{2+} levels than almost any other eukaryotic cells. There is relatively little information on how they cope with these levels, which probably reach a steady state of ~10 μM throughout the cell body during maintained illumination. However, appropriate regulation is vital not only for performance, but also because cell death and retinal degeneration rapidly result when levels are either too high or too low (e.g., Sahly, I. *et al.*, 1994; Alloway, P. G. *et al.*, 2000; Kiselev, A. *et al.*, 2000a; Raghu, P. *et al.*, 2000b; Yoon, J. *et al.*, 2000; Wang, T. *et al.*, 2005a; 2005b). By far, the dominant extrusion mechanism is a Na^+/Ca^{2+} exchanger (encoded by the *calx* gene), which is highly expressed in the

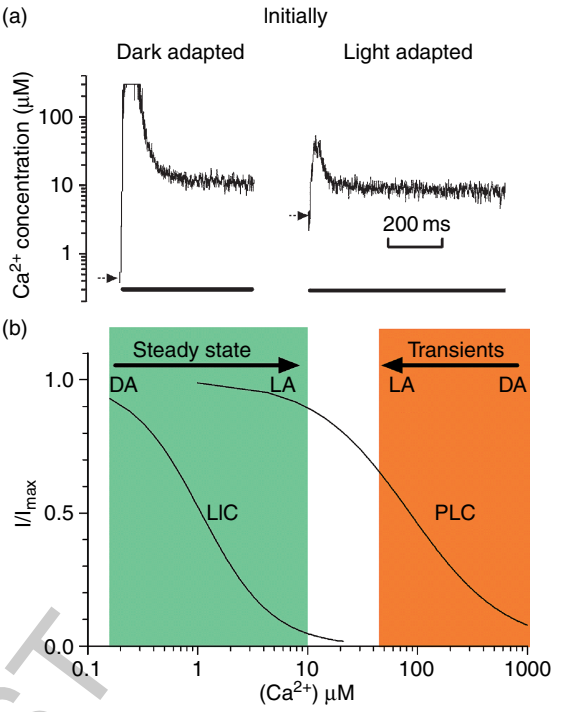

f0095

Figure 19 Ca^{2+} signals and adaptation strategy. (a) Ca^{2+} concentration measured in the rhabdomeres of the larger fly *Calliphora* in the intact animal using confocal imaging of the rhabdomeres via the intact optics. Cells were impaled with sharp intracellular microelectrodes containing the dye Oregon Green 5N. *Left*: in an initially dark adapted cell, Ca^{2+} rises from a submicromolar resting level (arrow) to values in excess of 200 μM (saturation level of the dye), before relaxing to a steady-state level of ~10 μM within ~200 ms. *Right*: in an initially light adapted cell, Ca^{2+} rises from an initial level of ~3 μM (arrow) to ~50 μM, relaxing now even more rapidly to a new steady state of 10 μM. (Adapted with permission from Oberwinkler, J. and Stavenga, D. G., 2000.) (b) Based on these findings, as well as on detailed theoretical considerations, the global steady-state Ca^{2+} levels in the microvilli and cell body are believed to vary from ~150 nM in the dark to ~10 μM as background intensity is raised, whilst the transients experienced during incremental flashes (and at the level of microvilli, in response to single photons) vary from ~1 mM in dark adapted cells to ~50 μM in light-adapted cells. The curves show the Ca^{2+} dependence of the inhibition of the light-induced current and channels (LIC) with an IC_{50} of ~1 μM, and of PLC (IC_{50} ~75 μM) determined by manipulation of the Na^+/Ca^{2+} exchanger. This suggests that the gain during steady-state adaptation is primarily determined by the Ca^{2+}-dependent inhibition of TRP channels, whilst the transients experienced during the quantum bumps are sufficient to inhibit PLC, thereby preventing excessive PIP_2 hydrolysis. (Adapted with permission from Gu, Y. *et al.*, 2005.)

microvillar membrane, where it can generate electrogenic Na^+/Ca^{2+} currents of at least 100 pA during Ca^{2+} extrusion. *calx* mutants show greatly reduced sensitivity to light, and response inactivation during continued illumination due to the Ca^{2+} overload, as well as severe and rapid light-dependent retinal degeneration due to Ca^{2+} cytotoxicity (Wang, T. *et al*., 2005b).

p0385 The cell body also contains Ca^{2+} stores, which can release enough Ca^{2+} to raise intracellular Ca^{2+} by a few 100 nM when their thapsigargin-sensitive Ca ATPase is inhibited. Although it is debatable whether the stores normally play any direct role in transduction, the Ca^{2+} relased following application of thapsigargin or ionomycin is sufficient to facilitate responses to light recorded in Ca^{2+}-free solutions (Hardie, R. C., 1996a). The cell body and microvilli also contain a variety of Ca^{2+}-binding proteins that may function as Ca^{2+} buffers. Firstly, the microvilli have an unusually high level (~0.5 mM) of CaM (Porter, J. A. *et al*., 1993), which may function as a buffer in addition to other roles described below (Calmodulin). Because of the high surface area-to-volume ratio in the microvillar lumen, low-affinity Ca^{2+} binding to negatively charged phospholipids may also be important. The cell body expresses at least two major Ca^{2+}-binding proteins, calphotin and calnexin. Calphotin is a novel Ca^{2+}-binding protein, which is enriched in the eye and found throughout a large, but distinct central region of the cell body. This region was also found to precipitate Ca oxalate, leading to speculation that it may represent a Ca^{2+}-sequestering sponge (Ballinger, D. G. *et al*., 1993; Martin, J. H. *et al*., 1993). Photoreceptors in *calphotin* mutants show severe developmental abnormalities, but calphotin's role as a buffer has not been further investigated (Yang, Y. and Ballinger, D., 1994). Calnexin is a molecular chaperone, and is required, along with the cyclophilin *ninaA* for Rh1 folding and targeting. However, it also appears to play a role as a Ca^{2+} buffer, since Ca^{2+} measurements reveal that abnormally high Ca^{2+} levels are reached during maintained illumination in *calnexin* mutants, whilst the photoreceptors also undergo light-dependent retinal degeneration that cannot be attributed to calnexin's role as a chaperone (Rosenbaum, E. E. *et al*., 2006).

6.63.6.2 Ca^{2+}-Dependent Negative Feedback

s0210

p0390 Although a number of Ca^{2+}-dependent feedback targets have been identified in the transduction cascade (Table 3), until recently their respective contribution to light adaptation and response termination was rather poorly defined. A major advance in this respect was made recently by exploring the Ca^{2+} dependence of phototransduction by exploiting the properties of the Na^+/Ca^{2+} exchanger (CalX) to manipulate

t0015 **Table 3** Molecular targets for Ca^{2+}-dependent feedback

Transduction protein	***Biochemical information***	***Function of feedback***
TRP	*In vivo* PKC substrate; contains CaM-binding site (CBS)	Ca^{2+}-dependent facilitation and inhibition
TRPL	*In vitro* PKC substrate; two CBS	Ca^{2+}-dependent inhibition
PLC (*norpA*)	Contains a Ca^{2+}-binding C2 motif. Inhibition is PKC dependent	Ca^{2+}-dependent regulation
INAD	*In vivo* PKC substrate; CBS	Unknown
Arrestin 2	CaMKII substrate	Prevents sequestration with M
Arrestin 1	CaMKII substrate	Unknown
	Substrates/binding partners	***Function***
Mediators (Ca^{2+}-dependent enzymes/binding protein)		
PKC (*inaC*)	TRP, INAD, NINAC	Ca^{2+}- (and DAG)-dependent inactivation
Rh phosphatase (*rdgC*)	CaCaM dependent	Rhodopsin dephosphorylation
CaMKII	Arr2 and Arr1	Pigment cycle
Calmodulin (*cam*)	TRP, TRPL, CaMKII, NINAC, INAD, RDGC	Ca^{2+}-dependent inactivation

Proteins reported to be subject to Ca^{2+}-dependent regulation. Protein targets have been separated into transduction proteins and mediators – i.e., Ca^{2+}-dependent enzymes and binding proteins. See text for further details and reference (Ca^{2+}-Dependent Feedback and Mechanisms of Adaptation and Molecular Strategies of Quantum Bump Generation and Adaptation).

cytosolic Ca^{2+} in the microvilli (Gu, Y. *et al*., 2005). The CalX exchanger, which is highly expressed in the microvilli (Wang, T. *et al*., 2005b), belongs to the NCX family of exchangers, which have a stoichiometry of $3Na^{+}$:$1Ca^{2+}$, and as such should drive cytosolic Ca^{2+} toward an equilibrium determined by membrane voltage, the transmembrane Na^{+} gradient and extracellular Ca^{2+}. By simply varying external Na^{+}, therefore, it is possible in principle to systematically manipulate cytosolic Ca^{2+} concentration to virtually any desired level. Using this approach it was shown that the LIC was sensitively inhibited by Ca^{2+} in the range 0.1–10 μM with an IC_{50} of ~1 μM Ca^{2+} (Gu, Y. *et al*., 2005). Raising Ca^{2+} in this range in the dark also quantitatively mimicked the major features of light adaptation (gain reduction, parallel shift of V/log I curves and response acceleration). In marked contrast, PLC activity, monitored using the PIP_2 biosensor channels (Kir2.1), was completely unaffected over this range and was only inhibited by much higher Ca^{2+} levels (IC_{50} ~ 75 μM) indicating that the major features of light adaptation are mediated downstream of PLC (Figure 19, Gu, Y. *et al*., 2005). An obvious target is the TRP channel that was also found to be inhibited by Ca^{2+} with an IC_{50} of ~1 μM. The very rapid time constant (1–2 ms) of Ca^{2+}-dependent inactivation of TRP, previously determined by applying hyperpolarizing voltage steps or by release of caged Ca^{2+}, suggests a direct mechanism, possibly with the involvement of CaM (Hardie, R. C. and Minke, B., 1994a; Hardie, R. C., 1995). These results thus suggested that the major features of light adaptation appear to be accounted for by Ca^{2+}-dependent inhibition of the light-sensitive channels, the final output stage of the transduction cascade.

p0395 Whilst apparently not directly contributing to light adaptation, the inhibition of PLC activity by higher levels of Ca^{2+}, which probably occur only during the Ca^{2+} transients, appears to be an essential mechanism to prevent depletion of PIP_2 during illumination. This inhibition fails not only in the absence of external Ca^{2+}, but also in *trp* mutants, apparently because the reduced Ca^{2+} influx through the less abundant, and less Ca^{2+}-permeable TRP channels is insufficient to generate the high Ca^{2+} levels required to inhibit PLC activity. The evidence for this again came from experiments using Kir2.1 biosensor channels to monitor PIP_2 hydrolysis (Figure 20): under normal conditions, illumination equivalent to bright daylight results in only very modest reductions of PIP_2 levels in the rhabdomere; however, in *trp* mutants even much weaker

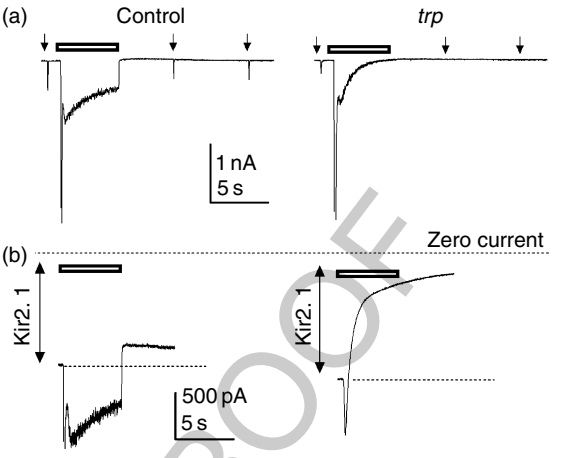

f0100 **Figure 20** The *trp* decay phenotype is associated with depletion of PIP_2. (a) Whole-cell recordings of response in wild type (WT) (control) and *trp* mutant to a 5-s light stimulus (~30 000 photons per second). Whilst the WT response shows the typical peak–plateau transition due to light adaptation, the response in *trp* decays to baseline. Furthermore, responses to brief test flashes are completely eliminated following the decay in *trp*. (b) The same stimulus, now applied to WT and *trp* mutants expressing the PIP_2-sensitive Kir2.1 channel (see Figure 14). In both cases, the constitutive current of 1–2 nA (double arrows) indicates the response of Kir2.1 to prevailing dark levels of PIP_2. In the WT fly, following illumination there is only a minor reduction in the Kir2.1 current; however, in *trp* the Kir2.1 current is almost entirely suppressed, indicating hydrolysis of the majority of PIP_2. This suggests that Ca^{2+} influx via the TRP channel is required to inhibit PLC activity, and that failure of this inhibition leads to a catastrophic loss of PIP_2, accounting for the *trp* phenotype (Hardie, R. C. *et al.*, 2001).

illumination results in hydrolysis of virtually all detectable PIP_2 (Hardie, R. C. *et al*., 2001), with an intensity dependence similar to that of the *trp* decay phenotype (Hardie, R. C. *et al*., 2004). The exhaustion of PLC substrate (PIP_2) due to failure of Ca^{2+}-dependent inhibition of PLC activity thus provides a satisfying explanation for the long debated transient receptor potential *trp* phenotype, which had previously been attributed to depletion of intracellular Ca^{2+} stores (Cook, B. and Minke, B., 1999) or Ca^{2+}-/CaM-dependent inactivation of the TRPL channel (Scott, K. *et al*., 1997).

p0400 The mechanism by which such high levels of Ca^{2+} inhibit PLC activity remains unsolved. Gu Y. *et al.* (2005) also found that PIP_2 levels were depleted by illumination in the PKC mutant *inaC* even more sensitively than is the case in the *trp* mutant, suggesting that the inhibition of PLC is PKC dependent (see Protein Kinase C).

s0215 ### 6.63.6.2.1 Calmodulin

p0405 Effects of Ca^{2+} are often mediated by small Ca^{2+}-binding proteins (EF hand proteins), several of which have been implicated in feedback control in vertebrate rods and cones (see Yau K-W., this volume). In *Drosophila*, however, only one, the ubiquitously expressed CaM, has been implicated in phototransduction, where it acts on several target proteins (Table 3). CaM is highly localized in the microvilli, where it is expressed at unusually high levels (~0.5 mM), potentially enough to function as a Ca^{2+} buffer in addition to more direct roles (Porter, J. A. *et al.*, 1993). The major CaM-binding protein in the eye is the NINAC class III myosin (Myosin Kinase NINAC) (Porter, J. A. *et al.*, 1992), and the concentration of CaM in the microvilli is greatly reduced in *ninaC* mutants lacking the microvillar 174-kDa splice variant (Porter, J. A. *et al.*, 1993). These $ninaC^{\Delta 174}$ mutants also have a response deactivation defect and an abnormally large plateau response, which appears to be largely attributable to the reduced CaM level, since it can be mimicked in a mutant in which the CaM-binding site (CBS) alone has been deleted from the NINAC protein (Arnon, A. *et al.*, 1997a).

p0410 Further insight into CaM function has come from analysis of CaM hypomorphic mutants (*cam*) expressing less than 10% of the normal protein levels. *cam* mutants have even more pronounced defects in response termination than *ninaC*, and the kinetics of response termination no longer show an obvious dependence on external Ca^{2+} concentration (Scott, K. *et al.*, 1997). Closer examination revealed that the slow responses are predominantly a consequence of multiple bump trains in response to single-photon absorptions. Since these are similar to responses in *arr2* mutants (Figure 10), and are more or less abolished on a *Gαq* mutant background, Scott, K. *et al.* (1997) concluded that the defect was upstream of G protein and represented a defect in rhodopsin inactivation. They also found that the CaMKII phosphorylation of Arr2 was largely abolished in these flies. As discussed above (Arrestin Phosphorylation) however, Arr2 phosphorylation *per se* is not required for M inactivation by Arr2, so this result implies either an alternative role of CaM in M inactivation, or, as appears to be the case in the $Arr2^{S366A}$ mutant (which lacks the CaMKII phosphorylation site), that Arr2 in these flies becomes unavailable due to permanent sequestration in M–Arr2 complexes. As discussed in Rhodopsin Kinase and Phosphatase, another CaM target is rhodopsin phosphatase (encoded by *rdgC*), which is a Ca–CaM-dependent enzyme, though again the dephosphorylation of rhodopsin is not believed to impact directly upon the light response.

p0415 Both TRP and TRPL proteins also have one or more CBSs (Warr, C. G. and Kelly, L. E., 1996; Chevesich, J. *et al.*, 1997) and both channels are subject to Ca^{2+}-dependent inactivation (Hardie, R. C. and Minke, B., 1994a; Reuss, H. *et al.*, 1997; Scott, K. *et al.*, 1997). The TRP protein has one consensus CBS in the C-terminal; peptide fragments containing this region bind CaM in a Ca^{2+}-dependent manner *in vitro* (Chevesich, J. *et al.*, 1997), but the role of the TRP CBS has not been analyzed *in vivo*. *In vitro* studies indicate that one of the two CBS's in TRPL is conventional, binding CaM in a Ca^{2+}-dependent fashion, whilst the other (CBS2) binds the Ca^{2+}-free form of CaM, with dissociation occurring at high Ca^{2+} concentrations (>10 μM) (Warr, C. G. and Kelly, L. E., 1996). Warr C. G. and Kelly L. E. (1996) also found that CaM binding to the conventional CBS1 was modulated by both PKA and PKC phosphorylation *in vitro*. Scott K. *et al.* (1997) reported that transgenic flies expressing TRPL protein in which CBS1 had been deleted had abnormally long light responses with reduced Ca^{2+}-dependent inactivation.

s0220 ### 6.63.6.2.2 Protein kinase C INAC

p0420 An eye-enriched PKC is a core member of the INAD signaling complex (Figure 6, Scaffolding Protein INAD), and is encoded by the *inaC* gene (Smith, D. P. *et al.*, 1991). The *inaC* PKC is a classical PKC with >50% identity to vertebrate PKCβs and PKCαs. Like them, it is presumed to be activated by a combination of DAG and Ca^{2+} via its two putative C1 domains (DAG binding) and one Ca^{2+}-binding C2 domain (reviewed in Shieh, B. H. *et al.*, 2002). INAC has at least two known *in vivo* substrates in the eye, namely the TRP channel and the INAD scaffolding protein (Huber, A. *et al.*, 1996b; 1998; Liu, M. *et al.*, 2000). The TRPL protein and the class III myosin NINAC have also been reported as *in vitro* targets for PKC phosphorylation (Warr, C. G. and Kelly, L. E., 1996; Li, H. S. *et al.*, 1998).

p0425 The *inaC* mutant has a specific deactivation defect, with flash responses showing a residual tail that decays slowly over 1–2 s (Figure 10) (Smith, D. P. *et al.*, 1991; Hardie, R. C. *et al.*, 1993). The deactivation phenotype is masked in recordings made in Ca^{2+}-free solutions (i.e., WT and *inaC* mutant responses are now similar), consistent with a defect in Ca^{2+}-dependent inactivation (Ranganathan, R. *et al.*, 1991). Although the deactivation defect in

macroscopic responses resembles that in the *arr2* mutant, in *arr2* this results from each photon giving rise to a train of apparently normal bumps (Scott, K. *et al.*, 1997), whilst in *inaC* the defect occurs at the level of individual quantum bumps, which also show a similar waveform (Figure 10, Hardie, R. C. *et al.*, 1993). During sustained bright illumination, the response in *inaC* eventually decays to baseline, reminiscent of the *trp* phenotype (Hardie, R. C. *et al.*, 1993). Experiments using the Kir2.1 PIP_2 biosensor indicated that such responses are associated with a complete loss of PIP_2. This was interpreted as a requirement for PKC for the Ca^{2+}-dependent inhibition of PLC (Gu, Y. *et al.*, 2005). Failure to terminate PLC activity may thus explain the major features of the *inaC* phenotype:

(1) the prolonged response, which could be interpreted as prolonged production of excitatory messenger (DAG and/or PIP2 reduction), and
(2) the response decay with prolonged illumination due to PIP_2 depletion.

p0430 The mechanism by which PKC might inactivate PLC remains unclear, since PLC is not believed to be a direct substrate of PKC. However, since PLC is coupled to INAD in the signalplex, one possibility is that PLC activity could be modulated indirectly by the phosphorylation of INAD.

p0435 Recently, PKC was also shown to have an additional, and separable effect on the TRP channel. Popescu D. C. *et al.* (2006) identified a PKC phosphorylation site (Ser^{982}) on the TRP protein, and found that flies expressing TRP channels in which the site was mutated to alanine (TRP^{S982A}) showed a deactivation defect, which was, however, less pronounced than that in an *inaC* null mutant. Interestingly though, the phenotype was very similar to that observed in the $InaD^{P215}$ mutant, which has a point mutation in the PDZ domain responsible for binding TRP (Shieh, B. H. and Zhu, M. Y., 1996). This suggests that the association of TRP with INAD is required for its efficient phosphorylation by PKC. Despite this demonstration of PKC's role in TRP channel termination, it is important to note that the Ca^{2+}-dependent inhibition of the TRP channel is still essentially unaltered in *inaC* mutants (Gu, Y. *et al.*, 2005).

s0225 6.63.7 Phosphoinositide Metabolism

p0440 Maintenance of the substrate for PLC, PIP_2 is crucial to the functioning of the transduction cascade, as witnessed by the loss of all response when PIP_2 levels collapse, after failure of the Ca^{2+}-dependent inhibition of PLC in the *trp* mutant. PIP_2 recycling involves a number of steps, summarized in Figure 17, which are believed to take place partly in the microvillar membrane and partly in the ER (i.e., the underlying SMC). Following complete depletion of PIP_2 in the rhabdomere by illumination in the *trp* or *trpl;trp* mutant, PIP_2 levels are restored with a halftime of ~60 s, as monitored either by Kir2.1 channels (see Figure 14), or by the time course for the recovery of the light response in the *trp* mutant (Hardie, R. C. *et al.*, 2001; Hardie, R. C. *et al.*, 2004). Indirect arguments suggest that the final steps in the microvilli (sequential phosphorylation of PI by PI and PIP kinases) are likely to be fast (seconds or subsecond), supplying PIP_2 essentially on demand (Hardie, R. C. *et al.*, 2001). This suggests that the rate-limiting step in recycling is likely to reside in a different part of the cycle, possibly slow transfer of lipids (e.g., PI) between the microvillar membrane and the ER, which form separate membrane containing compartments.

6.63.7.1 RDGA, CDP–DAG Synthase, and PI Synthase s0230

p0445 The first step in PI recycling after PIP_2 hydrolysis is the phosphorylation of DAG by DGK (encoded by *rdgA*) to form phosphatidic acid (PA), which also appears to be a key event in the termination of the light response (Evidence for Activation by Lipid Messengers). As discussed in PIP_2 Depletion, the reverse reaction (dephosphorylation of PA to DAG) is catalyzed by LPP. The balance of activity between DGK and LPP appears to be crucial in determining the amount of PA available for PI recycling, and accordingly, *rdgA* mutants have significantly reduced PI and PIP_2 levels (Hardie, R. C. *et al.*, 2004; Garcia-Murillas, I. *et al.*, 2006). Recent evidence, suggests that PA derived from DAG is the major source of PA for PI recycling in the photoreceptors (Garcia-Murillas, I. *et al.*, 2006), but it may not be the only source. PA can be synthesized *de novo* (by acylation of glycerophosphate) and can also be generated by hydrolysis of phosphatidylcholine (PC) by the action of phospholipase D (PLD). Two recent studies of a *Drosophila* PLD mutant have suggested that PA derived from PC may also play a role in phototransduction and/or PI recycling (Lalonde, M. M. *et al.*, 2005; Kwon, Y. and Montell, C., 2006). However, an earlier biochemical study failed to find any evidence

for involvement of PLD in PA synthesis in the *Drosophila* eye (Inoue, H. *et al.*, 1989).

p0450 PA is combined with CTP to form CDP–DAG by CDP–DAG synthase. A mutant in an eye-enriched isoform of this enzyme (*cds*) has a rather similar phenotype to *trp*, showing a loss of response after repeated stimulation, which could be restored by providing PIP_2 to the cell via the patch pipette (Wu, L. *et al.*, 1995). Strong evidence for essentially irreversible depletion of PIP_2 during continuous illumination was also provided by expressing the PIP_2 Kir2.1 biosensor channels in *cds* mutants (Hardie, R. C. *et al.*, 2002). In common with other mutants in the PI recycling pathway, *cds* mutants also undergo a light-dependent degeneration, which is rescued by the *norpA* (PLC) mutation PLC (Wu, L. *et al.*, 1995).

p0455 The next step in the PI cycle is the condensation of inositol and CDP–DAG to form phosphatidylinositol (PI) via the enzyme PI synthase. *Drosophila* contains only one PI synthase gene, and interestingly, its transcript levels are significantly reduced in the *rdgA* mutant and almost eliminated when LPP (*laza*) is overexpressed on the *rdgA* background (Garcia-Murillas, I. *et al.*, 2006). This suggests that PA, which is also severely reduced in these genetic backgrounds, may be a transcriptional regulator of this gene.

s0235 6.63.7.2 RDGB and PI Kinases

p0460 The reactions catalyzed by CDP–DAG synthase and PI synthase are presumed to take place in an ER compartment, probably the SMC. PI is then believed to be returned to the microvillar membrane by a PI transfer protein (PITP) encoded by the *rdgB* gene (Vihtelic, T. S. *et al.*, 1991; 1993), originally isolated as another light-dependent retinal degeneration mutant. Unlike previously characterized PITPs, which are soluble ~35 kDa proteins, RDGB protein is a 161-kDa integral membrane protein. However its N-terminal has ~40% identity with the soluble PITP proteins, and in the meantime, mammalian homologues of *Drosophila rdgB* have been discovered, defining a new class (Class II) of mammalian PITP proteins with similar topology (reviewed in Cockcroft, S., 2001).

p0465 Experiments with PIP_2 biosensors confirmed that PIP_2 recycling is effectively blocked in *rdgB* mutants (Hardie, R. C. *et al.*, 2001); however, there are indications that RDGB may have additional roles in the photoreceptors. For example, a point mutation in the PI transfer domain (T59E) restored PI transfer capability in an in *vitro* assay, but still resulted in a dominant retinal degeneration phenotype, and in reduced levels of rhodopsin (Milligan, S. C. *et al.*, 1997). More generally, there is considerable evidence that mammalian *rdgB* homologues play multiple roles in membrane trafficking, including vesicle biogenesis and regulated exocytosis (Cockcroft, S., 2001; Allen-Baume, V. *et al.*, 2002).

p0470 Finally, PI must be sequentially phosphorylated by PI kinase and PIP kinase. There are several such kinases in the *Drosophila* genome, but which of them are involved in photoreceptors has yet to be unequivocally determined. The conventional route for PIP_2 synthesis would include phosphorylation of PI to PI(4)P by PI-4 kinase, followed by phosphorylation by a type I PIP kinase to PI(4,5) P_2. There are two type I PIP kinases in *Drosophila*, and one of these (*skittles*) has recently been implicated in the photoreceptors since *skittles* mutations were reported to enhance degeneration in *rdgA* (Garcia-Murillas, I. *et al.*, 2006).

s0240 6.63.8 Molecular Strategies of Quantum Bump Generation and Adaptation

p0475 As emphasized in the introduction, not only can *Drosophila* and other arthropod photoreceptors reliably detect single quanta of light with extremely fast response kinetics, but also they are able to light adapt over the full range of daylight light intensities. Although we do not yet fully understand the mechanism of channel activation and the precise mechanisms of Ca^{2+}-dependent regulation, our current knowledge of the transduction cascade allows us to draw some general conclusions about the strategies involved achieving in this performance. At any one adaptational state the voltage-clamped macroscopic flash response is remarkably linear, simply representing the summation of the underlying quantum bumps (Figure 2, Henderson, S. R. *et al.*, 2000). The bumps themselves, however, are extremely nonlinear events with many of the characteristics of an action potential, including a threshold, positive and negative feedback and a refractory period. A key to understanding how these bumps are generated, and continue to be generated during light adaptation, is the extreme compartmentalization provided by the microvilli and possibly the ultrastructural organization of the INAD complex.

s0245 ### 6.63.8.1 Compartmentalization and Local Signaling

p0480 The suggestion, that the signal transduction machinery driving single-photon responses is largely restricted to a single microvillus, dates back to observations that response saturation occurs at light levels equivalent to each microvillus absorbing just a single photon (Howard, J. *et al.*, 1987; Hochstrate, P. and Hamdorf, K., 1990). This is supported by the close congruence of the number of channels activated during a bump (~15) with biochemical estimates of the number (25) of TRP tetramers in a microvillus (Huber, A. *et al.*, 1996a). The restriction of activation to a single microvillus is also consistent with the relatively slow lateral diffusion expected in a membrane-delimited cascade, which is likely to prevent significant diffusion beyond the boundary of one microvillus during the relatively short latent period of the bump (Figure 21).

p0485 Each of the ~30–50 000 microvilli represents a tiny volume, ~1–2 μM in length and about 60 nm in diameter. The lumen of the microvillus is connected to the massive cell body via a narrow neck (Figure 1) allowing diffusional exchange of Ca^{2+}. The membrane of a single microvillus is densely packed with about 1000 rhodopsins, and contains only a limited number of the signal transduction components: estimated at about 50 G proteins, ~100 PLCs, ~25 TRP, and ~2 TRPL channels (Figure 21, Huber, A. *et al.*, 1996a). In *Drosophila* it is likely that only the G proteins and lipids are freely diffusible. In contrast, PLC and TRP channels are part of the INAD

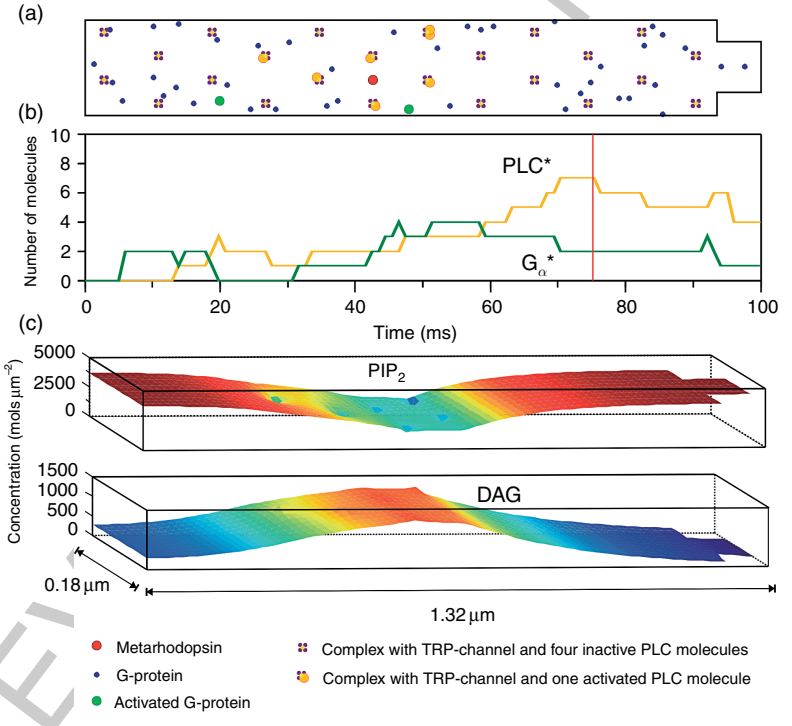

f0105 **Figure 21** Stochastic modeling of the cascade. (a) Stochastic simulation (random walk encounter) of the membrane surface of a single microvillus, 75 ms after the absorption of a single photon. In the 75 ms since absorption of a single photon, the active metarhodopsin (red) has activated 10 G proteins, eight of which have encountered and activated a PLC (yellow), and two of which (green) are still freely diffusing in the membrane. Two PLCs have also already deactivated due to the PLC-activated GTPase activity of $G_q\alpha$. (b) Time course of the numbers of activated G proteins and PLC as a function of time after photon absorption. (c) Estimated levels of PIP_2 and DAG over the surface of the microvillus generated after 75 ms by the activated PLC molecules. The simulation has used best estimates of the numbers of G proteins (50) and PLC (100) in the microvillus and typical values for diffusion coefficients of G proteins and membrane lipids from the literature. Note that, whilst finite levels of DAG have already reached ~70% of the surface area of the microvillus, no significant diffusion beyond the microvillar boundaries has occurred by this time (Postma, M. and Hardie, R. C., unpublished). According to the model of positive feedback suggested in Molecular Strategies of Quantum Bump Generation and Adaptation, once the first TRP channel opens (with relatively high DAG threshold), Ca^{2+} influx floods the microvillus within ~5 ms and facilitates activation of the remaining TRP channels to what were previously subthreshold levels of DAG (or derivative).

signaling complex (Figure 6, Scaffolding Protein INAD), which itself may be tethered to the cytoskeleton rendering it effectively immobile. Furthermore, by analogy to other arthropods (Goldsmith, T. H. and Wehner, R., 1977), it seems likely that rhodopsin itself is immobile on the timescale of transduction. Therefore G proteins are likely to act as diffusible shuttles that transduce the signal from the active M to the PLCs (Bahner, M. *et al.*, 2000). Importantly, a single rhodopsin can sequentially activate several G proteins, thereby amplifying the signal. The approximately fivefold reduction in bump amplitude in hypomorphic $G\alpha q$ mutants (Figure 12), where there is on average less than one G protein per microvillus, suggests that there may be five or so G proteins activated per rhodopsin, with an estimated minimal activation rate of 100–200 G proteins per second. After some delay, and at some distance from the activated rhodopsin, PLC molecules will be activated by $G_q\alpha$ subunits, and will start producing DAG, amplifying the signal further. DAG (or its derivative) will spread along the length of the microvillus and ultimately activate ~15 TRP channels (Figure 21).

s0250 **6.63.8.2 Fast NonLinear Response Kinetics**

p0490 The high Ca^{2+} permeability of the TRP channels and the restricted luminal volume of the microvillus results in Ca^{2+} rising as high as 1 mM throughout the microvillus during a single-photon response (see Ca^{2+} Transients in the Rhabdomeres, Figure 19, Postma, M. *et al.*, 1999; Oberwinkler, J. and Stavenga, D. G., 2000). This overwhelming Ca^{2+} rise is accompanied first by rapid facilitation, closely followed by complete inactivation of the current. Both the positive and negative feedback dominantly shape the waveform of the quantum bump (Figure 18).

p0495 The mechanism of facilitation is not known, but it is lacking in the *trp* mutant and therefore only appears to affect TRP channels. A plausible speculation is that it represents a Ca^{2+}-dependent shift in the affinity of the TRP channel for the active ligand, dramatically increasing its sensitivity, analogous perhaps to the shift in affinity to cGMP of the vertebrate CNG channels (Hsu, Y. T. and Molday, R. S., 1993). On this model, once the first channel opens, Ca^{2+} will flood the microvillus, thus further activating the TRP channels, which had been exposed to what were previously only subthreshold concentrations of the excitatory lipid messenger (e.g., DAG). Another possibility is the facilitation of PLC by Ca^{2+} (Running Deer, J. L. *et al.*, 1995; Hardie, R. C., 2005).

p0500 Most of the components of the phototransduction cascade appear to be subject to Ca^{2+}-dependent inactivation (Ca^{2+}-Dependent Negative Feedback, Table 3). Firstly, Ca^{2+}-dependent inactivation of the light-sensitive channels TRP and TRPL, either directly, or via CaM (Section 6.3), terminates the LIC AU5 (Hardie, R. C. and Minke, B., 1994a; Gu, Y. *et al.*, 2005). Secondly, the Ca^{2+}- and PKC-dependent inhibition of PLC is crucial to prevent further production of DAG and depletion of PIP_2 (Hardie, R. C. *et al.*, 2001; Gu, Y. *et al.*, 2005). Finally, recent studies strongly suggest that inactivation of *Drosophila* metarhodopsin by Arr2 is also dependent on Ca^{2+} influx (Hardie, R. C. *et al.*, in preparation-a). The requirement of Ca^{2+} influx for PLC and metarhodopsin inactivation has an elegant logic in that the upstream signals will only be terminated after the channels have been activated.

p0505 In summary, the key to fast response kinetics is a combination of the autocatalytic positive feedback loop caused by TRP channels leading to a massive Ca^{2+} influx in the restricted luminal volume of the microvillus, which then rapidly inactivates the cascade. Within 10–20 ms of the first channel opening, the single-photon response peaks and is then terminated with a time constant of about 8 ms. This contrasts with responses measured without Ca^{2+} influx, which peak at about 200 ms and have a decay time constant of about 200 ms with a ~10-fold reduction in quantum bump amplitude (Figure 18, Henderson, S. R. *et al.*, 2000). In addition, two further important concepts need to be considered, namely quantum bump latency and the refractory period.

6.63.8.3 Quantum Bump Latency s0255

p0510 After successful photon absorption, there is a finite delay before the response becomes apparent (e.g., Figure 2). This bump latency, with an average of ~45 ms, represents the time needed to open the first channel after photon absorption. Unlike vertebrate rods, which have rather invariant latencies, the bump latency in *Drosophila* is highly variable (20–100 ms), signifying on the one hand the stochastic nature of the phototransduction cascade, and on the other an effective threshold (and/or high cooperativity) for channel activation.

p0515 The stochastic variability in latency presumably originates from the low number of G proteins and

PLC molecules activated during the latent period of the quantum bump. Indeed, stochastic modeling of the cascade, based on realistic diffusion coefficients for G protein and lipids can accurately model the latency and its variability (Postma, M. and Hardie, R. C. unpublished, Figure 21). Modeling also indicates that the latency should allow sufficient time for finite quantities of a putative lipid messenger of excitation to spread by lateral diffusion throughout most of the microvillus. This may help to ensure that the majority of the TRP channels in the microvillus are activated by the Ca^{2+}-dependent positive feedback once the first channel has opened.

p0520 As well as contributing to a large gain, such a locally saturated all-or-none response could also provide an excellent mechanism for ensuring reproducibility of the single-photon response, which over the cell has a coefficient of variance of ~0.4 (Henderson, S. R. *et al.*, 2000). The variability in even this relatively tight distribution may result from variability between microvilli, because single bumps repeatedly activated in the same microvillus are even more reproducible in amplitude (Scott, K. and Zuker, C. S., 1998). This performance may be achieved however, as a trade-off against the speed of the response, since the latency distribution is somewhat slower and broader than the quantum bump waveform, and hence represents a major constraint on the macroscopic response kinetics (Figure 2).

s0260 **6.63.8.4 Refractory Period**

p0525 Another potentially important consequence of the microvillar design is that the massive Ca^{2+} influx renders the microvillus inactive for a refractory period of about 100 ms. Only when the Ca^{2+} is cleared from the microvillus and the inactivation is removed will it be responsive again. Clearance of Ca^{2+} is predicted to occur very quickly (<100 ms) by a combination of diffusion into the cell body and the Na^+/Ca^{2+} exchanger, which acts very powerfully on the microvillus because of the high surface area-to-volume ratio.

p0530 An indication of this refractory period is provided by at least two lines of evidence. Firstly, when a carefully calibrated flash is delivered, just sufficient to activate every microvillus, then a second flash delivered immediately afterward is completely ineffective. However, when delivered after ~80 ms it can generate an additional response (Hochstrate, P. and Hamdorf, K., 1990). Secondly, in certain mutants (e.g., *arr2* and *cam*), activated metarhodopsin fails to inactivate. In vertebrates, such mutants generate long-lasting quantum bumps that fail to terminate normally (Chen, J. *et al.*, 1995). However, in *Drosophila arr2* or *cam* mutants, single photons elicit a train of quantum bumps separated by an interbump interval of ~100 ms (e.g., Figure 10), but each quantum bump in the train terminates normally and is essentially indistinguishable from a WT bump (Scott, K. *et al.*, 1997). The interbump interval in such trains can thus be thought of as representing the refractory period during which activated rhodopsin can generate no response, but once this is over a second quantum bump can be generated again.

p0535 In a more conventional cascade such as in vertebrate rods, it is important that each and every stage of the transduction cascade is terminated rapidly, with the slowest step limiting the overall kinetics (see Yau, K-W., this volume). However, a strictly localized refractory period can in principle mask the effect of any moderately slow termination reactions, as long as they are completed within the refractory period. This means that the off-response kinetics at the level of the electrophysiological response can be determined by very fast Ca^{2+}-dependent channel inactivation (time constant of <10 ms), whilst other steps such as metarhodopsin–arrestin binding, GTPase activity of the G protein and PIP_2 resynthesis could in principle afford to proceed more slowly, e.g., 50–100 ms. Such a strategy could also reduce transducer noise associated with slower termination steps, which may be slow because of biophysical constraints, e.g., slow binding or enzymatic reactions.

6.63.8.5 Adaptation s0265

p0540 The microvillar design is also central to light adaptation, and in particular the ability of invertebrate photoreceptors to respond over the entire range of environmental intensities. With a refractory period of 100 ms (and probably less when light adapted), each individual microvillus should be able to generate quantum bumps at a rate of $\geq 10\,s^{-1}$. With ~45 000 microvilli in *Drosophila*, and more in the larger flies, this should allow the photoreceptors to process photon absorptions approaching $10^6\,s^{-1}$ – precisely the sorts of levels experienced under bright daylight conditions. This alone is not enough however, and to sustain such large photon fluxes without saturation, the light response needs to adapt by reducing gain. As in virtually all photoreceptors, this is achieved in the first instance by negative feedback regulation mediated primarily by Ca^{2+}, resulting in a progressive shifting

of the intensity-response function curve, optimizing the dynamic range around the prevailing background light intensity. Early shot noise analysis in the 1970s and 1980s indicated that discrete quantum bumps continue to underlie the macroscopic response even under bright backgrounds, but that their amplitude and duration progressively decrease, giving rise to the adapting bump model of light adaptation, which still holds today (Wu, C. F. and Pak, W. L., 1978; Wong, F. *et al*., 1980).

p0545 As discussed earlier (Ca^{2+} Signals), the microvillar design results in a distinction between

(1) global steady-state Ca^{2+} levels, (~150 nm in the dark to maximally ~10 μM in the light), that are reached throughout the cell, including the unstimulated microvilli, and
(2) the rapid microvillar transients, associated with each and every quantum bump that are maximally ~1 mM during the DA quantum bump, but only ~50–100 μM during the greatly attenuated LA quantum bumps (Figure 19).

p0550 In *Drosophila*, although Ca^{2+}-dependent feedback is found at virtually all stages of the cascade, our recent studies (see Ca^{2+}-Dependent Negative Feedback) suggest that the dominant mechanism for gain reduction during steady-state adaptation is the Ca^{2+}-dependent inhibition of the TRP (and TRPL) channels, which are inhibited with an IC_{50} of ~1 μM over a range that closely maps onto the global steady-state range of Ca^{2+} levels experienced during light adaptation (Figure 19). Although the mechanism is not fully understood, these relatively low concentrations of Ca^{2+} reduce the gain and shorten the duration of the quantum bump sufficiently to account for the major features of light adaptation, including the parallel shift of the response intensity function. By contrast, upstream activity of PLC appears not to be affected by these relatively low global Ca^{2+} levels, but importantly, it is inhibited over the range experienced during the rapid Ca^{2+} transients (Figure 19, Gu, Y. *et al*., 2005).

p0555 This bipartite strategy (Ca^{2+}-dependent inhibition of channels by low global Ca^{2+} levels, and inhibition of upstream components such as PLC and M by rapid transients) can be seen as an effective solution for light adaptation, allowing for rapid response kinetics without exhausting the finite supply of PIP_2 required for phototransduction. Bump latency is a major determinant of response kinetics, and is itself critically dependent upon PIP_2 hydrolysis to generate sufficient lipid messenger to overcome threshold for channel activation. Hence it is presumably important to maintain high PLC activity during light adaptation so as not to compromise latency. However, as shown by measurements with Kir2.1 PIP_2 biosensors (Figures 14, 20), the rate of light-induced PLC activity in the microvilli is so high that it is sufficient to deplete the entire microvillus of PIP_2 in less than 1 s. The solution therefore is to rapidly terminate PLC activity by Ca^{2+} influx, but only after the bump has been initiated. The collapse of the light response due to exhaustion of PIP_2 in the *trp* mutant, or in Ca^{2+}-free bath, shows the disastrous consequences when this Ca^{2+}- (and PKC)-dependent inhibition fails (Figure 20).

p0560 Whilst accounting for many of the major features of light adaptation, this overview of adaptation is clearly an oversimplification. The overall output of the cell during adaptation is also influenced by many other factors, working on a variety of timescales. In particular, the description above has considered only the voltage-clamped LIC. In the physiologically relevant voltage domain, gain and kinetics will be further moderated by the passive and active (mainly voltage-dependent K^+ channels) properties of the membrane (Potassium Channels); by the voltage-dependent Mg^{2+} block of the TRP channels, which reduces the effective single-channel conductance at depolarized membrane potentials (Channel Properties) and by synaptic feedback from higher-order interneurons (Zheng, L. *et al*., 2006). As described in Photoreceptor and Retinal Morphology every photoreceptor also has an autonomous pupil mechanism, whereby tiny pigment granules migrating toward the rhabdomere can reduce the effective light flux by up to two orders of magnitude. Photoreceptors in white-eyed mutants lacking this pupil saturate under bright illumination, indicating that this is an essential mechanism to avoid saturation under the brightest daylight intensities (Howard, J. *et al*., 1987). Finally translocation of transduction components like G proteins (G_q Translocation), TRPL channels (TRPL Translocation), and arrestin (Arrestin Translocation), can fine-tune the gain and sensitivity during long-term adaptation.

6.63.9 Phototransduction Mechanisms in Other Invertebrates s0270

6.63.9.1 Other Arthropods s0275

p0565 It seems likely that all arthropod photoreceptors respond to light using a G_q-/PLC-based cascade resulting in a membrane depolarization. However,

detailed information is restricted to relatively few preparations (notably *Limulus*, honeybee, crayfish, barnacle, and locust). Before the advent of molecular approaches, *Limulus* had been most extensively studied, and was the preferred preparation because of the large photoreceptors in the ventral eye, which allow stable intracellular recordings, and simultaneous impalement with several electrodes.

s0280 ### 6.63.9.1.1 *Limulus*

p0570 In *Limulus* ventral photoreceptors, the role of $InsP_3$ as a messenger of excitation is well established. Injections of $InsP_3$ and Ca^{2+} itself both mimic the response to light (Brown, J. *et al.*, 1984; Fein, A. *et al.*, 1984; Bolsover, S. and Brown, J., 1985; Payne, R. *et al.*, 1986) and it is clear that $InsP_3$ activates $InsP_3$ receptors on the SMC, resulting in release of Ca^{2+} from intracellular stores which can raise free cytosolic Ca^{2+} to $\sim$150 μM (Payne, R. *et al.*, 1986; Ukhanov, K. and Payne, R., 1995; Nasi, E. *et al.*, 2000). Despite compelling evidence for $InsP_3$ and Ca^{2+} as messengers of excitation in *Limulus*, the only substance that has been found to activate channels in excised patches from the microvillar membrane is cGMP (Bacigalupo, J. *et al.*, 1991). This has led to the proposal that generation of cGMP by a Ca^{2+}-dependent guanylate cyclase represents the final enzymatic component of the transduction cascade (Shin, J. *et al.*, 1993). Although there is no direct biochemical or molecular evidence for the presence of this enzyme, inhibitors of particulate guanylate cyclase severely attenuate the response to light (Garger, A. *et al.*, 2001), and a cGMP-gated ion channel has also recently been cloned from *Limulus*, which immunolocalizes to the microvillar membrane (Chen, F. H. *et al.*, 2001).

p0575 It has been suggested that this sequence of events accounts for the entire light response (Shin, J. *et al.*, 1993); however, a number of studies have reported that there may be three distinct classes of light-sensitive channels in *Limulus* (reviewed in: Nagy, K., 1991; Dorlochter, M. and Stieve, H., 1997; Nasi, E. *et al.*, 2000). These may correspond to three kinetic components of the light response that can be revealed by their differential recovery from light adaptation and distinct pharmacologies (Deckert, A. *et al.*, 1992; Nagy, K. *et al.*, 1993; Contzen, K. and Nagy, K., 1995; Nagy, K. and Contzen, K., 1997). This led to the suggestion that there may be parallel pathways involving three distinct G proteins, one operating via PLC and $InsP_3$, one via a guanylate cyclase, and one via adenylate cyclase (Dorlochter, M. and Stieve, H., 1997).

p0580 In an intriguing recent development, a *Limulus trp* homologue was cloned and found to be expressed in the ventral photoreceptors. Furthermore, the same authors found that a DAG analogue injected into the photoreceptors activate an inward current synergistically with Ca^{2+}, with electrical characteristics similar to the light-activated current (Bandyopadhyay, B. C. and Payne, R., 2004). This raises the possibility that at least one component of phototransduction in *Limulus* may be similar to *Drosophila*; i.e., a DAG-activated TRP channel. *Limulus* differs from *Drosophila* in that the light-induced current is essentially impermeable to Ca^{2+}, and therefore, the Ca^{2+}-dependent facilitation is provide by $InsP_3$-induced Ca^{2+} release, instead of Ca^{2+} influx as is the case in *Drosophila* (reviewed in Nasi, E. *et al.*, 2000).

p0585 Interestingly, quantum bumps in *Limulus* share many common features with those in *Drosophila*, including variable latency, low first stage (R-G) gain (Kirkwood, A. *et al.*, 1989), threshold, and positive and negative feedback by Ca^{2+}. However, there are also significant differences; firstly, the bump is mediated by several thousand channels spread over dozens of microvilli resulting in quantum bumps up to 4 nA in amplitude; secondly the Ca^{2+} originates primarily from Ca^{2+} release rather than influx. We can thus imagine that in *Limulus* the $InsP_3$ generated, initially in one microvillus, diffuses to the base of the microvillus where it releases Ca^{2+} from $InsP_3$-sensitive stores with sequential positive and negative feedback, probably being mediated by the bell-shaped Ca^{2+} sensitivity of the $InsP_3R$ (Payne, R. *et al.*, 1990). This results in a large, rapid, and relatively localized Ca^{2+} release signal, which can activate (possibly via GC) or facilitate ion channels over microvilli up to $\sim$2 μM distant from the release site.

6.63.9.1.2 *Bee and crayfish*

s0285

p0590 Bee photoreceptors have conspicuous and extensive SMC, which have functional $InsP_3$ receptors and also ryanodine receptors, which have been characterized in elegant studies using a permeabilized slice preparation (Baumann, O. and Walz, B., 1989; Walz, B. *et al.*, 1995). Whilst $InsP_3$-induced Ca^{2+} release almost certainly plays an important role in the bee, it is unknown whether the released Ca^{2+} is required for excitation or plays only roles in facilitation and adaptation, similar to the roles of Ca^{2+} influx in *Drosophila*. The large rhabdomeres in crayfish have been exploited for spectroscopic and biochemical

measurements, but whilst it is clear that they have a G_q protein and PLC (Terakita, A. *et al.*, 1993) there is little data on downstream pathways. Intriguingly though, a recent report has detected PUFA production in crayfish eyes following long exposure to light, putatively via phospholipase A2 (Kashiwagi, T. *et al.*, 2000), which would release PUFAs from phosphatidylcholine. Apart from the evidence from *Limulus* there is very little evidence to suggest that cGMP plays a role in excitation in other arthropods.

s0290

6.63.9.2 Mollusks

p0595 Some of the most detailed biochemical characterizations of phototransduction in any microvillar photoreceptors have been performed in cephalopods such as the squid. Their large eyes, combined with a distinctive photoreceptor ultrastructure, whereby the microvillar membrane is separated from the rest of the cell, allows the isolation of large amounts of photoreceptive membrane in similar quantities to that available from mammalian preparations. Hence it was possible for example to extract and characterize squid rhodopsin some 50 years ago (Hubbard, R. and St. George, R. C. C., 1958). More recently, several groups have exploited this material to purify, characterize, and eventually clone and sequence several components of the cascade, including rhodopsin, G_q and PLCβ, along with a TRP homologue (Monk, P. D. *et al.*, 1996; Lott, J. S. *et al.*, 1999), which is likely to represent a light-sensitive channel. Quantitative biochemical experiments have demonstrated light-activated PLC activity (Szuts, E. Z., 1993); however, there is little or no indication as to whether $InsP_3$ or DAG (or indeed PIP_2) is the active messenger of excitation. The status and role of Ca^{2+} stores is also not clear, although (Walrond, J. P. and Szuts, E. Z., 1992) reported a system of submicrovillar tubules, which they suggested might be the equivalent of the SMC and function as Ca^{2+} stores.

p0600 Unfortunately, cephalopod photoreceptors have proved a difficult preparation for electrophysiology (but see Nasi, E. and Gomez, M. d. P., 1992) and the most detailed physiological studies of transduction in mollusks come from the scallops, *Pecten* and *Lima.* Remarkably, these bivalve mollusks have two distinct retinae with different types of photoreceptor: the proximal retina contains depolarizing microvillar photoreceptors, whilst the distal retina contains ciliary photoreceptors, which hyperpolarize. In keeping with the proposal that ciliary photoreceptors use cyclic nucleotide signaling pathways, the light-sensitive channels in ciliary photoreceptors of the distal retina are cGMP-gated K^+ channels, and are probably activated by a cascade involving a G_o subclass of G protein and guanylate cyclase (Gomez, M. d. P. and Nasi, E., 1995; 2000). Uniquely amongst known photoreceptors, adaptation in these cells appears to be independent of Ca^{2+}, with sensitivity and kinetics of response completely unaffected by intracellular perfusion of 10-mM BAPTA (Gomez, M. d. P. and Nasi, E., 1997).

p0605 As in other microvillar photoreceptors, phototransduction in the proximal photoreceptors of *Lima* and *Pecten* is mediated by a PLC-based pathway, but once again the final mechanism of excitation is unclear (Nasi, E. *et al.*, 2000). There is clear evidence for light-induced release of Ca^{2+} from internal stores – presumably via $InsP_3$ – and $InsP_3$ injections have been reported to activate inward currents (Gomez, M. d. P. and Nasi, E., 1998). Since the light-sensitive channels (of which there are at least two classes) have only very limited permeability to Ca^{2+} (Gomez, M. d. P. and Nasi, E., 1996), the $InsP_3$ induced Ca^{2+} release is probably the major source of Ca^{2+} – whether it be for excitation, facilitation, or adaptation. In addition, DAG surrogates (phorbol esters), possibly acting via PKC, have also been reported to activate the light-sensitive channels (Gomez, M. d. P. and Nasi, E., 1998), whilst the most recent evidence has also suggested a direct role for PIP_2 depletion (Nasi, E. *et al.*, 2000; del Pilar Gomez, M. and Nasi, E., 2005).

s0295

6.63.9.3 Annelids

p0610 Leech photoreceptors, have a highly developed and extensive system of SMC, which have been shown to represent $InsP_3$-sensitive Ca^{2+} stores (Ukhanov, K. *et al.*, 2001). The photoreceptors have an unusual structure in which the microvilli enclose a large extracellular vacuole. This has been exploited by the development of a unique preparation of an inside-out cell, whereby the plasma membrane (but not the microvilli) is permeabilized, allowing unhindered intracellular perfusion of pharmacological agents, whilst an electrode can be inserted into the central vacuole to record conductance changes in the microvillar membrane. Using this preparation, it has been shown that Ca^{2+} can activate a depolarizing conductance with an EC_{50} of $\sim$1 μM. Agents that block $InsP_3$-induced Ca^{2+} release (such as heparin) block the plateau response to light, although a transient component appears relatively resistant to such agents (Walz, B. *et al.*, 2003).

6.63.10 Conclusion

p0615 Both vertebrate and invertebrate photoreceptors have been excellent models for our understanding of G protein-coupled signaling. The bovine ROS preparation, in particular, was instrumental in the molecular identification of most of the key components of G protein-coupled signaling (see Yau, K-W., this volume). *Drosophila* has been particularly important as a genetic model for PLC-based signaling, arguably the most widespread of the G protein-coupled signaling cascades. The discovery of the TRP ion channel family was undoubtedly the most influential example of a novel signaling molecule discovered in this system, though others such as the RDGB family of PI transfer proteins and the INAD scaffolding molecule also deserve mention. More than any other signal transduction cascade, phototransduction also lends itself to the most rigorous quantitative analysis, exemplified by the ability to analyze the responses to single photons. As such, the present detailed quantitative understanding of the molecular events underlying the photoresponse is unparalleled in other cellular signaling cascades.

p0620 Phototransduction in flies is often cited as the fastest known G protein-coupled signaling cascade, and in the light-adapted state, some of the more rapidly flying Diptera can follow flickering stimuli at up to 300 Hz with 3-dB cutoffs greater than 100 Hz (Weckström, M. *et al*., 1991). Remarkably, the same photoreceptors that sustain this performance under bright sunlight can still respond sensitively and rapidly to single photons in the dark. This is in marked contrast to vertebrates, which deploy two classes of photoreceptors to cover this range. Over 30 years of investigation, particularly in *Drosophila*, have now provided many of the answers as to how this performance is achieved. The key appears to be the extreme compartmentalization provided by the microvilli and possibly the INAD signaling complex. This minimizes diffusional delays, whilst allowing extremely rapid and highly localized Ca^{2+} transients, which accelerate the kinetics by sequential positive and negative feedback. There are nevertheless still important unanswered questions, the most pressing of which perhaps, are the exact mechanism of gating of the TRP channel, and how the dramatic facilitation by Ca^{2+} is achieved.

p0625 Although dipteran photoreceptors appear to outperform their vertebrate counterparts, their strategy is not without costs. The main metabolic demand on any neuron is reestablishing the ionic gradients, which are required for electrical signaling and dissipated by every channel opening. The maximum potential LIC in *Drosophila* is probably in excess of 100 nA, and although this is never realized due to Ca^{2+}-dependent inhibition, peak responses of many tens of nanoamperes can be measured, and the steady-state voltage-clamped current during maintained illumination is ~500 pA. This contrasts with currents in vertebrate rods and cones, which are maximally only ~20–50 pA in the dark, and only progressively reduce during light.

p0630 Finally, although not comprehensively covered in this chapter, it has long been apparent that mutations in virtually any component of the cascade in *Drosophila* can result in retinal degeneration. In many, though by no means all cases, disturbances in Ca^{2+} homeostasis appear to be the underlying cause. Despite their distant evolutionary histories, the equivalent mutations in vertebrates also often result in hereditary retinal disease, or degenerative diseases in other systems. It is even possible to mimic a variety of human neurodegenerative diseases in the *Drosophila* eye, including Huntington's and Parkinson's disease by overexpressing the relevant mutant protein. Not only has the molecular genetic potential of *Drosophila* been decisive in enabling the analysis of the phototransduction cascade, but also similar strategies, such as genome saturating mutagenesis, can be applied to pursue the underlying molecular etiology of some of these devastating diseases (Bonini, N. M. and Fortini, M. E., 2003; Michno, K. *et al*., 2005; Sang, T. K. and Jackson, G. R., 2005).

Acknowledgments

The authors wish to thank members of the lab, Drs. D. Ready, D. Stavenga, A. Satoh, and P. Raghu for helpful comments on drafts of the manuscript. The authors' own work described in this chapter was supported by grants from the BBSRC, MRC, and the Wellcome Trust.

References

b0005 Acharya, J. K., Jalink, K., Hardy, R. W., Hartenstein, V., and Zuker, C. S. 1997. $InsP_3$ receptor is essential for growth and differentiation but not for vision in *Drosophila*. Neuron 18, 881–887.

b0010 Agam, K., von Campenhausen, M., Levy, S., Ben-Ami, H. C., Cook, B., Kirschfeld, K., and Minke, B. 2000. Metabolic

stress reversibly activates the *Drosophila* light-sensitive channels TRP and TRPL *in vivo*. J. Neurosci. 20, 5748–5755.

b0015 Agam, K., Frechter, S., and Minke, B. 2004. Activation of the *Drosophila* TRP and TRPL channels requires both Ca^{2+} and protein dephosphorylation. Cell Calcium 35, 87–105.

b0020 Allen-Baume, V., Segui, B., and Cockcroft, S. 2002. Current thoughts on the phosphatidylinositol transfer protein family. FEBS Lett. 531, 74–80.

b0025 Alloway, P. G. and Dolph, P. J. 1999. A role for the light-dependent phosphorylation of visual arrestin. Proc. Natl. Acad. Sci. U. S. A. 96, 6072–6077.

b0030 Alloway, P. G., Howard, L., and Dolph, P. J. 2000. The formation of stable rhodopsin-arrestin complexes induces apoptosis and photoreceptor cell degeneration. Neuron 28, 129–138.

b0035 Anderson, J. and Hardie, R. C. 1996. Different photoreceptors within the same retina express unique combinations of potassium channels. J. Comp. Physiol. A 178, 513–522.

b0040 Arendt, D. 2003. Evolution of eyes and photoreceptor cell types. Int. J. Dev. Biol. 47, 563–571.

b0045 Arnon, A., Cook, B., Gillo, B., Montell, C., Sillinger, Z., and Minke, B. 1997a. Calmodulin regulation of light adaptation and store-operated dark current in *Drosophila* photoreceptors. Proc. Natl. Acad. Sci. U. S. A. 94, 5894–5899.

b0050 Arnon, A., Cook, B., Montell, C., Selinger, Z., and Minke, B. 1997b. Calmodulin regulation of calcium stores in phototransduction of *Drosophila*. Science 275, 1119–1121.

b0055 Arshavsky, V. Y. 2003. Protein translocation in photoreceptor light adaptation: a common theme in vertebrate and invertebrate vision. Sci. STKE 204, PE43.

b0060 Bacigalupo, J., Johnson, E. C., Vergara, C., and Lisman, J. E. 1991. Light-dependent channels from excised patches of *Limulus* ventral photoreceptors are opened by cGMP. Proc. Natl. Acad. Sci. U. S. A. 88, 7938–7942.

b0065 Bahner, M., Frechter, S., Da Silva, N., Minke, B., Paulsen, R., and Huber, A. 2002. Light-regulated subcellular translocation of *Drosophila* TRPL channels induces long-term adaptation and modifies the light-induced current. Neuron 34, 83–93.

b0070 Bahner, M., Sander, P., Paulsen, R., and Huber, A. 2000. The visual G protein of fly photoreceptors interacts with the PDZ domain assembled INAD signaling complex via direct binding of activated $G\alpha q$ to phospholipase $C\beta$. J. Biol. Chem. 275, 2901–2904.

b0075 Baker, E. K., Colley, N. J., and Zuker, C. S. 1994. The cyclophilin homolog NinaA functions as a chaperone, forming a stable complex in vivo with its protein target rhodopsin. EMBO J. 13, 4886–4895.

b0080 Ballinger, D. G., Xue, N., and Harshman, K. D. 1993. A *Drosophila* photoreceptor cell-specific protein, calphotin, binds calcium and contains a leucine zipper. Proc. Natl. Acad. Sci. U. S. A. 90, 1536–1540.

b0085 Bandyopadhyay, B. C. and Payne, R. 2004. Variants of TRP ion channel mRNA present in horseshoe crab ventral eye and brain. J. Neurochem. 91, 825–835.

b0090 Baumann, O. and Walz, B. 1989. Calcium- and inositol polyphosphate-sensitivity of the calcium-sequestering endoplasmic reticulum in the photoreceptor cells of the honeybee drone. J. Comp. Physiol. A 165, 627–636.

b0095 Bentrop, J. and Paulsen, R. 1986. Light-modulated ADP-ribosylation, protein phosphorylation and protein binding in isolated fly photoreceptor membranes. Eur. J. Biochem. 161, 61–67.

b0100 Bloomquist, B. T., Shortridge, R. D., Schneuwly, S., Pedrew, M., Montell, C., Steller, H., Rubin, G., and Pak, W. L. 1988. Isolation of putative phospholipase C gene of *Drosophila*, *norpA* and its role in phototransduction. Cell 54, 723–733.

b0105 Bolsover, S. and Brown, J. 1985. Calcium an intracellular messenger of light adaptation also participates in excitation of *Limulus* ventral photoreceptors. J. Physiol. (Lond.) 364, 381–393.

b0110 Bonini, N. M. and Fortini, M. E. 2003. Human neurodegenerative disease modeling using *Drosophila*. Annu. Rev. Neurosci. 10, 10.

b0115 Brown, J., Rubin, L., Ghalayini, A., Tarver, A. P., Irvine, R., Berridge, M., and Anderson, R. 1984. myo-inositol polyphosphate may be a messenger for visual excitation in *Limulus* photoreceptors. Nature 311, 160–163.

b0120 Byk, T., BarYaacov, M., Doza, Y. N., Minke, B., and Selinger, Z. 1993. Regulatory arrestin cycle secures the fidelity and maintenance of the fly photoreceptor cell. Proc. Natl. Acad. Sci. U. S. A. 90, 1907–1911.

b0125 Chen, F. H., Baumann, A., Payne, R., and Lisman, J. E. 2001. A cGMP-gated channel subunit in *Limulus* photoreceptors. Vis. Neurosci. 18, 517–526.

b0130 Chen, J., Makino, C. L., Peachey, N. S., Baylor, D. A., and Simon, M. I. 1995. Mechanisms of rhodopsin inactivation in vivo as revealed by a COOH- terminal truncation mutant. Science 267, 374–377.

b0135 Chevesich, J., Kreuz, A. J., and Montell, C. 1997. Requirement for the PDZ domain protein, INAD, for localization of the TRP store-operated channel to a signaling complex. Neuron 18, 95–105.

b0140 Chi, C. and Carlson, S. D. 1981. Lanthanum and freeze fracture studies on the retinular cell junction in the compound eye of the housefly. Cell Tissue Res. 214, 541–552.

b0145 Chyb, S., Hevers, W., Forte, M., Wolfgang, W. J., Selinger, Z., and Hardie, R. C. 1999a. Modulation of the light response by cAMP in *Drosophila* photoreceptors. J. Neurosci. 19, 8799–8807.

b0150 Chyb, S., Raghu, P., and Hardie, R. C. 1999b. Polyunsaturated fatty acids activate the *Drosophila* light-sensitive channels TRP and TRPL. Nature 397, 255–259.

b0155 Clapham, D. E. 2003. TRP channels as cellular sensors. Nature 426, 517–524.

b0160 Cockcroft, S. 2001. Phosphatidylinositol transfer proteins couple lipid transport to phosphoinositide synthesis. Semin. Cell Dev. Biol. 12, 183–191.

b0165 Combet, C., Jambon, M., Deleage, G., and Geourjon, C. 2002. Geno3D: automatic comparative molecular modelling of protein. Bioinformatics 18, 213–214.

b0170 Contzen, K. and Nagy, K. 1995. Current components stimulated by different G-proteins in *Limulus* ventral photoreceptor. NeuroReport 6, 1905–1908.

b0175 Cook, B., BarYaacov, M., BenAmi, H. C., Goldstein, R. E., Paroush, Z., Selinger, Z., and Minke, B. 2000. Phospholipase C and termination of G-protein-mediated signalling in vivo. Nat. Cell Biol. 2, 296–301.

b0180 Cook, B. and Minke, B. 1999. TRP and calcium stores in *Drosophila* phototransduction. Cell Calcium 25, 161–171.

b0185 Cosens, D. J. and Manning, A. 1969. Abnormal electroretinogram from a *Drosophila* mutant. Nature 224, 285–287.

b0190 Deckert, A., Nagy, K., Helricht, C. S., and Stieve, H. 1992. Three components in the light-induced current of the *Limulus* ventral photoreceptor. J. Physiol. (Lond.) 453, 69–96.

b0195 Deland, M. C. and Pak, W. L. 1973. Reversibly temperature sensitive phototransduction mutant of *Drosophila melanogaster*. Nat. New Biol. 244, 184–186.

b0200 Devary, O., Heichal, O., Blumenfeld, A., Cassel, D., Suss, E., Barash, S., Rubinstein, C. T., Minke, B., and Selinger, Z. 1987. Coupling of photoexcited rhodopsin to inositol phospholipid hydrolysis in fly photoreceptors. Proc. Natl. Acad. Sci. U. S. A. 84, 6939–6943.

b0205 Dolph, P. J., ManSonHing, H., Yarfitz, S., Colley, N. J., Running Deer, J., Spencer, M., Hurley, J. B., and Zuker, C. S. 1994. An eye-specific $G\beta$ subunit essential for termination of the phototransduction cascade. Nature 370, 59–61.

b0210 Dolph, P. J., Ranganathan, R., Colley, N. J., Hardy, R. W., Socolich, M., and Zuker, C. S. 1993. Arrestin function in inactivation of G protein-coupled receptor rhodopsin *in vivo*. Science 260, 1910–1916.

b0215 Dorlochter, M. and Stieve, H. 1997. The *Limulus* ventral photoreceptor: light response and the role of calcium in a classic preparation. Prog. Neurobiol. 53, 451–515.

b0220 Elia, N., Frechter, S., Gedi, Y., Minke, B., and Selinger, Z. 2005. Excess of $G\beta e$ over $Gq\alpha$ in vivo prevents dark, spontaneous activity of *Drosophila* photoreceptors. J. Cell Biol. 171, 517–526.

b0225 Estacion, M., Sinkins, W. G., and Schilling, W. P. 2001. Regulation of *Drosophila* transient receptor potential-like (TRPL) channels by phospholipase C-dependent mechanisms. J. Physiol. 530, 1–19.

b0230 Feiler, R., Bjornson, R., Kirschfeld, K., Mismer, D., Rubin, G. M., Smith, D. P., Socolich, M., and Zuker, C. S. 1992. Ectopic expression of ultraviolet-rhodopsins in the blue photoreceptor cells of *Drosophila*: visual physiology and photochemistry of transgenic animals. J. Neurosci. Res. 12, 3862–3868.

b0235 Fein, A., Payne, R., Corson, D. W., Berridge, M. J., and Irvine, R. F. 1984. Photoreceptor excitation and adaptation by inositol 1,4,5-trisphosphate. Nature 311, 157–160.

b0240 Ferreira, P. A. and Pak, W. L. 1994. Bovine phospholipase C highly homologous to the NorpA protein of *Drosophila* is expressed specifically in cones. J. Biol. Chem. 269, 3129–3131.

b0245 Frechter, S. and Minke, B. 2006. Light-regulated translocation of signaling proteins in *Drosophila* photoreceptors. J. Physiol. (Paris) 99, 133–139.

b0250 Fu, Y., Liao, H. W., Do, M. T., and Yau, K. W. 2005. Non-image-forming ocular photoreception in vertebrates. Curr. Opin. Neurobiol. 15, 415–422.

b0255 Garcia-Murillas, I., Pettitt, T., Macdonald, E., Okkenhaug, H., Georgiev, P., Trivedi, D., Hassan, B., Wakelam, M., and Raghu, P. 2006. *lazaro* encodes a lipid phosphate phosphohydrolase that regulates phosphatidylinositol turnover during *Drosophila* phototransduction. Neuron 49, 533–546.

b0260 Garger, A., Richard, E. A., and Lisman, J. E. 2001. Inhibitors of guanylate cyclase inhibit phototransduction in *Limulus* ventral photoreceptors. Vis. Neurosci. 18, 625–632.

b0265 Gärtner, W. 2000. Invertebrate Visual Pigments. In: Molecular Mechanisms in Visual Transduction (*eds*. D. G. Stavenga, W. J. DeGrip, and E. N. Pugh), pp. 297–388. Elsevier.

b0270 Geourjon, C., Combet, C., Blanchet, C., and Deleage, G. 2001. Identification of related proteins with weak sequence identity using secondary structure information. Protein Sci. 10, 788–797.

b0275 Gillo, B., Chorna, I., Cohen, H., Cook, B., Manistersky, I., Chorev, M., Arnon, A., Pollock, J. A., Selinger, Z., and Minke, B. 1996. Coexpression of *Drosophila* TRP and TRP-like proteins in *Xenopus* oocytes reconstitutes capacitative Ca^{2+} entry. Proc. Natl. Acad. Sci. U. S. A. 93, 14146–14151.

b0280 Goel, M., Garcia, R., Estacion, M., and Schilling, W. P. 2001. Regulation of *Drosophila* TRPL channels by immunophilin FKBP59. J. Biol. Chem. 276, 38762–38773.

b0285 Goldsmith, T. H. and Wehner, R. 1977. Restrictions of rotational and translational diffusion of pigment in the membranes of a rhabdomeric photoreceptor. J. Gen. Physiol. 70, 453–490.

b0290 Gomez, M.d. P. and Nasi, E. 1995. Activation of light-dependent K^+ channels in ciliary invertebrate photoreceptors involves cGMP but not the IP_3/Ca^{2+} cascade. Neuron 15, 607–618.

b0295 Gomez, M.d. P. and Nasi, E. 1996. Ion permeation through light-activated channels in rhabdomeric photoreceptors – role of divalent-cations. J. Gen. Physiol. 107, 715–730.

b0300 Gomez, M.d. P. and Nasi, E. 1997. Light adaptation in *Pecten* hyperpolarizing photoreceptors insensitivity to calcium manipulations. J. Gen. Physiol. 109, 371–384.

Gomez, M.d. P. and Nasi, E. 1998. Membrane current induced by protein kinase C activators in rhabdomeric photoreceptors: implications for visual excitation. J. Neurosci. 18, 5253–5263. b0305

Gomez, M.d. P. and Nasi, E. 2000. Light transduction in invertebrate hyperpolarizing photoreceptors: possible involvement of a G_o-regulated guanylate cyclase. J. Neurosci. 20, 5254–5263. b0310

Govardovskii, V. I., Fyhrquist, N., Reuter, T., Kuzmin, D. G., and Donner, K. 2000. In search of the visual pigment template. Vis. Neurosci. 17, 509–528. b0315

Gu, Y., Oberwinkler, J., Postma, M., and Hardie, R. C. 2005. Mechanisms of light adaptation in *Drosophila* photoreceptors. Curr. Biol. 15, 1228–1234. b0320

Gu, G., Yang, J., Mitchell, K. A., and O'Tousa, J. E. 2004. *Drosophila* NinaB and NinaD act outside of retina to produce rhodopsin chromophore. J. Biol. Chem. . AU6 b0325

Han, M., Gurevich, V. V., Vishnivetskiy, S. A., Sigler, P. B., and Schubert, C. 2001. Crystal structure of beta-arrestin at 1.9 A: possible mechanism of receptor binding and membrane translocation. Structure 9, 869–880. b0330

Hardie, R. C. 1979. Electrophysiological analysis of the fly retina I comparative properties of R1–6 and R7 and R8. J. Comp. Physiol. A 129, 19–33. b0335

Hardie, R. C. 1985. Functional organization of the fly retina. Prog. Sens. Physiol. 5, 1–79. b0340

Hardie, R. C. 1986. The photoreceptor array of the dipteran retina. Trends Neurosci. 9, 419–423. b0345

Hardie, R. C. 1989. A histamine-activated chloride channel involved in neurotransmission at a photoreceptor synapse. Nature 339, 704–706. b0350

Hardie, R. C. 1991a. Voltage-sensitive potassium channels in *Drosophila* photoreceptors. J. Neurosci. 11, 3079–3095. b0355

Hardie, R. C. 1991b. Whole-cell recordings of the light-induced current in *Drosophila* photoreceptors: evidence for feedback by calcium permeating the light sensitive channels. Proc. Roy. Soc. Lond. B 245, 203–210. b0360

Hardie, R. C. 1995. Photolysis of caged Ca^{2+} facilitates and inactivates but does not directly excite light-sensitive channels in *Drosophila* photoreceptors. J. Neurosci. 15, 889–902. b0365

Hardie, R. C. 1996a. Excitation of *Drosophila* photoreceptors by BAPTA and ionomycin: evidence for capacitative Ca^{2+} entry?. Cell Calcium 20, 315–327. b0370

Hardie, R. C. 1996b. INDO-1 measurements of absolute resting and light-induced Ca^{2+} concentration in *Drosophila* photoreceptors. J. Neurosci. 16, 2924–2933. b0375

Hardie, R. C. 2003. Regulation of TRP channels via lipid second messengers. Annu. Rev. Physiol. 65, 735–759. b0380

Hardie, R. C. 2005. Inhibition of phospholipase C activity in *Drosophila* photoreceptors by 1,2-bis(2-aminophenoxy)ethane *N*,*N*,*N*′,*N*′-tetraacetic acid (BAPTA) and di-bromo BAPTA. Cell Calcium 38, 547–556. b0385

Hardie, R. C. and Minke, B. 1992. The *trp* gene is essential for a light-activated Ca^{2+} channel in *Drosophila* photoreceptors. Neuron 8, 643–651. b0390

Hardie, R. C. and Minke, B. 1994a. Calcium-dependent inactivation of light-sensitive channels in *Drosophila* photoreceptors. J. Gen. Physiol. 103, 409–427. b0395

Hardie, R. C. and Minke, B. 1994b. Spontaneous activation of light-sensitive channels in *Drosophila* photoreceptors. J. Gen. Physiol. 103, 389–407. b0400

Hardie, R. C. and Mojet, M. H. 1995. Magnesium-dependent block of the light-activated and *trp*-dependent conductance in *Drosophila* photoreceptors. J. Neurophysiol. 74, 2590–2599. b0405

Hardie, R. C. and Raghu, P. 1998. Activation of heterologously expressed *Drosophila* TRPL channels: Ca^{2+} is not required and $InsP_3$ is not sufficient. Cell Calcium 24, 153–163. b0410

b0415 Hardie, R. C. and Raghu, P. 2001. Visual transduction in *Drosophila*. Nature 413, 186–193.

b0420 Hardie, R. C., Gu, Y., Martin, F., Sweeney, S. T., and Raghu, P. 2004. *In vivo* light-induced and basal phospholipase C activity in *Drosophila* photoreceptors measured with genetically targeted phosphatidylinositol 4,5-bisphosphate-sensitive ion channels (Kir2.1). J. Biol. Chem. 279, 47773–47782.

b0425 Hardie, R. C., Hsiung-Liu, C., Satoh, A. K., Postma, M., and Ready, D. F. In preparation-a. Ca^{2+} dependence of

AU7 Rhodopsin inactivation in *Drosophila* photoreceptors.

b0430 Hardie, R. C., Hsiung-Liu, C., Wang, T., Chan, E., Postma, M., Montell, C., and Obukhov, A. G. In preparation-b. *In vivo* identification of the Ca^{2+} selectivity filter in the *Drosophila*

AU8 TRP channel.

b0435 Hardie, R. C., Martin, F., Chyb, S., and Raghu, P. 2003. Rescue of light responses in the *Drosophila* ''null'' phospholipase C mutant, *norpA*^{P24}, by the diacylglycerol kinase mutant, *rdgA*, and by metabolic inhibition. J. Biol. Chem. 278, 18851–18858.

b0440 Hardie, R. C., Martin, F., Cochrane, G. W., Juusola, M., Georgiev, P., and Raghu, P. 2002. Molecular basis of amplification in *Drosophila* phototransduction. Roles for G protein, phospholipase C, and diacylglycerol kinase. Neuron 36, 689–701.

b0445 Hardie, R. C., Peretz, A., Suss-Toby, E., Rom-Glas, A., Bishop, S. A., Selinger, Z., and Minke, B. 1993. Protein kinase C is required for light adaptation in *Drosophila* photoreceptors. Nature 363, 634–637.

b0450 Hardie, R. C., Raghu, P., Moore, S., Juusola, M., Baines, R. A., and Sweeney, S. T. 2001. Calcium influx via TRP channels is required to maintain PIP_2 levels in *Drosophila* photoreceptors. Neuron 30, 149–159.

b0455 Hardie, R. C., Reuss, H., Lansdell, S. J., and Millar, N. S. 1997. Functional equivalence of native light-sensitive channels in the *Drosophila trp*^{301} mutant and TRPL cation channels expressed in a stably transfected *Drosophila* cell line. Cell Calcium 21, 431–440.

b0460 Hardie, R. C., Voss, D., Pongs, O., and Laughlin, S. B. 1991. Novel potassium channels encoded by the *Shaker* locus in *Drosophila* photoreceptors. Neuron 6, 477–486.

b0465 Harteneck, C., Obukhov, A. G., Zobel, A., Kalkbrenner, F., and Schultz, G. 1995. The *Drosophila* cation channel Trpl expressed in insect Sf9 cells is stimulated by agonists of G-protein-coupled receptors. FEBS Lett. 358, 297–300.

b0470 Haug-Collet, K., Pearson, B., Webel, R., Szerencsei, R. T., Winkfein, R. J., Schnetkamp, P. P., and Colley, N. J. 1999. Cloning and characterization of a potassium-dependent sodium/calcium exchanger in *Drosophila*. J. Cell Biol. 147, 659–670.

b0475 Henderson, S. R., Reuss, H., and Hardie, R. C. 2000. Single photon responses in *Drosophila* photoreceptors and their regulation by Ca^{2+}. J. Physiol. (Lond.) 524, 179–194.

b0480 Hevers, W. and Hardie, R. C. 1995. Serotonin modulates the voltage dependence of delayed rectifier and *Shaker* potassium channels in *Drosophila* photoreceptors. Neuron 14, 845–856.

b0485 Hicks, J. L., Liu, X., and Williams, D. S. 1996. Role of the NINAC proteins in photoreceptor cell structure: ultrastructure of *ninaC* deletion mutants and binding to actin filaments. Cell Motil. Cytoskeleton 35, 367–379.

b0490 Hillman, P., Hochstein, S., and Minke, B. 1983. Transduction in invertebrate photoreceptors: role of pigment bistability. Physiol. Rev. 63, 668–772.

b0495 Hochstrate, P. and Hamdorf, K. 1990. Microvillar components of light adaptation in blowflies. J. Gen. Physiol. 95, 891–910.

b0500 Hofstee, C. A. and Stavenga, D. G. 1996. Calcium homeostasis in photoreceptor cells of *Drosophila* mutants *inaC* and *trp* studied with the pupil mechanism. Vis. Neurosci. 13, 257–263.

Hofstee, C. A., Henderson, S., Hardie, R. C., and Stavenga, D. G. 1996. Differential effects of NINAC proteins (p132 and p174) on light-activated currents and pupil mechanism in *Drosophila* photoreceptors. Vis. Neurosci. 13, 897–906. b0505

Hotta, Y. and Benzer, S. 1970. Genetic dissection of the *Drosophila* nervous system by means of mosaics. Proc. Natl. Acad. Sci. U. S. A. 67, 1156–1163. b0510

Houdusse, A., Kalabokis, V. N., Himmel, D., Szent-Gyorgyi, A. G., and Cohen, C. 1999. Atomic structure of scallop myosin subfragment S1 complexed with MgADP: a novel conformation of the myosin head. Cell 97, 459–470. b0515

Howard, J., Blakeslee, B., and Laughlin, S. B. 1987. The intracellular pupil mechanism and the maintenance of photoreceptor signal: noise ratios in the blowfly *Lucilia cuprina*. Proc. R. Soc. Lond. B 231, 415–435. b0520

Hsu, Y. T. and Molday, R. S. 1993. Modulation of the cGMP-gated channel of rod photoreceptor cells by calmodulin. Nature 361, 76–79. b0525

Hu, Y., Vaca, L., Zhu, X., Birnbaumer, L., Kunze, D. L., and Schilling, W. P. 1994. Appearance of a novel Ca^{2+} influx pathway in Sf9 insect cells following expression of the transient receptor potential-like (*trpl*) protein of *Drosophila*. Biochem. Biophys. Res. Comm. 201, 1050–1056. b0530

Huang, F. D., Matthies, H. J., Speese, S. D., Smith, M. A., and Broadie, K. 2004. Rolling blackout, a newly identified PIP_2–DAG pathway lipase required for *Drosophila* phototransduction. Nat. Neurosci. 7, 1070–1078. b0535

Hubbard, R. and St. George, R. C. C. 1958. The rhodopsin system of the squid. J. Gen. Physiol. 41, 501–528. b0540

Huber, A. 2001. Scaffolding proteins organize multimolecular protein complexes for sensory signal transduction. Eur. J. Neurosci. 14, 769–776. b0545

Huber, A., Sander, P., Bahner, M., and Paulsen, R. 1998. The TRP Ca^{2+} channel assembled in a signaling complex by the PDZ domain protein INAD is phosphorylated through the interaction with protein kinase C (ePKC). FEBS Lett. 425, 317–322. b0550

Huber, A., Sander, P., Gobert, A., Bahner, M., Hermann, R., and Paulsen, R. 1996a. The transient receptor potential protein (Trp), a putative store-operated Ca^{2+} channel essential for phosphoinositide-mediated photoreception, forms a signaling complex with NorpA, InaC and InaD. EMBO J. 15, 7036–7045. b0555

Huber, A., Sander, P., and Paulsen, R. 1996b. Phosphorylation of the InaD gene product, a photoreceptor membrane protein required for recovery of visual excitation. J. Biol. Chem. 271, 11710–11717. b0560

van Huizen, R., Miller, K., Chen, D. M., Li, Y., Lai, Z. C., Raab, R. W., Stark, W. S., Shortridge, R. D., and Li, M. 1998. Two distantly positioned PDZ domains mediate multivalent INAD–phospholipase C interactions essential for G protein-coupled signaling. EMBO J. 17, 2285–2297. b0565

Hyde, D. R., Mecklenburg, K. L., Pollock, J. A., Vihtelic, T. S., and Benzer, S. 1990. Twenty *Drosophila* visual system cDNA clones: one is a homolog of human arrestin. Proc. Natl. Acad. Sci. U. S. A. 87, 1008–1012. b0570

Ikura, M., Clore, G. M., Gronenborn, A. M., Zhu, G., Klee, C. B., and Bax, A. 1992. Solution structure of a calmodulin-target peptide complex by multidimensional NMR. Science 256, 632–638. b0575

Inoue, H., Yoshioka, T., and Hotta, Y. 1985. A genetic study of inositol trisphosphate involvement in phototransduction using *Drosophila* mutants. Biochem. Biophys. Res. Commun. 132, 513–519. b0580

Inoue, H., Yoshioka, T., and Hotta, Y. 1989. Diacylglycerol kinase defect in a *Drosophila* retinal degeneration mutant *rdgA*. J. Biol. Chem. 264, 5996–6000. b0585

b0590 Jansonius, N. M. 1990. Properties of the sodium-pump in the blowfly photoreceptor cell. J. Comp. Physiol. A 167, 461–467.

b0595 Johnson, E. C. and Pak, W. L. 1986. Electrophysiological study of *Drosophila* rhodopsin mutants. J. Gen. Physiol. 88, 651–673.

b0600 Jors, S., Kazanski, V., Foik, A., Krautwurst, D., and Harteneck, C. 2006. Receptor-induced activation of *Drosophila* TRPgamma by polyunsaturated fatty acids. J. Biol. Chem. online.

AU9

b0605 Juusola, M. and Hardie, R. C. 2001. Light adaptation in *Drosophila* photoreceptors: I. Response dynamics and signaling efficiency at 25 degrees C. J. Gen. Physiol. 117, 3–25.

b0610 Kashiwagi, T., Meyer-Rochow, V. B., Nishimura, K., and Eguchi, E. 2000. Light activation of phospholipase A(2) in the photoreceptor of the crayfish (*Procambarus clarkii*). Acta Neurobiol. Exp. 60, 9–16.

b0615 Kiefer, C., Sumser, E., Wernet, M. F., and Von Lintig, J. 2002. A class B scavenger receptor mediates the cellular uptake of carotenoids in *Drosophila*. Proc. Natl. Acad. Sci. U. S. A. 99, 10581–10586.

b0620 Kimple, M. E., Siderovski, D. P., and Sondek, J. 2001. Functional relevance of the disulfide-linked complex of the N-terminal PDZ domain of InaD with NorpA. EMBO J. 20, 4414–4422.

b0625 Kirkwood, A., Weiner, D., and Lisman, J. E. 1989. An estimate of the number of G regulator proteins activated per excited rhodopsin in living *Limulus* ventral photoreceptors. Proc. Natl. Acad. Sci. U. S. A. 86, 3872–3876.

b0630 Kirschfeld, K. and Franceschini, N. 1977. Evidence for a sensitising pigment in fly photoreceptors. Nature 269, 386–390.

b0635 Kirschfeld, K. and Vogt, K. 1980. Calcium ions and pigment migration in fly photoreceptors. Naturwissenschaften 67, 516–517.

b0640 Kirschfeld, K., Feiler, R., Hardie, R., Vogt, K., and Franceschini, N. 1983. The sensitizing pigment in fly photoreceptors. Properties and candidates. Biophys. Struct. Mech. 10, 81–92.

b0645 Kiselev, A., Socolich, M., Vinos, J., Hardy, R. W., Zuker, C. S., and Ranganathan, R. 2000a. A molecular pathway for light-dependent photoreceptor apoptosis in *Drosophila*. Neuron 28, 139–152.

b0650 Kiselev, A., Sokolich, M., and Ranganathan, R. 2000b. Long-lived internalized phosphorylated Rh1 metarhodopsin/Arrestin-2/Clathrin complex mediates *Drosophila* photoreceptor cell apoptosis. *Drosophila*. Invest. Ophtalmol. Vis. Sci. 41, 4652B599.

b0655 Kosloff, M., Elia, N., Joel-Almagor, T., Timberg, R., Zars, T. D., Hyde, D. R., Minke, B., and Selinger, Z. 2003. Regulation of light-dependent G_q a translocation and morphological changes in fly photoreceptors. EMBO J. 22, 459–468.

b0660 Koundakjian, E. J., Cowan, D. M., Hardy, R. W., and Becker, A. H. 2004. The Zuker collection: a resource for the analysis of autosomal gene function in *Drosophila melanogaster*. Genetics 167, 203–206.

b0665 Kumar, J. P. and Ready, D. F 1995. Rhodopsin plays an essential structural role in *Drosophila* photoreceptor development. Development 121, 4359–4370.

b0670 Kwon, Y. and Montell, C. 2006. Dependence on the Lazaro phosphatidic acid phosphatase for the maximum light response. Curr. Biol. 16, 723–729.

b0675 Lalonde, M. M., Janssens, H., Rosenbaum, E., Choi, S. Y., Gergen, J. P., Colley, N. J., Stark, W. S., and Frohman, M. A. 2005. Regulation of phototransduction responsiveness and retinal degeneration by a phospholipase D-generated signaling lipid. J. Cell Biol. 169, 471–479.

b0680 Lan, L., Bawden, M. J., Auld, A. M., and Barritt, G. J. 1996. Expression of *Drosophila* Trpl cRNA in *Xenopus laevis* oocytes leads to the appearance of a Ca^{2+} channel activated by Ca^{2+} and Calmodulin, and by guanosine 5′[gamma-thio]triphosphate. Biochem. J. 316, 793–803.

Lee, S. J. and Montell, C. 2001. Regulation of the rhodopsin protein phosphatase, RDGC, through interaction with Calmodulin. Neuron 32, 1097–1106. b0685

Lee, S. J. and Montell, C. 2004. Light-dependent translocation of visual arrestin regulated by the NINAC myosin III. Neuron 43, 95–103. b0690

Lee, Y. J., Dobbs, M. B., Verardi, M. L., and Hyde, D. R. 1990. *dgq*: a *Drosophila* gene encoding a visual system-specific Galpha molecule. Neuron 5, 889–898. b0695

Lee, Y. J., Shah, S., Suzuki, E., Zars, T., Oday, P. M., and Hyde, D. R. 1994. The *Drosophila dgq* gene encodes a Ga protein that mediates phototransduction. Neuron 13, 1143–1157. b0700

Lee, S. J., Xu, H., Kang, L. W., Amzel, L. M., and Montell, C. 2003. Light adaptation through phosphoinositide-regulated translocation of *Drosophila* visual arrestin. Neuron 39, 121–132. b0705

Lee, S. J., Xu, H., and Montell, C. 2004. Rhodopsin kinase activity modulates the amplitude of the visual response in *Drosophila*. Proc. Natl. Acad. Sci. U. S. A. 101, 11874–11879. b0710

Leung, H. T., Geng, C., and Pak, W. L. 2000. Phenotypes of trpl mutants and interactions between the transient receptor potential (TRP) and TRP-like channels in *Drosophila*. J. Neurosci. 20, 6797–6803. b0715

Li, H. S. and Montell, C. 2000. TRP and the PDZ protein, INAD, form the core complex required for retention of the signalplex in *Drosophila* photoreceptor cells. J. Cell Biol. 150, 1411–1422. b0720

Li, C. J., Geng, C. X., Leung, H. T., Hong, Y. S., Strong, L. L. R., Schneuwly, S., and Pak, W. L. 1999. INAF, a protein required for transient receptor potential Ca^{2+} channel function. Proc. Natl. Acad. Sci. U. S. A. 96, 13474–13479. b0725

Li, H. S., Porter, J. A., and Montell, C. 1998. Requirement for the NINAC kinase/myosin for stable termination of the visual cascade. J. Neurosci. 18, 9601–9606. b0730

von Lintig, J. and Vogt, K. 2000. Filling the gap in vitamin A research. Molecular identification of an enzyme cleaving beta-carotene to retinal. J. Biol. Chem. 275, 11915–11920. b0735

von Lintig, J., Dreher, A., Kiefer, C., Wernet, M. F., and Vogt, K. 2001. Analysis of the blind *Drosophila* mutant *ninaB* identifies the gene encoding the key enzyme for vitamin A formation *in vivo*. Proc. Natl. Acad. Sci. U. S. A. 98, 1130–1135. b0740

Liu, M., Parker, L. L., Wadzinski, B. E., and Shieh, B. H. 2000. Reversible phosphorylation of the signal transduction complex in *Drosophila* photoreceptors. J. Biol. Chem. 275, 12194–12199. b0745

Lott, J. S., Wilde, J. I., Carne, A., Evans, N., and Findlay, J. B. C. 1999. The ordered visual transduction complex of the squid photoreceptor membrane. Mol. Neurobiol. 20, 61–80. b0750

Martin, J. H., Benzer, S., Rudnicka, M., and Miller, C. A. 1993. Calphotin: a *Drosophila* photoreceptor cell calcium-binding protein. Proc. Natl. Acad. Sci. U. S. A. 90, 1531–1535. b0755

Masai, I., Suzuki, E., Yoon, C. S., Kohyama, A., and Hotta, Y. 1997. Immunolocalization of *Drosophila* eye-specific diacylgylcerol kinase, RdgA, which is essential for the maintenance of the photoreceptor. J. Neurobiol. 32, 695–706. b0760

Matsumoto, H. and Pak, W. L. 1984. Light-induced phosphorylation of retina-specific polypeptides of *Drosophila in vivo*. Science 223, 184–186. b0765

Matsumoto, H., Kurien, B. T., Takagi, Y., Kahn, E. S., Kinumi, T., Komori, N., Yamada, T., Hayashi, F., Isono, K., Pak, W. L., Jackson, K. W., and Tobin, S. L. 1994. Phosrestin I undergoes the earliest light-induced phosphorylation by a calcium/calmodulin-dependent protein kinase in *Drosophila* photoreceptors. Neuron 12, 997–1010. b0770

b0775 McKay, R. R., Chen, D. M., Miller, K., Kim, S., Stark, W. S., and Shortridge, R. D. 1995. Phospholipase C rescues visual defect in norpA mutant of *Drosophila* melanogaster. J. Biol. Chem. 270, 13271–13276.

b0780 Melyan, Z., Tarttelin, E. E., Bellingham, J., Lucas, R. J., and Hankins, M. W. 2005. Addition of human melanopsin renders mammalian cells photoresponsive. Nature 433, 741–745.

b0785 Meyer, N. E., Joel-Almagor, T., Frechter, S., Minke, B., and Huber, A. 2006. Subcellular translocation of the eGFP-tagged TRPL channel in *Drosophila* photoreceptors requires activation of the phototransduction cascade. J. Cell Sci. 119, 2592–2603.

b0790 Michno, K., van de Hoef, D., Wu, H., and Boulianne, G. 2005. Demented flies? using *Drosophila* to model human neurodegenerative diseases. Clin. Genet. 67, 468–475.

b0795 Milligan, S. C., Alb, J. G., Elagina, R. B., Bankaitis, V. A., and Hyde, D. R. 1997. The phosphatidylinositol transfer protein domain of *Drosophila* retinal degeneration B protein is essential for photoreceptor cell survival and recovery from light stimulation. J. Cell Biol. 139, 351–363.

b0800 Minke, B. 1982. Light-induced reduction in excitation efficiency in the trp mutant of *Drosophila*. J. Gen. Physiol. 79, 361–385.

b0805 Minke, B. and Hardie, R. C. 2000. Genetic Dissection of *Drosophila* Phototransduction. In: Handbook of Biological Physics, Vol. 3 (*eds*. D. G. Stavenga, W. J. deGrip, and E. N. Pugh), pp. 449–525. Elsevier.

b0810 Minke, B. and Selinger, Z. 1992. Intracellular Messengers in Invertebrate Photoreceptors Studied in Mutant Flies. In: Intracellular Messengers (*eds*. A. Boulton, G. Baker, and C. Talyor), pp. 517–563. The Humana Press.

b0815 Minke, B., Wu, C.-F., and Pak, W. L. 1975. Induction of photoreceptor noise in the dark in a *Drosophila* mutant. Nature 258, 84–87.

b0820 Monk, P. D., Carne, A., Liu, S. H., Ford, J. W., Keen, J. N., and Findlay, J. B. C. 1996. Isolation, cloning, and characterisation of a *trp* homologue from squid (*Loligo forbesi*) photoreceptor membranes. J. Neurochem. 67, 2227–2235.

b0825 Montell, C. 1999. Visual transduction in *Drosophila*. Annu. Rev. Cell Dev. Biol. 15, 231–268.

b0830 Montell, C. 2005. The TRP superfamily of cation channels. Sci. STKE 272, re3.

b0835 Montell, C. and Rubin, G. M. 1988. The *Drosophila ninaC* locus encodes two photoreceptor cell specific proteins with domains homologous to protein kinases and the myosin heavy chain head. Cell 52, 757–772.

b0840 Montell, C. and Rubin, G. M. 1989. Molecular characterization of *Drosophila trp* locus, a putative integral membrane protein required for phototransduction. Neuron 2, 1313–1323.

b0845 Nagy, K. 1991. Biophysical processes in invertebrate photoreceptors: recent progress and a critical overview based on *Limulus* photoreceptors. Q. Rev. Biophys. 24, 165–226.

b0850 Nagy, K. and Contzen, K. 1997. Inhibition of phospholipase C by U-73122 blocks one component of the receptor current in *Limulus* photoreceptor. Vis. Neurosci. 14, 995–998.

b0855 Nagy, K., Contzen, K., and Stieve, H. 1993. Two components of the receptor current are developed from distinct elementary signals in *Limulus* ventral nerve photoreceptor. Eur. Biophys. J. 22, 341–350.

b0860 Nasi, E. and Gomez, M.d. P. 1992. Light-activated ion channels in solitary photoreceptors of the scallop *Pecten irradians*. J. Gen. Physiol. 99, 747–769.

b0865 Nasi, E., Gomez, M.d. P., and Payne, R. 2000. Phototransduction Mechanisms in Microvillar and Ciliary Photoreceptors of Invertebrates. In: Handbook of Biological Physics, Vol. 3 (*eds*. D. G. Stavenga, W. J. deGrip, and E. N. Pugh), pp. 389–448. Elsevier.

b0870 Niemeyer, B. A., Suzuki, E., Scott, K., Jalink, K., and Zuker, C. S. 1996. The *Drosophila* light-activated conductance is composed of the two channels TRP and TRPL. Cell 85, 651–659.

b0875 Niven, J. E., Vahasoyrinki, M., Kauranen, M., Hardie, R. C., Juusola, M., and Weckstrom, M. 2003. The contribution of *Shaker* K^+ channels to the information capacity of *Drosophila* photoreceptors. Nature 421, 630–634.

b0880 Oberwinkler, J. and Stavenga, D. G. 1998. Light dependence of calcium and membrane potential measured in blowfly photoreceptors in vivo. J. Gen. Physiol. 112, 113–124.

b0885 Oberwinkler, J. and Stavenga, D. G. 2000. Calcium transients in the rhabdomeres of dark- and light-adapted fly photoreceptor cells. J. Neurosci. 20, 1701–1709.

b0890 O'Tousa, J. E., Baehr, W., Martin, R. L., Hirsh, J., Pak, W. L., and Applebury, M. L. 1985. The *Drosophila ninaE* gene encodes an opsin. Cell 40, 839–850.

b0895 Pak, W. L. 1995. *Drosophila* in vision research: the Friedenwald lecture. Invest. Ophthalmol. Vis. Sci. 36, 2340–2357.

b0900 Pak, W. L. and Leung, H. T. 2003. Genetic approaches to visual transduction in *Drosophila melanogaster*. Receptors Channels 9, 149–167.

b0905 Pak, W. L., Grossfield, J., and Arnold, K. S. 1970. Mutants of the visual pathway of *Drosophila melanogaster*. Nature 227, 518–520.

b0910 Palczewski, K., Kumasaka, T., Hori, T., Behnke, C. A., Motoshima, H., Fox, B. A., Le Trong, I., Teller, D. C., Okada, T., Stenkamp, R. E., Yamamoto, M., and Miyano, M. 2000. Crystal structure of rhodopsin: a G protein-coupled receptor. Science 289, 739–745.

b0915 Panda, S., Nayak, S. K., Campo, B., Walker, J. R., Hogenesch, J. B., and Jegla, T. 2005. Illumination of the melanopsin signaling pathway. Science 307, 600–604.

b0920 Payne, R., Corson, D. W., and Fein, A. 1986. Pressure injection of calcium both excites and adapts *Limulus* ventral photoreceptors. J. Gen. Physiol. 88, 107–126.

b0925 Payne, R., Flores, T. M., and Fein, A. 1990. Feedback inhibition by calcium limits the release of calcium by inositol trisphosphate in *Limulus* ventral photoreceptors. Neuron 4, 547–555.

b0930 Pearn, M. T., Randall, L. L., Shortridge, R. D., Burg, M. G., and Pak, W. L. 1996. Molecular, biochemical, and electrophysiological characterization of *Drosophila norpA* mutants. J. Biol. Chem. 271, 4937–4945.

b0935 Peretz, A., Suss-Toby, E., Rom-Glas, A., Arnon, A., Payne, R., and Minke, B. 1994. The light response of *Drosophila* photoreceptors is accompanied by an increase in cellular calcium: effects of specific mutations. Neuron 12, 1257–1267.

b0940 Phillips, A. M., Bull, A., and Kelly, L. E. 1992. Identification of a *Drosophila* gene encoding a calmodulin-binding protein with homology to the trp phototransduction gene. Neuron 8, 631–642.

b0945 del Pilar Gomez, M. and Nasi, E. 2005. A direct signaling role for phosphatidylinositol 4,5-bisphosphate (PIP_2) in the visual excitation process of microvillar receptors. J. Biol. Chem. 280, 16784–16789.

b0950 Plangger, A., Malicki, D., Whitney, M., and Paulsen, R. 1994. Mechanism of arrestin 2 function in rhabdomeric photoreceptors. J. Biol. Chem. 269, 26969–26975.

b0955 Popescu, D. C., Ham, A.-J. L., and Shieh, B.-H. 2006. Scaffolding protein INAD regulates deactivation of vision by promoting phosphorylation of transient receptor potential by rye protein kinase C in *Drosophila*. J. Neurosci. 26, 8570–8577.

b0960 Porter, J. A. and Montell, C. 1993. Distinct roles of the *Drosophila ninaC* kinase and myosin domains revealed by systematic mutagenesis. J. Cell Biol. 122, 601–612.

b0965 Porter, J. A., Hicks, J. L., Williams, D. S., and Montell, C. 1992. Differential localizations of and requirements for the two *Drosophila ninaC* kinase/myosins in photoreceptor cells. J. Cell Biol. 116, 683–693.

b0970 Porter, J. A., Yu, M., Doberstein, S. K., Pollard, T. D., and Montell, C. 1993. Dependence of calmodulin localization in the retina on the NINAC unconventional myosin. Science 262, 1038–1042.

b0975 Postma, M., Oberwinkler, J., and Stavenga, D. G. 1999. Does Ca^{2+} reach millimolar concentrations after single photon absorption in *Drosophila* photoreceptor microvilli? Biophys. J. 77, 1811–1823.

b0980 Provencio, I., Jiang, G. S., DeGrip, W. J., Hayes, W. P., and Rollag, M. D. 1998. Melanopsin: an opsin in melanophores, brain, and eye. Proc. Natl. Acad. Sci. U. S. A. 95, 340–345.

b0985 Qiu, X., Kumbalasiri, T., Carlson, S. M., Wong, K. Y., Krishna, V., Provencio, I., and Berson, D. M. 2005. Induction of photosensitivity by heterologous expression of melanopsin. Nature 433, 745–749.

b0990 Raghu, P., Colley, N. J., Webel, R., James, T., Hasan, G., Danin, M., Selinger, Z., and Hardie, R. C. 2000a. Normal phototransduction in *Drosophila* photoreceptors lacking an $InsP_3$ receptor gene. Mol. Cell Neurosci. 15, 429–445.

b0995 Raghu, P., Usher, K., Jonas, S., Chyb, S., Polyanovsky, A., and Hardie, R. C. 2000b. Constitutive activity of the light-sensitive channels TRP and TRPL in the *Drosophila* diacylglycerol kinase mutant, *rdgA*. Neuron 26, 169–179.

b1000 Ramsey, I. S., Delling, M., and Clapham, D. E. 2006. An introduction to trp channels. Annu. Rev. Physiol. 68, 619–647.

b1005 Ranganathan, R., Bacskai, B. J., Tsien, R. Y., and Zuker, C. S. 1994. Cytosolic calcium transients: spatial localization and role in *Drosophila* photoreceptor cell function. Neuron 13, 837–848.

b1010 Ranganathan, R., Harris, G. L., Stevens, C. F., and Zuker, C. S. 1991. A *Drosophila* mutant defective in extracellular calcium-dependent photoreceptor deactivation and rapid desensitization. Nature 354, 230–232.

b1015 Ready, D. F. 1989. A multifaceted approach to neural development. Trends Neurosci. 12, 102–110.

b1020 Reuss, H., Mojet, M. H., Chyb, S., and Hardie, R. C. 1997. In vivo analysis of the *Drosophila* light-sensitive channels, TRP and TRPL. Neuron 19, 1249–1259.

b1025 Roebroek, J. G. H. and Stavenga, D. G. 1990. On the effective optical density of the pupil mechanism in fly photoreceptors. Vision Res. 30, 1235–1242.

b1030 Rosenbaum, E. E., Hardie, R. C., and Colley, N. J. 2006. Calnexin is essential for rhodopsin maturation, Ca^{2+} regulation, and photoreceptor cell survival. Neuron 49, 229–241.

b1035 Running Deer, J. L., Hurley, J. B., and Yarfitz, S. L. 1995. G protein control of *Drosophila* photoreceptor phospholipase C. J. Biol. Chem. 270, 12623–12628.

b1040 Sahly, I., Schroder, W. H., Zierold, K., and Minke, B. 1994. Accumulation of calcium in degenerating photoreceptors of several *Drosophila* mutants. Vis. Neurosci. 11, 763–772.

b1045 Salcedo, E., Huber, A., Henrich, S., Chadwell, L. V., Chou, W. H., Paulsen, R., and Britt, S. G. 1999. Blue- and green-absorbing visual pigments of *Drosophila*: ectopic expression and physiological characterization of the R8 photoreceptor cell-specific Rh5 and Rh6 rhodopsins. J. Neurosci. 19, 10716–10726.

b1050 Sang, T. K. and Jackson, G. R. 2005. *Drosophila* models of neurodegenerative disease. NeuroRx 2, 438–446.

b1055 Sarfare, S., Ahmad, S. T., Joyce, M. V., Boggess, B., and O'Tousa, J. E. 2005. The *Drosophila* ninaG oxidoreductase acts in visual pigment chromophore production. J. Biol. Chem. 280, 11895–11901.

b1060 Sarthy, P. V. 1991. Histamine: a neurotransmitter candidate for *Drosophila* photoreceptors. J. Neurochem. 57, 1757–1768.

b1065 Satoh, A. K. and Ready, D. F. 2005. Arrestin1 mediates light-dependent rhodopsin endocytosis and cell survival. Curr. Biol. 15, 1722–1733.

Scavarda, N. J., Otousa, J., and Pak, W. L. 1983. *Drosophila* locus with gene-dosage effects on rhodopsin. Proc. Natl. Acad. Sci. U. S. A. 80, 4441–4445. b1070

Schillo, S., Belusic, G., Hartmann, K., Franz, C., Kuhl, B., Brenner-Weiss, G., Paulsen, R., and Huber, A. 2004. Targeted mutagenesis of the farnesylation site of *Drosophila* Ggamma e disrupts membrane association of the G protein beta gamma complex and affects the light-sensitivity of the visual system. J. Biol. Chem. b1075 AU10

Schneuwly, S., Burg, M. G., Lending, C., Perdew, M. H., and Pak, W. L. 1991. Properties of photoreceptor-specific phospholipase C encoded by the norpA gene of *Drosophila* melanogaster. J. Biol. Chem. 266, 24314–34319. b1080

Schwarz, E. M. and Benzer, S. 1997. Calx, a Na–Ca exchanger gene of *Drosophila melanogaster*. Proc. Natl. Acad. Sci. U. S. A. 94, 10249–10254. b1085

Scott, K. and Zuker, C. S. 1998. Assembly of the *Drosophila* phototransduction cascade into a signalling complex shapes elementary responses. Nature 395, 805–808. b1090

Scott, K., Becker, A., Sun, Y., Hardy, R., and Zuker, C. 1995. G_q a protein function in vivo: genetic dissection of its role in photoreceptor cell physiology. Neuron 15, 919–927. b1095

Scott, K., Sun, Y. M., Beckingham, K., and Zuker, C. S. 1997. Calmodulin regulation of *Drosophila* light-activated channels and receptor function mediates termination of the light response in vivo. Cell 91, 375–383. b1100

Shieh, B. H. and Niemeyer, B. 1995. A novel protein encoded by the InaD gene regulates recovery of visual transduction in *Drosophila*. Neuron 14, 201–210. b1105

Shieh, B. H. and Zhu, M. Y. 1996. Regulation of the TRP Ca^{2+} channel by INAD in *Drosophila* photoreceptors. Neuron 16, 991–998. b1110

Shieh, B. H., Parker, L., and Popescu, D. 2002. Protein kinase C (PKC) isoforms in *Drosophila*. J. Biochem. (Tokyo) 132, 523–527. b1115

Shin, J., Richard, E. A., and Lisman, J. E. 1993. Ca^{2+} is an obligatory intermediate in the excitation cascade of *Limulus* photoreceptors. Neuron 11, 845–855. b1120

Smith, D. P., Ranganathan, R., Hardy, R. W., Marx, J., Tsuchida, T., and Zuker, C. S. 1991. Photoreceptor deactivation and retinal degeneration mediated by a photoreceptor-specific protein-kinase-C. Science 254, 1478–1484. b1125

Stavenga, D. G. 1996. Insect retinal pigments: spectral characteristics and physiological functions. Prog. Retin. Eye Res. 15, 231–259. b1130

Stavenga, D. G. 2004. Angular and spectral sensitivity of fly photoreceptors. III. Dependence on the pupil mechanism in the blowfly Calliphora. J. Comp. Physiol. A 190, 115–129. b1135

Steele, F. R., Washburn, T., Rieger, R., and Otousa, J. E. 1992. *Drosophila* retinal-degeneration-C (Rdgc) encodes a novel serine threonine protein phosphatase. Cell 69, 669–676. b1140

Sullivan, K. M. C., Scott, K., Zuker, C. S., and Rubin, G. M. 2000. The ryanodine receptor is essential for larval development in *Drosophila melanogaster*. Proc. Natl. Acad. Sci. U. S. A. 97, 5942–5947. b1145

Szuts, E. Z. 1993. Concentrations of phosphatidylinositol 4,5-bisphosphate and inositol 1,4,5-trisphosphate within the distal segment of squid photoreceptors. Vis. Neurosci. 10, 921–929. b1150

Taylor, D. A., Sack, J. S., Maune, J. F., Beckingham, K., and Quiocho, F. A. 1991. Structure of a recombinant calmodulin from *Drosophila melanogaster* refined at 2.2-A resolution. J. Biol. Chem. 266, 21375–21380. b1155

Terakita, A., Hariyama, T., Tsukahara, Y., Katsukura, Y., and Tashiro, H. 1993. Interaction of GTP-binding protein Gq with photoactivated rhodopsin in the photoreceptor membranes of crayfish. FEBS Lett. 330, 197–200. b1160

b1165 Toyoshima, S., Matsumoto, N., Wang, P., Inoue, H., Yoshioka, T., Hotta, Y., and Osawa, T. 1990. Purification and partial amino acid sequences of phosphoinositide-specific phospholipase C of *Drosophila* eye. J. Biol. Chem., 265, 14842–14848.

b1170 Tsunoda, S., Sierralta, J., Sun, Y. M., Bodner, R., Suzuki, E., Becker, A., Socolich, M., and Zuker, C. S. 1997. A multivalent PDZ-domain protein assembles signalling complexes in a G-protein-coupled cascade. Nature 388, 243–249.

b1175 Tsunoda, S., Sun, Y., Suzuki, E., and Zuker, C. 2001. Independent anchoring and assembly mechanisms of INAD signaling complexes in *Drosophila* photoreceptors. J. Neurosci. 21, 150–158.

b1180 Ugarte, G., Delgado, R., O'Day P, M., Farjah, F., Cid, L. P., Vergara, C., and Bacigalupo, J. 2005. Putative ClC-2 chloride channel mediates inward rectification in *Drosophila* retinal photoreceptors. J. Membr. Biol. 207, 151–160.

b1185 Ukhanov, K. and Payne, R. 1995. Light activated calcium release in *Limulus* ventral photoreceptors as revealed by laser confocal microscopy. Cell Calcium 18, 301–313.

b1190 Ukhanov, K., Mills, S. J., Potter, B. V., and Walz, B. 2001. $InsP_3$-induced Ca^{2+} release in permeabilized invertebrate photoreceptors: a link between phototransduction and Ca^{2+} stores. Cell Calcium 29, 335–345.

b1195 Vaca, L., Sinkins, W. G., Hu, Y., Kunze, D. L., and Schilling, W. P. 1994. Activation of recombinant trp by thapsigargin in Sf9 insect cells. Am. J. Physiol. Cell Physiol. 267, C1501–C1505.

b1200 Vahasoyrinki, M., Niven, J. E., Hardie, R. C., Weckstrom, M., and Juusola, M. 2006. Robustness of neural coding in *Drosophila* photoreceptors in the absence of slow delayed rectifier K^+ channels. J. Neurosci. 26, 2652–2660.

b1205 Vihtelic, T. S., Goebl, M., Milligan, S., O'Tousa, J. E., and Hyde, D. R. 1993. Localization of *Drosophila* retinal degeneration B, a membrane-associated phosphatidylinositol transfer protein. J. Cell Biol. 122, 1013–1022.

b1210 Vihtelic, T. S., Hyde, D. R., and Otousa, J. E. 1991. Isolation and characterization of the *Drosophila* retinal-degeneration-B (*rdgB*) gene. Genetics 127, 761–768.

b1215 Vinos, J., Jalink, K., Hardy, R. W., Britt, S. G., and Zuker, C. S. 1997. A G protein-coupled receptor phosphatase required for rhodopsin function. Science 277, 687–690.

b1220 Vogt, K. and Kirschfeld, K. 1984. The chemical identity of the chromophores of fly visual pigment. Z. Naturwiss. 71, 211–213.

b1225 Wall, M. A., Coleman, D. E., Lee, E., Iniguez-Lluhi, J. A., Posner, B. A., Gilman, A. G., and Sprang, S. R. 1995. The structure of the G protein heterotrimer Gi alpha 1 beta 1 gamma 2. Cell 83, 1047–1058.

b1230 Walrond, J. P. and Szuts, E. Z. 1992. Submicrovillar tubules in distal segments of squid photoreceptors detected by rapid freezing. J. Neurosci. 12, 1490–1501.

b1235 Walz, B., Baumann, O., Zimmermann, B., and Ciriacywantrup, E. V. 1995. Caffeine-sensitive and ryanodine-sensitive Ca^{2+}-induced Ca^{2+} release from the endoplasmic-reticulum in honeybee photoreceptors. J. Gen. Physiol. 105, 537–567.

b1240 Walz, B., Liebherr, H., and Ukhanov, K. 2003. Ca^{2+}-dependent and Ca^{2+} release-dependent excitation in leech photoreceptors: evidence from a novel ''inside-out'' cell model. Cell Calcium 34, 35–47.

b1245 Wang, T. and Montell, C. 2005. Rhodopsin formation in *Drosophila* is dependent on the PINTA retinoid-binding protein. J. Neurosci. 25, 5187–5194.

b1250 Wang, T., Jiao, Y., and Montell, C. 2005a. Dissecting independent channel and scaffolding roles of the *Drosophila* transient receptor potential channel. J. Cell Biol. 171, 685–694.

Wang, T., Xu, H., Oberwinkler, J., Gu, Y., Hardie, R. C., and Montell, C. 2005b. Light activation, adaptation, and cell survival functions of the Na^+/Ca^{2+} exchanger CalX. Neuron 45, 367–378. b1255

Warr, C. G. and Kelly, L. E. 1996. Identification and characterization of two distinct calmodulin-binding sites in the Trpl ion-channel protein of *Drosophila* melanogaster. Biochem. J. 314, 497–503. b1260

Weckström, M., Hardie, R. C., and Laughlin, S. B. 1991. Voltage-activated potassium channels in blowfly photoreceptors and their role in light adaptation. J. Physiol. (Lond.) 440, 635–657. b1265

Wehner, R. 1989. Neurobiology of polarization vision. Trends Neursoci. 12, 353–359. b1270

Wolfram, V. 2004. Impact of light history on processing of visual signals in *Drosophila* photoreceptors, Ph.D. thesis, Cambridge University. b1275

Wong, F., Knight, B. W., and Dodge, F. A. 1980. Dispersion of latencies in photoreceptors of *Limulus* and the adapting-bump model. J. Gen. Physiol. 76, 517–537. b1280

Wu, C. F. and Pak, W. L. 1975. Quantal basis of photoreceptor spectral sensitivity of *Drosophila melanogaster*. J. Gen. Physiol. 66, 149–168. b1285

Wu, C. F. and Pak, W. L. 1978. Light-induced voltage noise in the photoreceptor of *Drosophila melanogaster*. J. Gen. Physiol. 71, 249–268. b1290

Wu, L., Niemeyer, B., Colley, N., Socolich, M., and Zuker, C. S. 1995. Regulation of PLC-mediated signalling *in vivo* by CDP–diacylglycerol synthase. Nature 373, 216–222. b1295

Xu, X. Z. S., Chien, F., Butler, A., Salkoff, L., and Montell, C. 2000. TRP gamma, a *Drosophila* TRP-related subunit, forms a regulated cation channel with TRPL. Neuron 26, 647–657. b1300

Xu, X. Z. S., Choudhury, A., Li, X. L., and Montell, C. 1998. Coordination of an array of signaling proteins through homo- and heteromeric interactions between PDZ domains and target proteins. J. Cell Biol. 142, 545–555. b1305

Xu, X. Z. S., Li, H. S., Guggino, W. B., and Montell, C. 1997. Coassembly of TRP and TRPL produces a distinct store-operated conductance. Cell 89, 1155–1164. b1310

Yamada, T., Takeuchi, Y., Komori, N., Kobayashi, H., Sakai, Y., Hotta, Y., and Matsumoto, H. 1990. A 49-kilodalton phosphoprotein in the *Drosophila* photoreceptor is an arrestin homolog. Science 248, 483–486. b1315

Yang, Y. and Ballinger, D. 1994. Mutations in calphotin, the gene encoding a *Drosophila* photoreceptor cell-specific calcium-binding protein, reveal roles in cellular morphogenesis and survival. Genetics 138, 413–421. b1320

Yarfitz, S. L., Deer, J. L. R., Froelick, G., Colley, N. J., and Hurley, J. B. 1994. In situ assay of light-stimulated G protein activity in *Drosophila* photoreceptor G protein beta mutants. J. Biol. Chem. 269, 30340–30344. b1325

Yarfitz, S., Niemi, G. A., McConnell, J. L., Fitch, C. L., and Hurley, J. B. 1991. A G beta protein in the *Drosophila* compound eye is different from that in the brain. Neuron 7, 429–438. b1330

Yasuhara, J. C., Baumann, O., and Takeyasu, K. 2000. Localization of Na/K-ATPase in developing and adult *Drosophila melanogaster* photoreceptor. Cell Tissue Res. 300, 239–249. b1335

Yoon, J., Ben-Ami, H. C., Hong, Y. S., Park, S., Strong, L. L., Bowman, J., Geng, C., Baek, K., Minke, B., and Pak, W. L. 2000. Novel mechanism of massive photoreceptor degeneration caused by mutations in the trp gene of *Drosophila*. J. Neurosci. 20, 649–659. b1340

Yuan, J. P., Kiselyov, K., Shin, D. M., Chen, J., Shcheynikov, N., Kang, S. H., Dehoff, M. H., Schwarz, M. K., Seeburg, P. H., Muallem, S., and Worley, P. F. 2003. Homer binds TRPC family channels and is required for gating of TRPC1 by IP_3 receptors. Cell 114, 777–789. b1345

b1350 Zheng, L., de Polavieja, G. G., Wolfram, V., Asyali, M. H., Hardie, R. C., and Juusola, M. 2006. Feedback network controls photoreceptor output at the layer of first visual synapses in *Drosophila*. J. Gen. Physiol. 127, 495–510.

Relevant Websites

http://flybase.bio.indiana.edu/– Flybase: detailed information and annotation on all *Drosophila* genes and mutant phenotypes, including links to sequences, primary references, extensive stocklists and much more.

http://www.fruitfly.org/– Home page for the Berkeley *Drosophila* Gene Project (BDGP). Definitive sequence and annotation for the *Drosophila* Genome. Plus P element-mediated mutagenesis on a scale unprecedented in metazoans.

Author's Contact Information

AU1 **Roger C. Hardie**
Department of Physiology Development and Neuroscience
University of Cambridge
Downing Street
Cambridge CB2 3DY
UK
Tel: 01223-339771
Fax: 01223-333786
E-mail: rch14@hermes.cam.ac.uk

Keywords: adaptation; arrestin; calcium; calmodulin; diacylglycerol; DAK kinase; *Drosophila*; G protein; lipid signaling; microvillus; NINAC; PDZ domain; phospholipase C; phosphoinostide; photoreceptors; PIP_2; rhodopsin; translocation; TRP channels

Abstract

Invertebrate microvillar photoreceptors depolarize in response to light by opening nonselective cation channels. Often the same cells can respond sensitively and rapidly to single photons, and yet light adapt to encode fluctuations of intensity under full sunlight. The underlying molecular mechanisms have been most extensively studied in the fruitfly *Drosophila*. Incident light is absorbed in the rhabdomere, a 1- to 2-μm diameter, 100-μm-long waveguide composed of ~40 000 tightly packed microvilli, which contain the visual pigment rhodopsin and all the major components of the cascade. The extreme compartmentalization provided by this microvillar design is key to understanding the combination of sensitivity, rapid kinetics, and large dynamic range. Excitation is mediated by activation of G_q protein and phospholipase C (PLC) resulting in activation of two classes of Ca^{2+}-permeable channel. These are encoded by the transient receptor potential (*trp*) and *trp-like* (*trpl*) genes, the founding members of the large and diverse TRP (light-activated nonspecific cation channel encoded by *trp* gene) superfamily of nonvoltage-gated cation channels. Several components of the cascade, including TRP, PLC, and protein kinase C (PKC) are assembled into a multimolecular signaling complex by the scaffolding protein INAD. Recent evidence suggests that the primary activator of the channels is likely to be a lipid messenger derived from the hydrolysis of phosphatidylinositol 4,5-bisphosphate (PIP_2) by PLC. Candidates include diacylglycerol (DAG), polyunsaturated acids (PUFAs), or the reduction in PIP_2. Ca^{2+} influx via TRP channels is essential for rapid kinetics, amplification, and light adaptation, and mediates both positive and negative feedback via multiple downstream targets, including calmodulin (CaM), both TRP and TRPL (light-activated nonspecific cation channel encoded by *trpl* gene) channels, PKC, and PLC. Ca^{2+} influx is also required for proper functioning of the visual pigment cycle, which involves CaMKII-dependent phosphorylation of arrestin and Ca^{2+} CaM-dependent dephosphorylation of rhodopsin.